

nuclear science and technology

Long-term behaviour of glass: Improving the glass source term and substantiating the basic hypotheses (GLASTAB)

I. Ribet, S. Gin, N. Godon, P. Jollivet, Y. Minet (CEA-Valrho, France – coordinator)
B. Grambow, A. Abdelouas, K. Ferrand (Subatech, France)
K. Lemmens, M. Aertsens, V. Pirlet, D. Jacques (SCK•CEN, Belgium)
J. L. Crovisier, A. Clément, B. Fritz, I. Munier (CGS, France)
M. Del Nero, A. Ozgümüs (IRES, France)
E. Curti (PSI, Switzerland)
B. Luckscheiter (FZK, Germany)
B. Schwyn (Nagra, Switzerland)

Contract N° FIKW-CT-2000-00007

Final report

Work performed as part of the European Atomic Energy Community's R&T specific programme Nuclear Energy 1998-2002, key action Nuclear Fission Safety
Area: Safety of the fuel cycle

Directorate-General for Research
Euratom

Project coordinator

Bundesanstalt für Geowissenschaften und Rohstoffe (BGR), DE

Project partners

1. Gesellschaft für Anlagen- und Reaktorsicherheit mbH (GRS), DE
2. Empresa Nacional de Residuos Radiactivos SA (ENRESA), ES
3. Asociación para la Investigación y Desarrollo Industrial de los Recursos Naturales (AITEMIN), ES
4. Centre International de Méthodes Numériques en Ingéniería (CIMNE), ES
5. Nationale Genossenschaft für die Lagerung radioaktiver Abfälle (Nagra), CH
6. Eidgenössische Technische Hochschule Zürich, Institut für Geotechnik (ETHZ), CH
7. Colenco Power Engineering Ltd (Colenco), CH
8. Rothpletz Lienhard + Cie AG (RL), CH

Table of contents

1	Executive summary	1
1.1	Objectives of the project	1
1.2	Challenges to be met	1
1.3	Achievements	1
2	Objectives and strategic aspects	3
2.1	Scientific objectives	3
2.2	Socio-economic objectives and strategic aspects	3
3	Scientific and technical description of the results	5
3.1	Observation and characterisation of the alteration products	5
3.2	Modelling of alteration kinetics and gel formation	26
3.3	Glass corrosion in near-field conditions	61
3.4	Retention behaviour of actinides and lanthanides in gel/solution systems	75
3.5	Performance calculations: long-term glass package behaviour under integral conditions ..	92
4	General conclusion	99

1 Executive summary

1.1 Objectives of the project

The disposal of vitrified waste forms in a geological repository requires predictions of their very long-term behaviour in complex media, where water will be both the main alteration factor and the main radiotoxicity vector from the repository site to the biosphere. Prediction on time scales beyond the realm of human experimentation makes it indispensable to understand all the phenomena involved in the interaction between the glass and the environment. The GLASTAB project was undertaken to improve our knowledge of nuclear glass behaviour, and thus to increase the dependability of glass source term models under representative repository conditions. Adopting an integrated approach to the interactions and coupled phenomena controlling the long-term glass stability in the near field of disposal sites enhances the realism of the models. The overly conservative approach of previous models based on the maximum glass rate alteration is thus no longer necessary.

1.2 Challenges to be met

The measurement and calculation of the altered glass quantity according to the time and alteration conditions have been investigated for many years in an effort to better understand the phenomena involved and to develop more realistic models. The difficulties arise not only from the complexity of the systems considered (nuclear glass compositions, and the range of environmental materials under consideration for the repository) but also from the excellent intrinsic performance of many nuclear glasses (only a few nanometres altered per year under residual rate conditions), requiring sophisticated equipment to observe and characterize the alteration products.

Two approaches have therefore been combined under the GLASTAB project: an experimental approach to acquire missing data on the alteration characteristics, and modelling to test hypotheses concerning the mechanisms governing alteration. Combining these two approaches has led to substantial progress in understanding the phenomena involved, and thus to the construction of performance models.

1.3 Achievements

1.3.1 OBSERVATION AND CHARACTERIZATION OF THE ALTERATION PRODUCTS

Glass alteration by water results in the formation of alteration products (crystallized secondary phases and an amorphous “gel” phase) which in turn affect the alteration kinetics. One of the project objectives was to observe and characterize the alteration products to better understand their role and integrate it into the alteration rate model. The studies carried out within the framework of the GLASTAB programme confirmed that the nature and properties of the alteration layer were highly dependent on both the glass composition and the alteration conditions (temperature, pH, water flow rate, etc.), and that they evolved with the reaction progress. These observations were corroborated by studies of natural analogues of the alteration gels (palagonite).

1.3.2 MODELLING OF ALTERATION KINETICS AND GEL FORMATION

The formation of the alteration layer systematically corresponds to a significant drop in the glass alteration rate, which in the case of SON68 glass at 90 °C can diminish from about $0.3 \mu\text{m}\cdot\text{d}^{-1}$ to $3\cdot 10^{-5} \mu\text{m}\cdot\text{d}^{-1}$. Various models have been developed under the GLASTAB project both for the formation of the alteration gel and for the glass surface alteration rate. The

methods range from microscopic approaches such as Monte Carlo modelling to macroscopic approaches combining silicon retention in the gel, silicon diffusion in the gel and possibly in the hydrated glass layer, and the onset of silicon saturation at the glass/gel interface. Attempts have also been undertaken to model the gel formation from the standpoint of the chemical composition based on the use of geochemical models taking account of the formation of solid solutions, and from a texture standpoint using coupled transport-chemistry models to describe the evolution of the gel porosity. The drop in the alteration rate is indeed modelled according to the alteration conditions, although it is still necessary to use empirical parameters. The next objective will be to model the long-term rate conditions following the rate drop.

1.3.3 GLASS ALTERATION IN THE PRESENCE OF NEAR-FIELD MATERIALS

The presence of near-field materials — in particular clays (some of which, such as boom clay or FoCa7 clay, were specifically investigated under the GLASTAB project) — modifies the glass alteration kinetics observed during alteration in aqueous media. A major effort has been undertaken to characterize the properties of these materials in order to progress towards a coupled description of the glass evolution in contact with clay. Significant differences in behaviour can be observed depending on the nature of the materials. The main phenomena likely to account for the effects of clay are silicon sorption on the clay and the precipitation of secondary phases containing silicon. Nevertheless, these phenomena do not prevent very low glass alteration rates from being reached after a time period that depends on the quantity of clay involved.

1.3.4 RADIONUCLIDE RETENTION

Sorption and co-precipitation are also the two major phenomena considered to account for radionuclide retention in the glass alteration products. Experiments in complex glass-gel-solution systems have confirmed that the behaviour of elements and the predominant sorption mechanism depend on the physico-chemical conditions: Trivalent elements released by glass dissolution are incorporated by (ad)sorption on gels at near-neutral pH. Under basic pH, there is competition between adsorption and aqueous carbonate complexation, leading to decreased retention (the solubility-limiting phases could be carbonates). In $MgCl_2$ brines the predominant sorption mechanism is ion exchange (low efficiency). Over the long term, the behaviour of actinides and lanthanides is controlled by precipitation of poorly soluble mineral phases.

1.3.5 PERFORMANCE ASSESSMENT

All the preceding results have been incorporated into an overall view of glass performance to substantiate the hypotheses supporting the operational models of glass alteration: These are simple, robust models with varying degrees of realism, to be coupled with environmental models for performance assessment calculations. The conclusion is that glass performance is highly dependent on the reactivity of the surrounding environment, on the residual alteration rate (i.e. the rate observed over the very long term), and on the hypotheses postulated concerning the repository constituents that must be taken into account. Performance assessments have shown that when the alteration conditions are compatible with the onset of a residual rate, the glass matrix has a significant barrier function within the considered system which includes a bentonite barrier.

2 Objectives and strategic aspects

2.1 Scientific objectives

The GLASTAB project was intended to increase the confidence in glass source term modelling for representative geological disposal conditions. By using an integrated approach to the interactions and coupled phenomena controlling the long-term stability of glass in the near field of geological disposal sites, the project aimed at increasing the realism of modelling and decreasing the over-conservatism of previous approaches.

The objective of this project was to enhance the scientific exactitude of models used for long-term glass performance assessment, to substantiate them, to resolve contradictory modelling approaches, and to seek experimental confirmation by integral mock-up tests. The successive steps of the project were the following:

1. quantifying the passivating properties of alteration gels in an integral-field system
2. assessing the stability of the potentially protective alteration layers
3. integrating the properties of the gel in the glass alteration kinetics
4. assessing coupling phenomena in an integral near-field system
5. modelling of long-term glass package behaviour under integral conditions
6. synthesising and communicating the scientific knowledge acquired.

2.2 Socio-economic objectives and strategic aspects

Nuclear fission energy plays a key role in the supply of electric power in the European Union and is particularly relevant to reduce the greenhouse effect. To be able to fulfil this important role, the safety of the nuclear fuel cycle and of the management and disposal of high-level and long-lived radioactive waste in particular must continuously be demonstrated and improved. Especially the general public, which to a large extent determines the acceptance of this energy source, wants clear proof of the safe and effective management and final disposal of radioactive waste.

Vitrification is a widely applied technique to immobilise the high-level and long-lived radioactive waste originating from the reprocessing of spent fuel. Various Member States of the European Union will have to safely dispose of their amounts of vitrified high-level waste (HLW). In the Member States concerned, disposal of HLW in a deep and stable geological formation (clay, granite or salt), based on the multi-barrier concept, is intensively studied as a safe option. The scale and common aspects of the problem, both in terms of scientific and financial aspects, justify the past and present European programmes. The proposed project will provide reliable data for modelling of HLW glass corrosion and radionuclide release out of the waste package. The modelling approach will enable to establish laboratory- and in situ-based long-term HLW glass performance predictions and therefore contribute to strengthen the scientific basis for the management and disposal of HLW glass. If the results of the in situ test from the cluster project CORALUS-2 agree with the laboratory-based predictions, this will also be a clear demonstration that HLW glass forms an important barrier and that the proposed disposal concept is safe.

From a scientific point of view, the modelling of long-term behaviour of nuclear glasses is a very complex issue. Thus different approaches have been attempted by the various scientific laboratories in charge of this problem. These approaches are not together consistent, inducing a lack of confidence in the way governments will deal with the problem of the nuclear waste. The GLASTAB project will allow combining the expertise of numerous European scientific teams and so contribute to building a consensus on the way to model the long-term behaviour of nuclear glass. This common knowledge could then be relayed outside the European Union.

The GLASTAB project will directly contribute

- to a safe disposal of vitrified high-level and long-lived radioactive waste, since the results of the modelling will lead to a performance assessment of waste packages
- to the enhancement of public confidence in the disposal concept for HLW glass by editing a summary document specially devoted to non-specialists.

The results of the GLASTAB project will also be useful to EU Member States that are facing the disposal of other types of vitrified waste, including non-radioactive waste.

3 Scientific and technical description of the results

The GLASTAB project was divided into 6 work packages and 40 tasks, corresponding either to bibliographic surveys, experimental investigations or modelling exercises. The details of the tasks are given in the management reports. These tasks can be split into 5 major topics of interest:

- Observation and characterisation of alteration gel layers
- Modelling of alteration kinetics and gel formation
- Glass corrosion in near-field conditions
- Retention behaviour of actinides and lanthanides in gel/solution systems
- Performance calculations: long-term glass package behaviour under integral conditions

The main results are presented below.

3.1 Observation and characterisation of the alteration products

The work packages related to the different topics are listed in the table below.

TOPIC	WORK PACKAGES	PARTNER
SEM and TEM observations on different kinds of gel (long-term experiment on nuclear glasses, natural analogues)	WP1-2, WP1-3, WP1-6, WP2-3-3	CGS, PSI, CEA
Measure of diffusion coefficients	WP1-1, WP3-3	CEA, SUBATECH
Gel leaching	WP2-7	CEA, xxx
In-situ irradiation	WP2-7-5	SUBATECH
Gel stability	WP2-8, WP4-2	CGS, CEA

3.1.1 INTRODUCTION

A common property of nuclear and basaltic glasses is the formation of an alteration layer on the surface. This layer is commonly called **gel** for nuclear glass and **palagonite** for basaltic glasses. What are the common properties of these gel layers, what are the differences? What teachings for nuclear glasses can one get of the survey of the basaltic glasses altered during several thousand or millions of years in nature?

This chapter was initially entitled “Characterising the gel” and it was decided, during the final meeting of GLASTAB, to give a definition of the gels.

For some of the participants a gel is an amorphous, hydrated and porous product formed by recondensation of silica of the glass. Some others consider a gel as the result of recondensation or co-precipitation of silica with “other elements”.

Enzo Curti considers the gel in the glass science field as "a dense network of polymerised SiO₂ filled with water. The pore sizes are so small and the tortuosity so large that diffusion of species is strongly reduced". This participant distinguish glass

science from a classical sense (chemistry) where a gel is "a dense, self-supporting colloidal dispersion, generated for instance by a coagulation process. The dispersion medium may be water (hydro gel) or another solvent".

So why should we distinguish between a general sense and a restricted one reduced to glasses?

Bernd Grambow pointed out that "if we stick to the classical sense, we are obliged to distinguish two phases: the dispersed phase, and the dispersing media. This means that the hydrated glass is not a gel, it is still a glass. Water is integrated in this glass phase as a solid solution. There are no phase boundaries. But there is recondensation of silanol groups, reorganisation of the network to replace alkali ion by water/H⁺ etc. He proposed two mechanisms for gel formation: (1) dissolution/precipitation and (2) augmentation of water content in the glass beyond the solubility limit and "precipitation" of water droplets in the glass. In the first case, the gel is formed by glass corrosion, in the second case by water diffusion. Such a clear separation of gel and hydrated glass allows for a better thermodynamic treatment of both phases. It is compatible with both a smooth transition between glass and hydrated glass and with a sharp interface between both. Karine Ferrand (SUBATECH) shall look at the IR data to see whether there is evidence for a water phase in the hydrated glass, or whether there are just individual water molecules. May be this can also be resolved by small angle X-ray ... keep on discussing".

Another question is to decide if a gel is amorphous or if a local order can exist and if yes how far? In the sol-gel science, it is considered that most of the gels are amorphous. However, the aging of numerous gels at room temperature can lead to their crystallisation, for example by formation of carbonated phases (BRINKER and SCHERER, 1990 and references therein). Do they continue to be called gels? If a gel is amorphous or even "isotropic", then WP1-1-2 and WP1-2 ("Study of alteration layers from basaltic glasses"; "Diffusion through palagonite layer"), and WP1-6 ("Study of alteration layers from nuclear glasses") do not deal with gels So it was decided to rename the Chapter 1: "Characterising the alteration layers".

As can be noticed in the following 1.2 review, a comparable discussion already took place in the community of geologists about the nature of "palagonite gel layers" (see also CROVISIER et al., 2003).

3.1.2 PALAGONITE: NATURAL ANALOGUE OF EXPERIMENTALLY FORMED LAYERS ON NUCLEAR GLASS

3.1.2.1 About a definition

Palagonite, first described in 1845 by von Waltershausen (1845), was named for Palagonia, a locality in the Iblei Mountains of Sicily. It is an alteration product around the outer rind of basaltic glasses subjected to the action of water. Its structure and especially its chemical composition vary significantly from one sample to another. There is generally a very distinct border between the pristine glass, or sideromelane, and the alteration rind; observed by optical microscopy, the latter is characterized by its orange-yellow coloration in natural light and sometimes by slight birefringence in polarized light, while the glass itself is isotropic and honey-coloured (Figure 1).

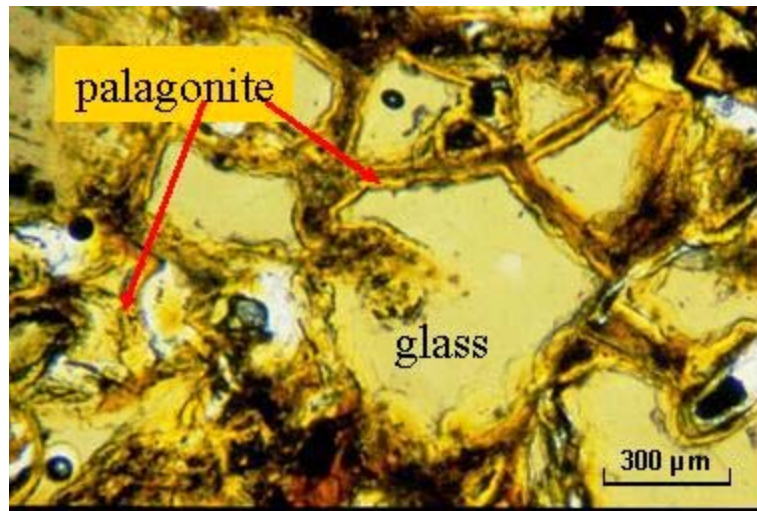


Figure 1. Palagonitized Icelandic glass (Hahryggur) 90 000 years. (CROVISIER et al., 2003)

No simple definition of this product was found in the literature. It was once considered a mineraloid distinct from species such as korite, hyblite or notite (WALTERSHAUSEN, 1845). Des Cloizeaux (1862) wrote: “Mr Sartorius de Waltershausen identified as korite a dark brown variety of palagonite disseminated in the Sudafell palagonitic tuff in Iceland and in the Val di Nito; he finally acknowledged that a similar tombac-brown substance found in the Tonnara tuff of Cap Passaro consisted of 75 % siderosilicite and 25 % trinacrite. There is little need to point out that since palagonite is itself a rock rather than a well-defined mineral, all these names can be applied only to essentially variable mixtures.” Penck (1879) was of the same opinion: “*es existiert kein Mineral Palagonite ...*”. Nevertheless, Peacock (1930) made a distinction between palagonite and chlorophaeite. Today its chemical composition is known to be largely dependent on the temperature, composition and flow rate of the alteration fluids, and on the time during which these solutions are in contact with the glass (CROVISIER, 1989; LE GAL et al., 1999; MURAKAMI et al., 1988; TECHER et al., 2000). (HONNOREZ, 1967; HONNOREZ, 1972) suggests that the term “palagonite” is confusing and should no longer be used as it designates poorly defined and highly diverse products. He recommends the use of expressions such as residual glass, altered glass or palagonitized glass to designate alteration layers containing no clearly identifiable mineral. Some terms are difficult to get rid of, however, and “palagonite” is often used in the literature.

It may also be noted that palagonitic layers do not form systematically in fresh water. FIELDDES et al. (1956), SINGER (1974) noted that a palagonitic layer is systematically observed when the principal alteration mineral is montmorillonite. In this case, the layer itself consists of poorly organized montmorillonite. Conversely, when the principal alteration mineral is halloysite, it directly replaces the glass without forming an alteration layer per se that can be discriminated from the clayey intergranular material (WADA and MIZOTA, 1982).

3.1.2.2 Structure and texture

The spectra obtained by X-ray diffraction in these alteration rinds are those of amorphous or slightly crystallized products; they exhibit some characteristics of

smectitic phyllosilicates (CROVISIER et al., 1987; EGGLETON and KELLER, 1982; HONNOREZ, 1972; JERCINOVIC and EWING, 1987; MATTEWS, 1962; SUMMERS, 1976). Their crystallinity generally increases over time as shown, for example, by a study of basalt samples altered in the Eas Pacific Rise and in the North Atlantic Ridge (NOACK and CROVISIER, 1980). An example is given in Figure 2 (palagonitized hyaloclastite from Hahryggur, Iceland). A broad, low-amplitude peak centered on 13 Å is visible (untreated sample, Figure 2a). After treatment with ethylene glycol, the peak became broader and shifted to about 17 Å (Figure 2b). Heating the sample to 490°C caused the peak to collapse to about 10 Å (Figure 2c). This behaviour is characteristic of a poorly crystallized smectite. Some samples, such as one from the Contrada Acqua Amara (Palagonia, Sicily), were completely destroyed by heating (HONNOREZ, 1967; HONNOREZ, 1972; CROVISIER, 1989).

3.1.2.3 Properties

The data summarized hereafter are detailed in (CROVISIER et al., 2003). They indicate that dedicated petrographic examination of natural basaltic glasses and leach tests conducted on synthetic glasses can shed light on the geochemical alteration mechanisms and kinetics.

The activation energies associated with the initial alteration reactions of basaltic glass and nuclear glass are identical (73-71 kJ.mol⁻¹). This similarity indicates that similar mechanisms are involved during aqueous dissolution, including hydrolysis of the silicate network. Laboratory leaching experiments have also shown that the basaltic glass alteration rate diminishes very rapidly with the reaction progress. The drop in the dissolution kinetics may reach several orders of magnitude at advanced stages of reaction progress. A similar trend is observed for nuclear borosilicate glass altered under the same experimental conditions (temperature, water/glass ratio and interaction time). The protectiveness of the alteration layer could account for the drop in the alteration rate. At the same time, the chemical composition of the alteration solution influences the alteration reaction processes. Measurements of the thickness of the alteration layers on volcanic glasses weathered in the natural environment (palagonites) have shown that the long-term alteration rates are very low, of the same order of magnitude as those measured in the laboratory.

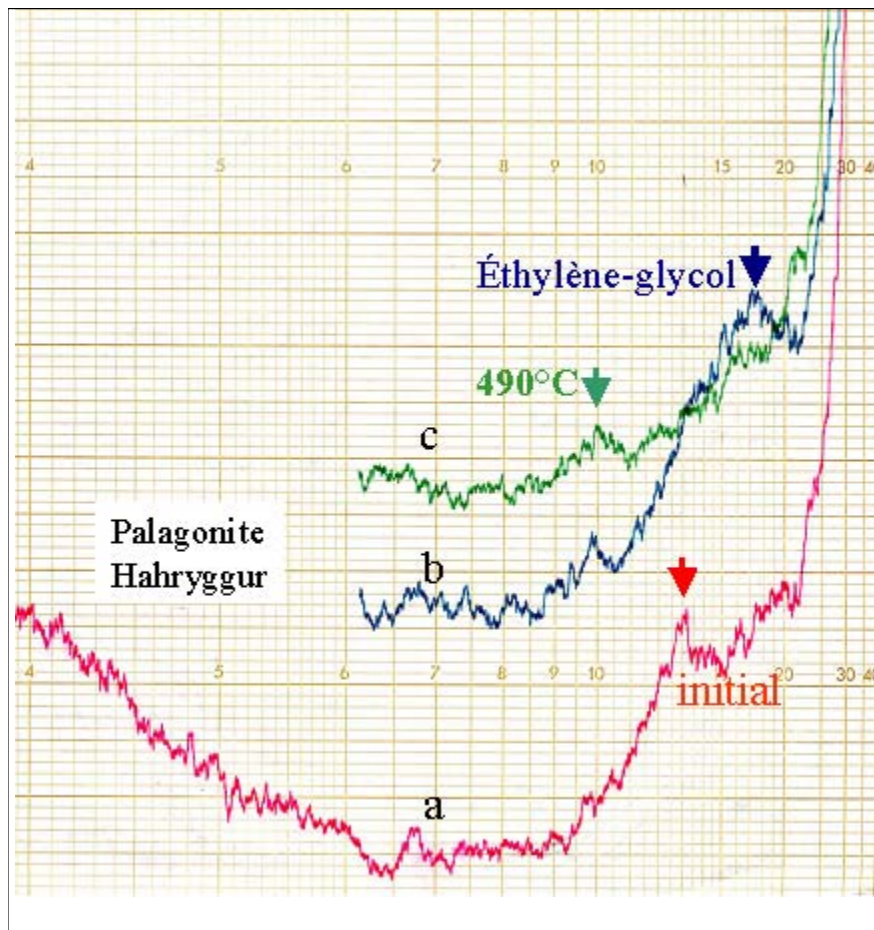


Figure 2. Spectra obtained by X-ray diffraction in altered rind of a Hahryggur glass sample (Iceland): (a) as sampled; (b) after treatment with ethylene glycol; (c) after heating. (CROVISIER et al., 2003)

3.1.3 GELS FORMED DURING LONG-TERM EXPERIMENTS (SON68 AND MW WASTE FORM GLASSES)

The dissolution kinetics of nuclear waste glasses has been intensively investigated in the past decades. Kinetic investigations are essential to formulate a source term for the release of hazardous radioactive elements into the environment. However, since important fractions of most radionuclides are retained in the gel layer and/or secondary surface precipitates, glass dissolution rates are not sufficient to predict their release. In many cases, the radionuclide release is strongly limited by incorporation in secondary solids. The first step to understand the fate of such radionuclides is thus the identification of such host minerals.

In this task, we studied the alteration of two reference glasses (SON68 and MW) representative of vitrified high-level waste arising from nuclear power plants in Switzerland. The main objective was the identification and mineralogical characterization of the alteration phases formed during the long-term leaching (up to 13 years) of powder samples, with special emphasis on systematic differences between the two glass formulations. We also performed complementary chemical calculations on the analysed leachant solutions, in order to detect (or verify) solid phases in saturation equilibrium. Finally, we determined retention factors for a number of radionuclides. The main techniques used were electron microscopy

(SEM/TEM/STEM) on altered glass samples separated after 5.7 and 12.2 years corrosion time and concentration measurements of dissolved elements (ICP-AES). Details on the experimental setup and a kinetic analysis of these tests can be found in the reporting of WP 5-5.

During the project, two sets of altered glass samples (5.7 years and 12.2 years reaction time) were investigated. For the MW-glass, three material types could be distinguished on the base of SEM/TEM pictures: *unaltered glass*, thin (μm -thick) *coatings* of altered glass enveloping the grains (Fig. 3) and a $\sim 1\text{mm}$ -thick *crust* formed by coalescing alteration products (mainly clay minerals). In the altered SON68 samples a similar coating adhering to the grains was found but no crust. The TEM images revealed that the grain coatings around MW glass grains can be subdivided in an XRD-amorphous *porous zone* and an external *clay zone* dominated by crystalline clay minerals (Fig. 4). Well-developed clay crystals were found only occasionally in the SON68 sample and do not form a well-differentiated rim as for the MW glass. For both glasses, the morphology of the alteration products did not change significantly during the 6.5 years corrosion time elapsed between the two sample extractions. Only the thickness of the MW-glass alteration rim increased from ~ 1.5 to ~ 2.3 μm .

Semi quantitative chemical analyses of the glass and of alteration products were carried out on TEM thin sections by analysing the characteristic X-ray fluorescence with an EDS detector. The nominal composition of unaltered glass could be reproduced satisfactorily after correction for Na volatilisation and for the elements not included in the EDS analyses. This demonstrates the reliability of the performed chemical analyses. The MW glass revealed a variety of alteration phases: besides Mg-dominated clays (probably saponites), several small particles enriched in phosphate and lanthanides could be detected. Because the calculated $(\Sigma\text{Ln})/\text{P}$ stoichiometric ratios are close to unity, these phases are probably simple lanthanide phosphates with stoichiometric formula LnPO_4 . The average formula resulting from 5 analyses is $\text{Nd}_{0.42} \text{La}_{0.21} \text{Pr}_{0.14} \text{Ce}_{0.05} \text{Ln}_{0.18} \text{PO}_4$ (where Ln represents non-analysed lanthanides). Similar Ln-phosphate micro phases have been found also in natural basalts (STEINMANN et al., 1999). Furthermore, opaque particles enriched in Zr, lanthanides and phosphate, have been detected at the interface between glass and alteration products.

Clay minerals in the SON68 samples are not well-developed as in the MW glass and do not show a diffraction pattern. However, a homogeneous compositional picture emerges, with notable enrichments in Zn (9-11 w% oxides), Fe (8-9 w%) and Ni (~ 4 w%). In contrast to the MW glass, no distinct phosphate phases have been detected. Nevertheless, EDS analyses of spots containing mixed phases revealed positive correlations between the concentrations of phosphate and Ln, as well as phosphate and Ca, suggesting the presence of nanoparticles of lanthanide phosphates and Ca-phosphates (e.g. apatite, $\text{Ca}_5\text{OH}[\text{PO}_4]_3$).

In general, the average composition of the porous alteration zone was found to be close to that of crystalline clay minerals in both altered glasses. Furthermore, compositional changes with time are minor. As notable exception, Zn concentrations in the clay minerals of SON68 samples increase from ~ 9 w% in the 5.7 years samples to ~ 11 w% in the 12.2 years samples - at the expense of Al, which decreases from ~ 8 to 6 w%.

Chemical analyses (ICP-AES) of the leachant solutions were performed in order to determine retention factors of major and minor elements present in the glass (Table 1).

The results indicate that most elements representing radionuclides (Fe, Ni, Zr, Ln) will be largely retained in the solid alteration products described above. Thus, their concentrations will be controlled by solubility products of these solid solution phases. Sr retention is also very high (95-97 %) but we were not able to detect the phase(s) to which this element is associated. Cs retention is high as well (~ 90 %), and with TEM we could detect spots enriched with this element in the altered MW glass. However, tests showed that such enrichments disappeared after washing the altered samples with distilled water. Hence, Cs in these samples is probably present either as outer sphere sorbate or in a soluble salt.

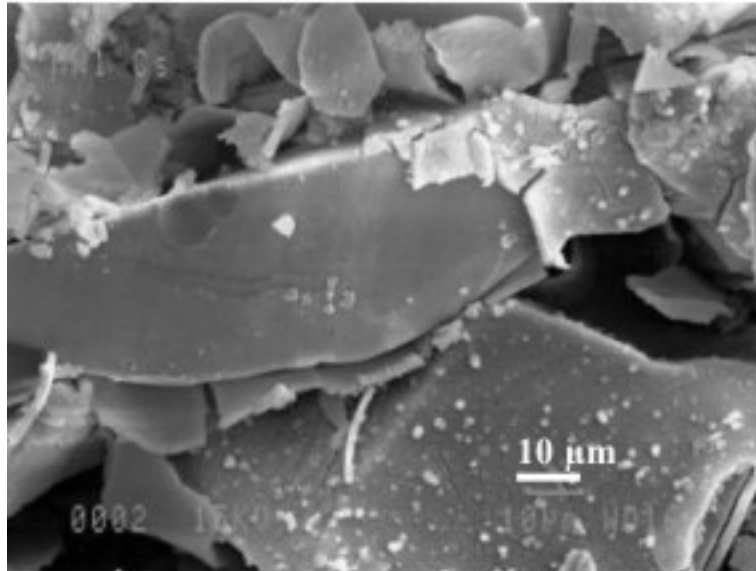


Figure 3: SEM image of MW glass corroded during 5.7 years, showing a glass grain with exfoliated alteration coating.

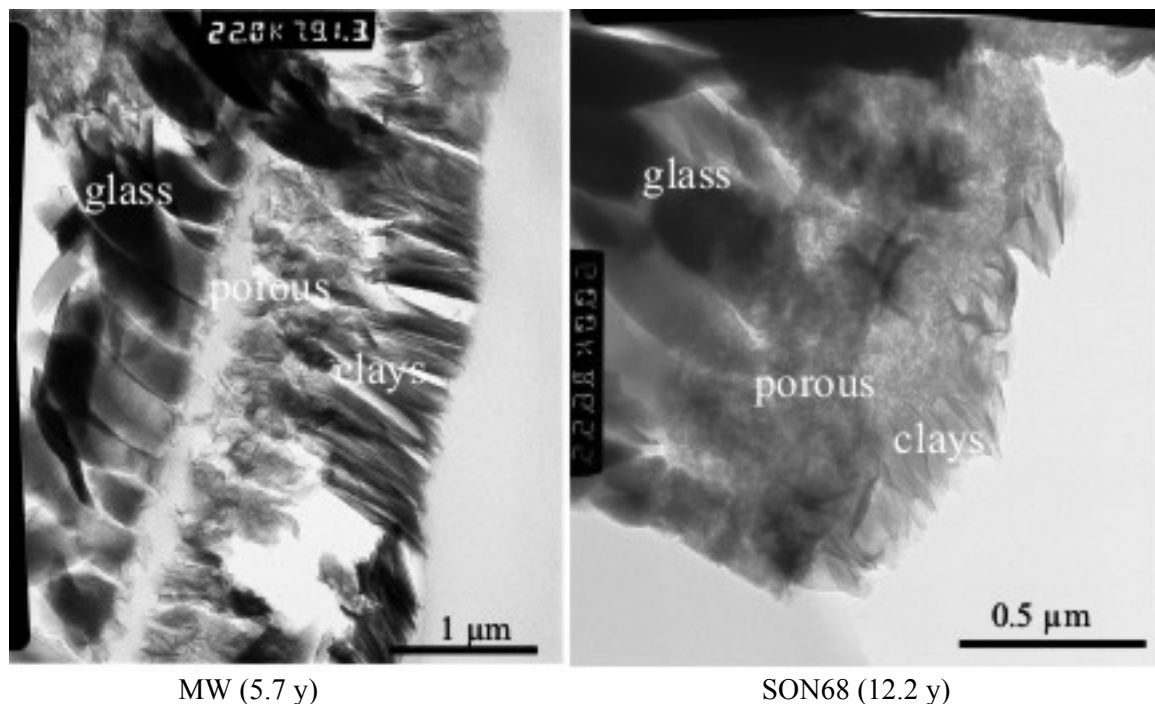


Figure 4: TEM images of MW and SON68 grains. Cross sections through unaltered glass, porous zone and clay zone.

Table 1: Molar concentrations and calculated retention factors for selected elements in MW and SON68 altered glass samples.

12.2 y samples	concentration (mol/l)		Retention Factor (%)	
	MW	SON68	MW	SON68
	Al	1.30E-04	3.90E-05	99.1
B	6.70E-02	8.90E-03		7.1
Ca	2.10E-06	1.60E-05	97.3	99
Ce	4.80E-06	1.30E-07	99.4	99.9
Cs	4.90E-05	2.90E-05	95.7	87.8
Fe	1.20E-05	3.70E-06	99.7	99.6
La	1.10E-05	1.20E-07	97.6	99.9
Li	2.90E-02	3.20E-03	18.6	
Mg	8.70E-05	1.90E-06	99.6	
Mo	7.30E-04	1.50E-04	62.2	52.8
Na	2.10E-02	4.30E-03	42	43.8
Nd	6.20E-06	1.40E-07	99.5	99.9
Ni	1.70E-06	1.30E-06	99.7	99.5
P	3.30E-05	1.30E-05	90.8	85.8
Pr	1.70E-06	1.10E-07	99.8	99.8
Si	5.00E-03	3.60E-03	95.4	79.8
Sm	7.10E-07	1.00E-07	99.7	
Sr	1.50E-06	4.10E-07	99.7	99.5
Y	9.20E-07	4.20E-08	99.6	99.9
Zn	1.10E-07	6.30E-06		99.1
Zr	4.70E-06	3.80E-07	99.8	99.9

3.1.4 MEASURE OF DIFFUSION COEFFICIENTS OF WATER, AN ALKALI METAL AND SILICA IN AN ALTERATION LAYER OF A NUCLEAR GLASS AND IN PALAGONITE

The objective of this work package of the GLASTAB project is a better knowledge of diffusion phenomena through the measurement of the diffusion coefficient of three species: water, silicon and an alkali metal, namely sodium, in the alteration layer of various materials. Materials of interest here are SON68 glass, a non-radioactive analogue of the French R7T7 nuclear glass, and two varieties (a “young” and an “old” one) of altered basaltic glass (palagonite). Palagonite is not considered here as a direct analogue for nuclear glass; the idea is rather that comparison between varieties of different age will shed some light on the evolution of transport and retention properties of altered layer.

3.1.4.1 Material

Altered SON68 glass has been supplied under the form of a powder with a mean initial diameter of 25 μm , lixiviated at a temperature of 90 $^{\circ}\text{C}$ for one year under dynamic conditions, with a daily renewal rate of the solution of 0.4. These alteration conditions lead to a glass dissolution rate r of 0.05 $\text{g}/\text{m}^2/\text{d}$ which corresponds to the ratio $r_0/20$ (r_0 is the initial dissolution rate). This ratio indicates that the gel formed in this study is slightly protective (for a strongly protective gel, ratio r/r_0 is around 10 000).

Total available mass is about 22 g. To avoid cracking of the gel layer, the material was preserved in a 1 mol/L NaCl solution.

“Young” palagonite with an estimated age of 90 000 years (CROVISIER et al., 1989) could be separated from samples of altered basaltic glass. After sieving, 4.4 grams of dry palagonite grains were obtained, with a mean diameter of 80 μm . It was humidified by contact with a saturation solution obtained by lixiviating SON68 glass.

One last material was intended to be “old” palagonite (1.3 M years). About 4.6 grams could be obtained, with a size distribution between 40 and 63 μm . The samples contain a significant fraction of zeolite (chabazite), which unfortunately proved impossible to separate from palagonite. It is not known at this time whether the properties of each mineral can be discriminated. Work on old palagonite has therefore been suspended until adequate methods are developed to overcome this difficulty.

3.1.4.2 Methods

The problem to be addressed here is the measurement of the diffusion coefficient of reactive and non reactive species in the gel layer, considered as a porous structure. Among various classical techniques, the use of tracers in a chromatographic column has been selected for several reasons: it has been successfully applied to characterization of ion exchangers, a very similar problem; it allows a realistic liquid to mass ratio while requiring only limited amounts of material; no mechanical stress is imposed on the particles.

The technique consists in packing the material in a column fed with a continuous flow of an adequate eluent, in our case a NaCl solution, in which a tracer of the species under study is injected under the form of a pulse. Restitution of the tracer is monitored at the outlet of the column. This experiment yields several informations:

The area of the restitution curve makes it possible to establish a tracer balance, which indicates which proportion (if any) is irreversibly fixed in the material.

The mean residence time of the tracer allows calculating the porosity ε (both porosity between the grains and inside them) that the tracer can access, in the case it does not interact with the material. In the opposite case, the retardation factor R characterizing this physico-chemical interaction is obtained.

When the up-front of the tracer pulse goes through the column, tracer diffuses into the grains; conversely, it diffuses out of them after the end the pulse. Diffusion in/out of the internal porosity of the grains results in a modification of the restitution curve, usually under the appearance of a large tail. Using an adequate model, it is possible to determine a characteristic diffusion time t_d from which the apparent diffusion coefficient D_a can be deduced by $D_a = r^2 / kt_d$ (r : characteristic dimension of the grains, k : shape factor – many diffusion coefficients can be defined in porous media, D_a is the one that actually controls the transient concentration profile in the gel layer, i.e. the one that is truly relevant for studies on long-term behaviour).

The method has however two pitfalls: it requires that characteristic diffusion time t_d bear some relation with the mean residence time in the column (hence the feed flow rate); the resulting D_a is quite sensitive to the size distribution of the grains because of the r^2 dependence.

This technique has been applied using four different tracers: a deficit in the NaCl concentration in the eluent (monitored by a conductimeter at the exit of the column); tritiated water (HTO) as a tracer for water, monitored by an on-line β counter; ^{22}Na

under the form $^{22}\text{NaCl}$ as a tracer for the sodium ion (γ counter); ^{32}Si as Si^{4+} as a tracer for silicon (β counter again).

Column length is typically 4 cm, for a diameter of 1 cm. Eluent flow rate can be varied between 1 and 60 mL/h; most tracer experiments (HTO , ^{22}Na , ^{32}Si) were conducted at low NaCl concentrations (0.5 to $1 \cdot 10^{-2}$ mol/L).

3.1.4.3 Results

Porosity of the altered layer as a function of eluent ionic strength

Though apparently not directly related to the objectives of the work package, this point provides interesting information on the compared behaviour of nuclear glass and palagonite. It has been chiefly investigated by monitoring pulses of salt concentration deficit at the outlet and measuring the pressure drop in the column.

In the case of **SON68 glass**, there is consistent evidence that the **altered layer contracts with increasing ionic strength** (the overall porosity of the column increases, from about 45 % at $4 \cdot 10^{-3}$ mol/L NaCl to 75 % at 1 mol/L, whereas the pressure drop decreases). This effect is well known in ion-exchangers. The size of the grains being a function of ionic strength, simultaneous determination of inter-granular and intra-granular porosity is not possible.

Palagonite shows notably different behaviour: the pressure drop in the column shows **no indications of swelling or contraction** as a function of ionic strength. On the other hand, the apparent porosity determined from the salt deficit pulses is more than 100 % at low ionic strength (less than 10^{-2} mol/L NaCl), which is interpreted as a sign of some **interaction between NaCl as a whole and palagonite**. Literature suggests Donnan partition as a plausible interpretation.

The reason for the difference between SON68 glass and palagonite has not been investigated so far.

Diffusion coefficient for water

With the available equipment the mean residence time of the eluent cannot be reduced under 90 to 120 s (depending on the material and the quality of packing). This means that we cannot hope to measure t_d values less than a few percents of this quantity. Restitution curves obtained with tritiated water show no sign of deformation due to diffusion into the grains, which indicates that the actual value of t_d for water is less than the measurable limit. The column experiments therefore did not allow to measure the diffusion coefficient of water in SON68 glass nor in palagonite; for the measurement to be effective, much larger flow rates would be required, which does not seem practical because of excessive pressure drops, or a much smaller column – for example a short capillary. Another alternative would be to use larger particles (which is possible with nuclear glass, but obviously unpractical with palagonite).

Having an upper limit for t_d however allows to calculate a lower bound for D_a : in the case of nuclear glass, the latter can be expected to be more than $4 \cdot 10^{-12}$ m²/s (not a very valuable information since apparent diffusion coefficients of water is often much higher in porous media); the corresponding lower limit for palagonite being, more interestingly, $3 \cdot 10^{-11}$ m²/s. The difference in orders of magnitude is entirely due to the smaller size of the palagonite grains, not to the nature of the materials.

Diffusion coefficient for silicon

The results of the ^{32}Si tracer experiments are available for the SON68 glass only at this date. They highlight several facts:

Restitution of injected ^{32}Si is very low (1.6 % in our operating conditions), which indicates, not surprisingly, a **high** amount of **irreversible fixation of silicon** in the altered layer of the glass.

The restitution curve has two peaks; the first one is only little retarded/deformed with respect to a passive tracer and can therefore not be used to measure diffusive effects. Possible origins might be a) transport by colloids b) fixation on and transport by phyllosilicates present in the alteration layer. Available data does not allow discriminating between these assumptions.

The second peak can be analysed by the methods described above. It results in an estimate of the **diffusion coefficient for silicon in altered nuclear glass of $5 \cdot 10^{-14}$ to $10^{-13} \text{ m}^2/\text{s}$** . This value is consistent with existing correlations.

Lastly, the second peak corresponds to a **retardation factor of about 30** with respect to a non-interactive species.

The corresponding experiments are under way for palagonite.

Diffusion coefficient for sodium

Tracer experiments with $^{22}\text{NaCl}$ were successful for both SON68 glass and palagonite. Irreversible fixation was observed in neither case. Analysis resulted in the following estimates for the apparent diffusion coefficient and the retardation factor:

Material	D_a (m^2/s)	R (-)
Altered SON68 glass	$0.7\text{-}2 \cdot 10^{-13}$	110-350
Palagonite	$3 \cdot 10^{-12}\text{-}2 \cdot 10^{-11}$	4.5-6.5

The apparent diffusion coefficient for sodium in nuclear glass is about 2 orders of magnitude lower than in palagonite; the retardation factor 30 to 60 times larger. Product RD_a , a diffusion coefficient corrected for the effects of interaction, consistently has the same order of magnitude for both materials.

3.1.5 LONG-TERM IMPACT ASSESSMENT OF WATER DIFFUSION PROCESSES IN THE PRISTINE GLASS VERSUS HYDROLYSIS REACTIONS, BY MEANS OF LEACH TESTS AT IMPOSED PH

SON 68 glass corrosion experiments were conducted in a dynamic system at imposed pH (4.8, 7.2 and 9.8) at 50 and 90 °C. The tests were conducted in a synthetic solution containing silicon (127 mg/L), boron (380 mg/L) and sodium (1015 mg/L). Solutions of this composition are typically observed during SON 68 leaching of glass powder at $S/V = 20000 \text{ m}^{-1}$ and $T = 90 \text{ °C}$ (TOVENA, 1995).

The kinetics of glass corrosion were determined by measuring Lithium, Caesium and Molybdenum concentrations in solution with the ICP-MS. Glass hydration was studied using a Fourier Transform Infrared spectrophotometer (FTIR) between 400

and 4000 cm⁻¹. Glass surface was observed under scanning and transmission electron microscopes.

Alteration kinetics Normalized dissolution rates of Li, Cs and Mo were calculated using the formula:

$$NL_{t+1} = \frac{\left(\frac{NC_t - NC_{t+1}}{(t+1) - t} \right) + \left(\frac{F}{V} \times NC_{t+1} \right)}{S/V}$$

$$\text{With } NC = \frac{C_{\text{element}}}{\% \text{element in pristine glass}}$$

t (days), F/V is the ratio of the solution flow (mL.d⁻¹) to solution volume (mL), S/V (m⁻¹) is the ratio of the glass surface (m²) to solution volume (m³), NL is the normalized leaching rate (g.m⁻².d⁻¹), C is the element concentration (g.m⁻³), NC is the normalized element concentration (g.m⁻³).

An example of alteration data obtained at pH 4.8 is plotted in figure 5. Leaching rates measured for Li and Cs were quite similar and slightly decreased indicating that Li and Cs release was controlled by diffusion as indicated by the slope of about -1/2. At the end of experiment with powder, the leaching rate measured by Li was about 2.10⁻³ g.m².d⁻¹ and 100 times lower for Mo that is often used to monitor glass matrix dissolution.

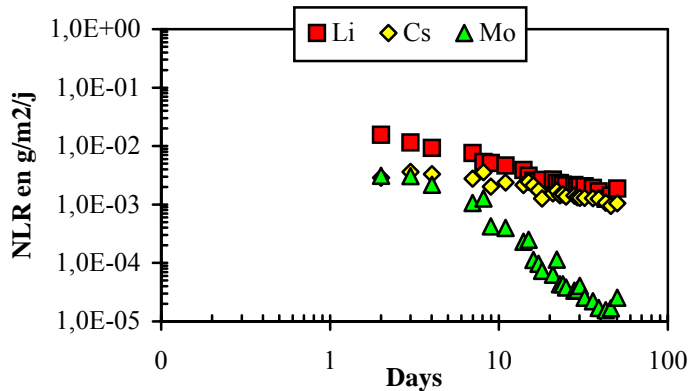


Figure 5. Normalized leaching rates as a function of time for glass powders altered in a synthetic solution at pH 4.8 and 50 °C.

Similar trends were observed for experiments at pH 7.2 and 9.8 but also for experiments at 90 °C. Corrosion rates were calculated and are given in table 2. For dissolution at pH 4.8 and 7.2 there was no effect of the temperature increase on the corrosion rates. However at pH 9.8, glass matrix corrosion and ionic exchange were about 10 times higher at 90 °C.

Table 2. SON 68 glass normalized leaching rates in $\text{g}\cdot\text{m}^{-2}\cdot\text{d}^{-1}$.

Material	Element	50 °C			90 °C		
		pH			pH		
		4.8	7.2	9.8	4.8	7.2	9.8
Chip	Li	$2\cdot 10^{-3}$	$3\cdot 10^{-3}$	-	$5\cdot 10^{-3}$	$5\cdot 10^{-3}$	10^{-2}
	Mo	$5\cdot 10^{-5}$	-	10^{-4}	$2\cdot 10^{-5*}$	$3\cdot 10^{-4}$	10^{-3}
Powder	Li	$2\cdot 10^{-3}$	$2\cdot 10^{-3}$	$6\cdot 10^{-5}$	$5\cdot 10^{-3}$	$2\cdot 10^{-3}$	$2\cdot 10^{-3}$
	Mo	$3\cdot 10^{-5}$	10^{-4*}	10^{-5}	$2\cdot 10^{-5}$	10^{-4}	$3\cdot 10^{-4}$

* Steady state was not reached in these experiments

Surface analysis No gel layer was observed under the scanning electron microscope except for experiment at pH 4.8 and 90 °C (Figure 6). According to transmission electron microscopy and compared to pristine glass, the gel is enriched in silicon, aluminium and had lost up to 60 % of the initial sodium (Table 3).

Element	Pristine glass	Alteration layer
Si	49	52.6 ± 2.3
Al	6	6.8 ± 1.0
Na	16.8	1.2 ± 0.6
Ca	6.7	1.7 ± 0.2
Fe	4.7	3.0 ± 0.2
Zn	4.6	17.0 ± 4.0
Zr	4.5	6.9 ± 1.1
Mo	2.6	5.6 ± 0.9
La	1.8	2.7 ± 0.3
Nd	3.1	2.6 ± 0.3
total	99.8	100

Table 3. Composition of pristine and alteration layer formed at pH 4.8 and 90 °C (in cation weight%, average of 8 analyses, ignoring oxygen and boron).

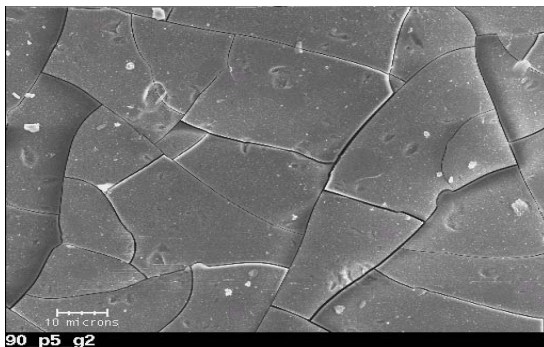


Figure 6. Alteration layer formed on the glass chip corroded at 90 °C and pH 4.8.

3.1.5.1 Water analysis

Figure 7 shows FTIR spectra of glass hydrated at 90°C and pH 4.8. According to Beer-Lambert law and taking extinction coefficients given by literature (GEOTTI-BIANCHINI et al., 1999; YANAGISAWA et al., 1997) $\epsilon_{\text{SiOH}} = 70 \text{ L}\cdot\text{mol}^{-1}\cdot\text{cm}^{-1}$ and $\epsilon_{\text{H}_2\text{O(I\&II)}} = 81 \text{ L}\cdot\text{mol}^{-1}\cdot\text{cm}^{-1}$, water and silanol concentrations were calculated. In all set of data, water concentration was higher than silanol concentration and hydration increased when pH decreased. The plot of hydrogen concentration in the corroded glass surface as a function of the alkalis released from the glass gives a molar ratio of H/Na+Li+Cs near 3 as shown in Figure 8. This may suggest the exchange reaction $\text{H}_3\text{O}^+ \leftrightarrow \text{A}^+$ (A = alkali).

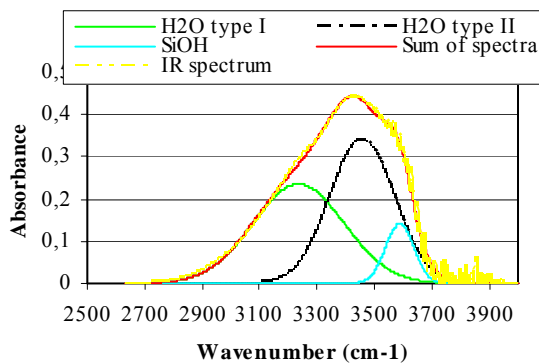


Figure 7. Peak separations of the 2500-4000 cm^{-1} FTIR water-related bands using three Gaussian bands for glass powder hydrated for SON68 glass powder hydrated for 14 days in a synthetic saturated solution at pH 4.8 and 90 °C.

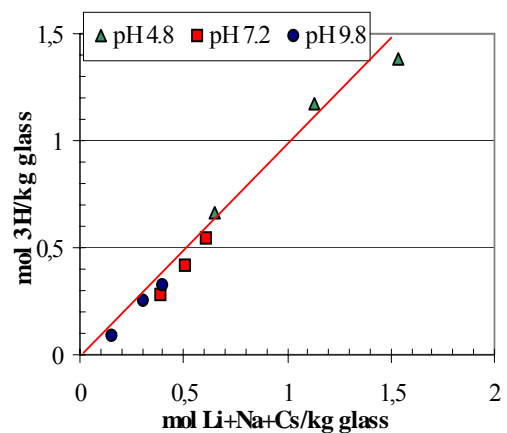


Figure 8. 3H (mol)/glass (kg) calculated from FTIR data as a function of alkali (mol)/glass (kg) for powder corroded at 90 °C.

Water diffusion coefficients To describe the experimental data and to fit the water diffusion coefficients we used the model proposed by (GRAMBOW and MÜLLER, 2001). This model describes glass alteration by an affinity driven corrosion of the glass matrix coupled to a diffusion controlled glass hydration process. Fixing most model parameters (silica saturation constant, forward rate of glass corrosion, diffusion coefficient of dissolved silica in the gel) to values given in the paper by Grambow and Müller the model was used to fit the water diffusion coefficients (Table 4). For experiments at 50°C, and pH 4.8 and 7.2 with glass powder, the coefficient was about 10^{-22} - $10^{-23} \text{ m}^2\cdot\text{s}^{-1}$. At 90 °C, water diffusion coefficients were one order of magnitude higher.

Table 4. Water diffusion coefficients ($\text{m}^2 \cdot \text{s}^{-1}$) in SON 68 glass.

Temperature	50°C			90°C		
pH	4.8	7.2	9.8	4.8	7.2	9.8
Powder $\varnothing \leq 20$ μm	$4 \cdot 10^{-22}$	$6 \cdot 10^{-23}$	$3 \cdot 10^{-24}$	$3 \cdot 10^{-21}$	$5 \cdot 10^{-22}$	10^{-22}
Powder $\varnothing \leq 5$ μm	$8 \cdot 10^{-23}$	$5.3 \cdot 10^{-23}$	-	10^{-21}	$1.5 \cdot 10^{-22}$	$6 \cdot 10^{-23}$
Glass chip	$2.5 \cdot 10^{-21}$	$1.5 \cdot 10^{-22}$	-	$6 \cdot 10^{-19}$	$4 \cdot 10^{-21}$	$2 \cdot 10^{-21}$

3.1.5.2 Discussion

Under saturation conditions final SON 68 glass matrix corrosion rates were found similar to those obtained in static conditions for over 11 years in the order of 10^{-4} - 10^{-5} $\text{g} \cdot \text{m}^{-2} \cdot \text{d}^{-1}$. Modelling of the experimental results suggests that the continuing glass alteration under low affinity conditions was controlled by water diffusion with diffusion coefficients in the order of 10^{-21} $\text{m}^2 \cdot \text{s}^{-1}$. Under storage conditions where the pH is expected to reach a value higher than 9 the water diffusion coefficients are very low 10^{-21} - 10^{-24} $\text{m}^2 \cdot \text{s}^{-1}$.

3.1.6 IN SITU IRRADIATION

For alpha and gamma irradiation alteration experiments were conducted with SON 68 glass and saturated solution as described in WP3-3 but in a static system. The gamma irradiation experiments were conducted at the University of Orsay (France) with a ^{60}Co source. The alpha irradiation experiments were done in a cyclotron at the CERI (CNRS, France).

The results of gamma irradiation are plotted in figures 9-10. For low doses the pH dropped only slightly while for high total dose the pH significantly decreased (figure 9). Total doses below 4380 Gy did not affect the corrosion behaviour of the glass within 92 days. A total dose of 57714 Gy had led to a pH decrease, which enhanced the leaching rate of Li (figure 10). To confirm this hypothesis and to simulate the effect of gamma irradiation alteration experiments were conducted and the pH was lowered from 9.7 to about 9 as it was the case with the irradiation experiment. The leaching rate of Li in non-irradiated experiment is similar to that in the irradiated experiment after 28 days and is higher than that in the blank experiment.

The irradiation with alpha, where the total dose did not exceed 1800 Gy, did not affect the alteration behaviour of the glass.

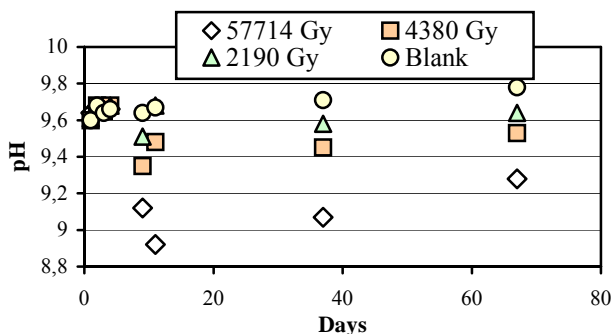


Figure 9. Evolution of pH as a function of gamma dose rate delivered to the glass/solution system.

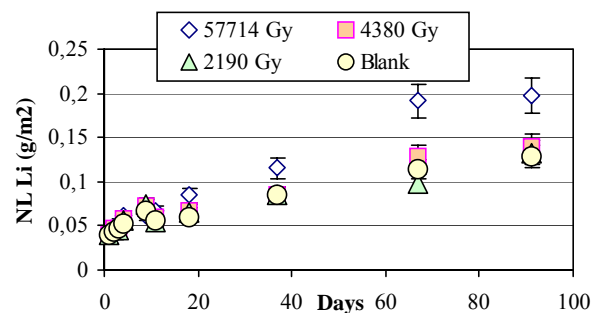


Figure 10. Li-normalized mass loss as a function of gamma dose rate delivered to the glass/solution system.

3.1.7 STABILITY OF THE GELS

The experiments proposed in this WP were designed to assess the stability of a protective gel. Different types of perturbations were applied to SON68 glass samples previously altered in static mode at high S/V ratios to verify to what extent the pre-existing gel conserves its diffusion barrier properties.

The protective gel was formed during static mode alteration at 90°C of SON68 glass powder for 56 days at a high S/V ratio. The tests were performed in PTFE containers with 5.77 g of SON68 glass (the 40–63 μm fraction with a specific surface area of 1300 cm²·g⁻¹ measured by the BET method) in contact with 150 mL of ultra pure water, yielding an S/V ratio of 50 cm⁻¹. The solution was agitated by a magnetic stirring bar. The pH was measured at regular intervals at the test temperature. Solution samples were taken after 14, 28 and 56 days. The samples were acidified then analyzed by ICP-AES for Si, B, Na, Al, Ca, and Li. After 56 days the glass alteration rate was estimated to be near 5 × 10⁻⁴ g·m⁻²·d⁻¹, which corresponds to about $r_0/2000$ under these temperature and pH conditions. The resulting gel was 80 nm thick and could be considered highly protective. Eight tests of this type were performed. Seven of them were perturbed after 56 days, and the eighth constituted the control specimen.

Two types of perturbations were applied. In one series of tests the solution pH was modified, and pH values of 4.2, 9.5, 10, 10.7 and 11.5 were imposed by adding dilute HCl or KOH solutions. In another series, the solutions were diluted with pure water (1:2 and 1:150). The effect of these perturbations was compared with the control experiment in which the glass was not perturbed.

3.1.7.1 pH perturbations

The results of the pH variation tests are shown in **Figure 11**.

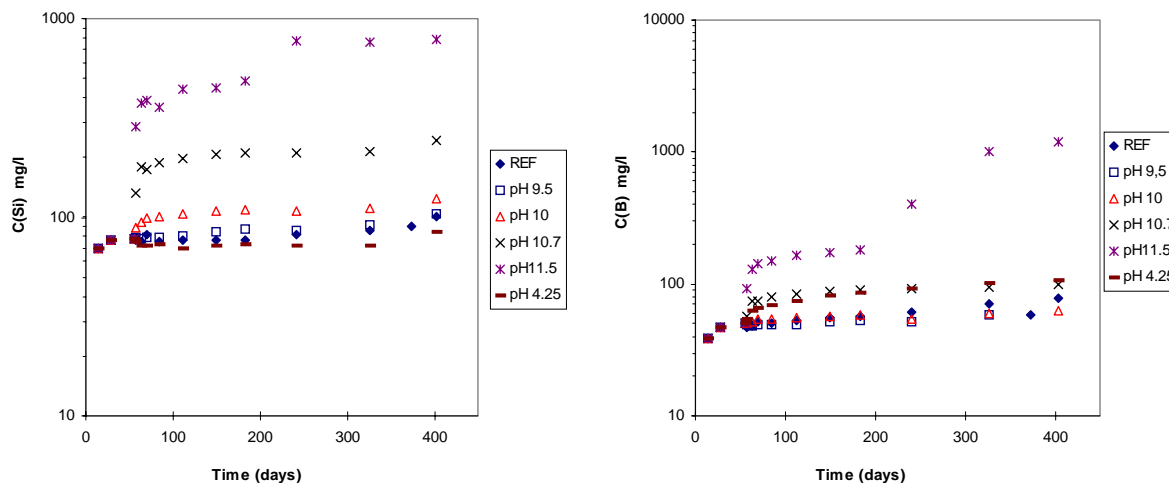


Figure 11. Silicon (left) and boron (right) concentrations versus time for the control test and pH perturbation tests.

In the undisturbed solution under these temperature and S/V conditions, the equilibrium pH of the solution was approximately 9.1 at 90 °C.

Lowering the pH to 4.25 had the following effects: the pH rapidly increased (in less than a day) to above 7, then more slowly to about 8.5; the silica concentration slowly diminished (from 78 ppm to 70 ppm in 56 days) followed by a slow increase; the glass alteration increased significantly (+ 57 % compared with the control sample at the end of the test). Most of this increase occurred during the first ten days after the perturbation, corresponding to alteration at a pH between 7 and 8.5. The behaviour of SON68 glass under these conditions corroborates the results obtained during experiments at imposed pH values showing that minimum alteration occurred between pH 9 and pH 10 (GIN and MESTRE, 2001).

The perturbations at pH 9.5 and 10 had virtually no effect on the glass behaviour. The pH tended to revert very slowly toward the equilibrium value (from pH 10 to pH 9.7 in 400 days), and the boron and silicon concentrations were practically unaffected by these perturbations. As before, this result is consistent with published data and confirms that the gel formed on SON68 glass is stable and protective between pH 9 and 10.

The pH 10.7 and 11.5 perturbations resulted in a significant increase in glass alteration. In the pH 10.7 experiment the pH remained stable at this value, silica was highly solubilized ($\times 2.5$ compared with the control sample) and the glass was more extensively altered than in the control test ($\times 2$ after 400 days), particularly during the first few days after the perturbation. In this case, the glass reacted strongly to the perturbation but no resumption of alteration occurred during the test, even after long time intervals.

The pH 11.5 perturbation resulted in a gradual decrease in the pH, considerable silica solubilization, and a major resumption of alteration about 200 days after the perturbation. The renewed alteration had already been observed during the tests at imposed pH values (GIN and MESTRE, 2001); the mechanism was attributed to precipitation of zeolites whose growth destabilized the protective gel notably by consuming the aluminum it contained. The latency time before the resumption of alteration is attributable to the zeolite nucleation phase; this step is associated with a gradual decline in the dissolved aluminium concentration. It is important to note that

the severe glass alteration released boron into solution in sufficient quantities for the pH to diminish to the point at which the zeolite growth ceased. Consequently, after a simple perturbation resulting in a highly basic pH the system slowly returns to equilibrium.

These tests during which the pH was perturbed can be interpreted on the basis of prior experiments at imposed pH values. There do not appear to be any particular mechanisms related to the reactivity of the pre-existing gel.

3.1.7.2 Perturbation by dilution

The results of the dilution tests are shown in Figure 12.

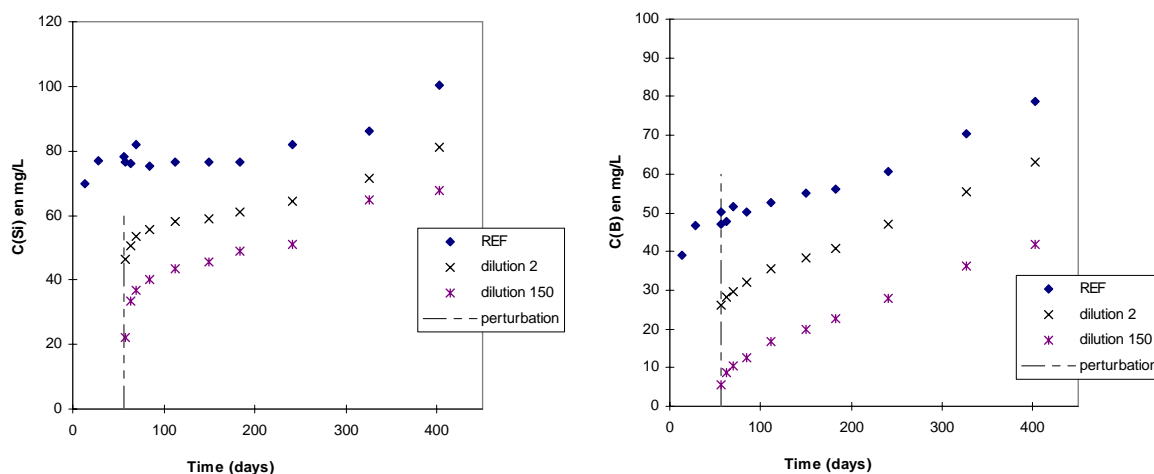


Figure 12: Silicon (left) and boron (right) concentrations versus time for the control test and dilution tests

Between 50 and 400 days in the control medium the glass was altered at a rate considered constant at experimental scale, equal to $4 \times 10^{-4} \text{ g} \cdot \text{m}^{-2} \cdot \text{d}^{-1}$. About 28 days after the perturbation in the two media that were diluted, the rates also stabilized at $4 \times 10^{-4} \text{ g} \cdot \text{m}^{-2} \cdot \text{d}^{-1}$. Dilution by factors of 2 and 150 caused the altered glass quantity at the end of the test to increase by 12 and 16 %, respectively, compared with the control medium. Although these increases were limited, this result suggests that when the gel is subjected to dilution it is not stable and partially loses its protective properties. Figure 12 shows that silica dissolved to a greater extent in the more disturbed medium, providing further support for the preceding argument. This result is consistent with earlier tests in which the alteration kinetics were measured for samples previously altered at high S/V ratios and then placed in pure water (GIN, 2000). These experiments showed that a protective gel placed in pure water partially dissolved until the solution reached new quasi steady-state conditions under which the residual kinetics were about 4 orders of magnitude lower than the initial rate. It may be noted that a steady-state silica concentration was not reached in this series of tests. As this result demonstrates, a persistent residual rate is not directly correlated with the evolution of the solution toward silica saturation conditions; this is consistent with the idea that the drop in the glass alteration rate is attributable primarily to a limitation in the transport of reactive species within the gel under conditions far from thermodynamic equilibrium.

In conclusion, and as suggested by considerable experimental work with SON68 glass (VERNAZ and GIN, 2001; VERNAZ et al., 2001), these results appear to confirm that the alteration kinetics of this nuclear glass are controlled by processes in which species are transported within the gel.

These experiments highlight the stability domain of the gel formed during alteration of SON68 nuclear glass, and the persistence of its diffusion behaviour. These results demonstrate the following features:

- Up to pH 10.7, a basic perturbation has no effect on the protective gel.
- A strong resumption of alteration is observed above pH 11 that may be related to the precipitation of zeolites whose growth destabilizes the gel.
- An acidic perturbation has little effect insofar as the pH very rapidly becomes basic again (pH 8.5).
- Dilution with pure water has extremely limited effects, confirming the excellent performance of the gel formed in static mode at 90 °C.

3.1.8 CONCLUSIONS

The survey of natural alteration layers (palagonite) clearly shows that the alteration of a same glass may lead to the **formation of alteration rims whose chemical and physical properties differ considerably from one environment to another (WP1-2)**. Besides, the alteration of basaltic glass does not necessarily lead to an alteration layer *sensu stricto* (WADA and MIZOTA, 1982). Interestingly, no gel layer was observed in experiments performed with nuclear glass in near saturation conditions (**WP3-3**). Thus, the differences observed between the SON68 alteration layers (swelling or contraction as a function of ionic strength, **WP1-1**) don't imply at all that palagonite would be a bad analogue for nuclear glasses. These differences must make us think to the fact that most laboratory experiments concerning nuclear glasses are made at the same temperature (90 °C) and in conditions necessarily simplified compared to the real storage site.

Our microscopic investigations (**WP1-6**) allow us to draw important conclusions on the impact of long-term glass alteration on the release of radionuclides into the geosphere:

- **A number of safety-relevant fission products have been shown to be immobilised in secondary alteration products** Ni(II) and Fe(II,III) concentrate in clay minerals; Zr(IV) and Ln(III) in phosphates. On the base of well-established chemical analogies it can be suggested that trivalent and tetravalent actinides would also concentrate in phosphates.
- **The nature of the secondary phases controlling the solubility of radionuclides depends to a large extent on glass composition.** For instance, the presence of only 5 w% MgO in the MW glass favored the formation of Mg-rich clays. In contrast, alteration of the Mg-free SON68 glass produced much smaller amounts of clay minerals, which contained Zn(II), Ni(II) and Fe(II,III) as octahedral cations in the place of Mg(II).
- Therefore, in order to predict the release and migration of radionuclides in a high-level waste repository environment, **it is essential to gain glass-specific information on the solubility-controlling alteration phases.** Clearly, there will be no generic solution to this problem, but only site-specific solutions.

Experiments performed under saturation conditions for SON 68 glass (WP3-3) indicate that:

- **Matrix corrosion rates are similar to those obtained in static conditions for over 11 years in the order of 10^{-4} - 10^{-5} g.m⁻².d⁻¹.**
- Modelling of the experimental results suggests that the continuing glass alteration under low affinity conditions was controlled by water diffusion with diffusion coefficients in the order of 10^{-21} m².s⁻¹. **Under storage conditions where the pH is expected to reach a value higher than 9 the water diffusion coefficients are very low 10^{-21} - 10^{-24} m².s⁻¹.**

High doses of gamma irradiation may enhance the corrosion of the glass due to acidification of solution. Therefore, detailed experiments are needed to better quantify the role of irradiation

The experiments conducted in WP 4-2 highlight the stability domain of the gel formed during alteration of SON68 nuclear glass, and the persistence of its diffusion behaviour:

- Up to pH 10.7, a basic perturbation has no effect on the protective gel.
- A strong resumption of alteration is observed above pH 11 **that may be related to the precipitation of zeolites whose growth destabilizes the gel.**
- An acidic perturbation has little effect insofar as the pH very rapidly becomes basic again (pH 8.5).
- Dilution with pure water has extremely limited effects, **confirming the excellent performance of the gel formed in static mode at 90 °C.**

3.1.9 REFERENCES

Brinker C. J. and Scherer G. W. (1990) Sol-Gel Science. The physics and chemistry of sol-gel processing. Academic Press, Inc., Harcourt Brace Jovanovich, Publishers, 908p.

Crovisier J. L. (1989) Dissolution des verres basaltiques dans l'eau de mer et dans l'eau douce. Essai de modélisation. PhD, Université Louis Pasteur, Strasbourg, 253p.

Crovisier J. L., Honnorez J., and Eberhart J. P. (1987) Dissolution of basaltic glass in seawater: Mechanism and rate. *Geochimica et Cosmochimica Acta* 51, 2977-2990.

Crovisier J.-L., Advocat T., and Dussossoy J.-L. (2003) Nature and role of natural alteration gels formed on the surface of ancient volcanic glasses (Natural analogs of waste containment glasses). *Journal of Nuclear Materials* 321(1), 91-109.

Des Cloizeaux A. (1862) Manuel de Minéralogie. Dunod, Paris 572p.

Eggleton R. A. and Keller J. (1982) The palagonitization of limburgite glass - A TEM study. *N. Jb. Miner. Mh.* 7, 321-336.

Fieldes M., Walker I., and Williams P. P. (1956) Clay mineralogy of New Zealand soils. -III. Infrared absorption spectra of soil clays. *New Zealand Journal of Sciences and Technology* 38, 31-43.

Geotti-Bianchini F., Geibler H., Krämer F., and Smith I. H. (1999) Recommended procedure for the IR spectroscopic determination of water in soda-lime-silica glass. *Glastech. Ber. Glass Sci. Technol.* 72 (4).

- Gin S. (2000) Protective effect of the alteration gel: A key mechanism in the long-term behaviour of nuclear waste glass. In *Scientific Basis for Nuclear Waste Management XXIV*, Mater. Res. Soc. Proc. (ed. K. Hart and G. R. Lumpkin), 207-216.
- Gin S. and Mestre J. P. (2001) SON 68 nuclear glass alteration kinetics between pH 7 and pH 11.5. *Journal of Nuclear Materials* 295(1), 83-96.
- Grambow B. and Müller R. (2001) First-order dissolution rate law and the role of surface layers in glass performance assessment. *Journal of Nuclear Materials* 298, 112-124.
- Honnorez J. (1967) La palagonitisation : l'altération sous marine du verre volcanique basique de Palagonia (Sicile). Thèse Université Libre de Bruxelles, 227p.
- Honnorez J. (1972) La palagonitisation : l'altération sous marine du verre volcanique basique de Palagonia (Sicile). Vulkaninstitut Immanuel Friedlaender. Birkhäuser Verlag, Basel, 9, 131p.
- Jercinovic M. J. and Ewing R. C. (1987) Basaltic glasses from Iceland and the deep sea : natural analogues to borosilicate nuclear waste-form glass, pp. 221. Swedish Nuclear Fuel and Waste Management Co, Tech. Report JSS 88-01.
- Le Gal X., Crovisier J.-L., Gauthier-Lafaye F., Honnorez J., and Grambow B. (1999) Meteoric alteration of Icelandic volcanic glass: long-term changes in the mechanism. *Comptes Rendus de l'Académie de Sciences, Paris - Série IIa: Sciences de la Terre et des Planètes* 329, 175-181.
- Mattews D. H. (1962) Altered lavas from the floor of the eastern North Atlantic. *Nature* 194, 368-369.
- Murakami T., Ewing R. C., and Bunker B. C. (1988) Analytical electron microscopy of leached layers on synthetic basalt glass. In: *Scientific Basis for Nuclear Waste Management XI*, (Ed. Michael, J. Apted and Richard E. Westerman), Mat. Res. Soc. Proc., 737-748.
- Noack Y. and Crovisier J. L. (1980) Evolution de la densité et de la réfractivité spécifique lors de l'altération sous marine des verres basaltiques. *Bull. Minéral.* 103, 523-527.
- Peacock M. A. (1930) The distinction between chlorophaeite and palagonite. *Geological Magazine* 67, 170-177.
- Penck A. (1879) Über palagonit und basalttuff. *Zeitschrift der Deutschen Geologischen Gesellschaft* 31, 504-577.
- Singer A. (1974) Mineralogy of palagonitic material from the Golan heights, Israel. *Clays and Clay Minerals* 22, 231-240.
- Steinmann M., Stille P., Bernotat W., and Knipping B. (1999) The corrosion of basaltic dykes in evaporites: Ar-Sr-Nd isotope and rare earth elements evidence. *Chemical Geology* 153, 259-279.
- Summers K. V. (1976) The clay component of the Columbia River palagonites. *American Mineralogist* 61, 492-494.
- Techer I., Advocat T., Lancelot J., and Liotard J.-M. (2000) Basaltic glass: alteration mechanisms and analogy with nuclear waste glasses. *Journal of Nuclear Materials* 282, 40-46.

Tovena I. (1995) Influence de la composition des verres nucléaires sur leur altérabilité. Ph.D. Thesis, Université de Montpellier II, France, 230 p.

Vernaz E. and Gin S. (2001) Apparent solubility limit of nuclear glass. In Scientific Basis for Nuclear Waste Management XXIV, Mater. Res. Soc. Proc. (ed. K. Hart and G. R. Lumpkin), 217-226.

Vernaz E., Gin S., Jégou C., and Ribet I. (2001) Present understanding of R7T7 glass alteration kinetics and their impact on long-term behaviour modeling. Journal of Nuclear Materials 298(1,2), 27-36.

Wada S. I. and Mizota C. (1982) Iron-rich halloysite (10 Å) with crumpled lamellar morphology from Hokkaido, Japan. Clays and Clay Minerals 30, 315-317.

Waltershausen S. v. (1845) Ueber die Submarinen vulkanischen Ausbrüche in der tertiären Formation des Val di Noto im Vergleich mit verwandten Erscheinungen am Aetna. Göttingen Studien I, 371-431.

Yanagisawa N., Fujimoto K., Nakashima S., Kurata Y., and Sanada N. (1997) micro-FT-IR study of the hydration-layer during dissolution of silica glass. Geochimica et Cosmochimica Acta 61(6), 1165-1170.

3.2 Modelling of alteration kinetics and gel formation

The work packages related to the different topics are listed in the table below.

TOPIC	WORK PACKAGES	PARTNER
Literature review	WP2-2, WP5-1	SUBATECH, CEA
Kinetics modelling	WP3-1, WP3-2	SUBATECH, CEA
Solid-solution modelling	WP2-1, WP2-3-4	CGS
KIRMAT	WP2-4, WP2-5	CGS, SUBATECH
Monte-Carlo modelling	WP2-9, WP5-7	SCK.CEN, CEA

3.2.1 LITERATURE REVIEW ON MODELLING GLASS DISSOLUTION

3.2.1.1 Alteration kinetics

The storage of nuclear waste within a vitreous matrix has raised the question of modelling the long-term alteration of this type of glass. The initial step of any glass-water reaction is the detachment of the ionic bound mobile and water accessible atoms at the glass surface, the alkali ions, by means of an exchange with hydrogen ions in presence of water molecules from solution. Alkali ions are not only exchanged at the outer glass surface but by diffusion of water molecules and alkali ions also from the surface region beneath, with release rates decreasing with time. The hydrolysis of

iono-covalent bonds of the glass network is a reaction, which occurs simultaneously with ion exchange. This reaction defines a corrosion front, which moves with an initially more or less constant rate into the glass. It leads to the release of silica and mobile glass constituents into solution and/or to the transformation of the glass phase into a gel-like surface layer. For nuclear waste glass it takes in most cases only few hours until the release rate of alkali ions becomes slow enough that also alkali ions are controlled by this corrosion reaction. This is why most rate laws for nuclear waste glass corrosion (exception McGrail et al. (2001b) for a low activity glass exposed to low temperature alteration) ignore ion exchange and describe only the corrosion reaction.

Wallace and Wicks (1983) derived a first model for the nuclear glass corrosion reaction, combining a notion of effects of silica concentrations and glass dissolution rates. The model considered the surface layers are generally protective. A similar approach has been presented by Jégou *et al.* (2000) The approach of Wallace and Wicks (1983) was later invalidated in its general applicability, well admitting that there are cases where surface layers are protective (Grambow, Strachan 1984).

A first order dissolution rate law for nuclear waste glass dissolution with silica as principal species was developed (Grambow 1983), later being integrated (Grambow 1984) into a general transition state theory based rate law for silicate mineral dissolution proposed by Aagaard and Helgeson (1982) which has been modified by divers approaches which may be in the general way as proposed by McGrail et al. (2001):

$$r = k \cdot a_{H^+}^{-\eta} \cdot \exp\left(\frac{-E_a}{RT}\right) \left[1 - \left(\frac{Q}{K_g(T)} \right)^\sigma \right] \cdot \prod_j a_j^{n_j}$$

where r is rate of the corrosion reaction, k the rate constant, a_{H^+} and η are the hydrogen ion activity and corresponding stoichiometric reaction coefficient, a_j and n_j the activity and stoichiometric coefficient of the superficial species j having an inhibiting effect on the overall reaction, E_a is the activation energy for the initial corrosion reaction, Q is the ion activity product and K_g the temperature dependent pseudo-equilibrium constant, σ is the stoichiometric coefficient (Temkin coefficient) which relates the stoichiometry of the rate limiting elementary reaction to overall glass dissolution, R the ideal gas constant, T the absolute temperature.

This rate law considers that the dissolution rate depends directly on the affinity of the rate limiting step of the dissolution reaction. Grambow (1984, 1985) postulated that the limiting step of the glass dissolution is desorption (hydrolysis) of a purely siliceous surface complex leading to

$$\frac{Q}{K_g} = \frac{[H_4SiO_4^0]}{[H_4SiO_4^0]_{sat}} \quad (\sigma \text{ was } 1 \text{ and all } n_j \text{ were } 0, \text{ the}$$

pH dependency was not formulated). Hydrolysis and condensation thus control the affinity and the corresponding “saturation” constant K_g in this reaction. Since a simple first order dissolution rate law would predict a stop of reaction at saturation in contrast to experimental observations it was proposed that the reaction would continue, governed by a constant final rate

This rate equation or corresponding equations with concentrations replacing activities have been applied to the alteration of basaltic (Grambow et al. 1985, Techer et al. 2001) and to a large set of experimental data with nuclear waste glasses (Werme et al. 1990, Advocat 1991).

Some authors modified the rate law, by considering the influence of elements, such as inhibitors Al^{3+} or H_4SiO_4 on r_0 ((Knauss *et al.* 1990, Carroll *et al.* 1994, Advocat *et al.* 1998, Techer *et al.* 2001, Oelkers and Gislason 2001) or of Al, Fe, Si on the affinity term (McGrail 1997, Gin 1996, Daux *et al.* 1997), or by setting $\sigma=0.33$ for basalt glass (Berger *et al.* 1994) or $\sigma=0.1$ for nuclear waste glass (Bourcier *et al.* 1994).

The dissolving solid phase whose dissolution affinity is rate controlling is supposed to be either the desalkalized glass surface (Grambow 1984), the altered and hydrated glass (Daux *et al.* 1997) or a solid solution of constant composition representing the gel-layer at the surface (Bourcier *et al.* 1990). Some authors tried to take the overall chemical affinity for the glass/water reaction into account, calculating the stability constant K_g by a solid solution representation of component oxides (Paul 1977) with a free energy of mixing (Leturcq *et al.* 1999, Advocat *et al.* 1998, Jégou *et al.* 2000, Techer *et al.* 2001).

All of these models only describe one aspect of glass corrosion: the surface reaction, without taking transport processes of reactants and of soluble products to or from the surface and across various surface reaction products into account. Thus, it seems to be necessary to take into account the role of gel as a diffusion barrier (Techer *et al.* 2001, Advocat 1991, Guy 1989, Leturcq *et al.* 1999, Jégou *et al.* 2000, Gin *et al.* 2001). Transport processes of dissolved silica in the growing gel layer were coupled to the first order dissolution rate law by Grambow *et al.* (1986) and by Delage (1992) to describe a protective effect of gel-layers, which is particularly obvious in corrosion tests in flowing solutions. A linear concentration gradient for dissolved orthosilicic acid was assumed to establish in the gel layer between the pristine glass and the bulk solution. The coupling was performed in numerical codes such as GLASOL (Grambow 1987) and Lixiver. Later it was realised that in the long term, when the corrosion reaction slows down due to saturation and protective effects, the ion exchange reaction may again become rate limiting governed by the diffusion of water into a saturation-stabilised glass network (Grambow *et al.* 2001, Ferrand *et al.* 2004), leading to the formation of a hydrated alkali-depleted glass at the glass/gel interface. The coupling of the affinity rate law with protective effects of the gel and with water diffusion is realised in the model GM2001 (Grambow 2001).

Since the overall reaction mechanism comprises different steps, it is clear that the first order rate law alone does not explain all of the experimental results, especially at silica super-saturated conditions (Gin 1996, Advocat *et al.* 1998, Jégou 1998, Jégou *et al.* 2000). Indeed, for a same activity of orthosilicic acid, at steady state, the dissolution rate does not depend only on orthosilicic acid activity but on flow rate, on S/V ratio as well (Advocat 1991, Advocat *et al.* 1998). It appears especially when considering the long-term dissolution where the models are far from reproducing the drop of the dissolution rate. This lead some authors (Jégou *et al.* 2000) to the conclusion that the above described affinity law is not valid for glass dissolution. Since the affinity law still explains quite a lot of data it was concluded that the apparent solubility constant K_g has no thermodynamic significance, but rather is a fitting variable representing a dynamic equilibrium between the quantity of silica hydrolyzed from the glass and gel and the quantity of silica condensed in the gel. It was suggested that this is a dynamic – and not a thermodynamic – equilibrium that depends on the conditions under which the equilibrium was reached (S/V ratio, silica removal kinetics, etc.) and not only on the concentrations in solution (Vernaz 2002). However, when considering overall coupling of the affinity law with silica transport

in the gel and water diffusion in the glass network, a satisfactory quantitative explanation of rate drop at near saturation conditions can also be obtained (Grambow et al. 2001).

3.2.1.2 Surface alteration products

Observed surface alterations on nuclear and basaltic glass

The alteration of glass results first in the formation of a hydrated, desalkalized interdiffusion region of few nm (Crovisier, 1987 ; Michaux, 1992), which moves with time into the glass and transforms itself into a hydrolysed, largely amorphous to crypto-crystalline reaction product which is often called a gel. The density of the gel is initially low and increases with time and with S/V due to condensation of silanol groups and accumulation of heavy elements. Deruelle (1997) observed a pore distribution between 2 and 4 nm, and a porosity of 33%. Pores were larger under dynamic than under static leach conditions. At the outer surface of the gel and also within the gel, crystalline phases, in particular sheet silicates can grow (Caurel et al. 1990). The composition of these sheet-silicates is constant within the altered layer. The composition of the gel evolves during alteration and is at 150°C similar to the composition of clays (except enrichment in Zr and rare earths). Valle (2000) showed that the sheet silicates have the isotopic signature for Si of the alteration solution. Since the isotopic composition of the gel is also strongly influenced by the solution, the gel is not a residual glass, but a new phase: a reaction product. At 250°C, the formation of the *gel* and *sheet-silicates* are also observed (Caurel et al. 1990). *Analcime* precipitates rapidly. *Smectites* are also observed as well as *zeolites* and *hydrated calcium silicates (tobermorite or gyrolite)*. At this temperature compositions of the gel and of the sheet silicates differ (Crovisier et al. 1992b).

Rare earth elements are strongly retained either on exchangeable interlayer position in the sheet silicates (Bonnot, 1982; Jaffrezic, 1982; Vidal, 1995) or as REE phosphates (Noguès, 1984; Fillet, 1987). After some time, the REE are principally fixed in the gel and not in the phyllosilicates (Gin 2000).

As for solution alteration, vapor phase alteration products of R7T7 glass at 200°C (Gong et al. 1998), are *amorphous gel*, *smectites*, *analcime*, *hydrate calcium silicate phases (tobermorite)*, *wecksite*, but additionally *amorphous silica (opal)*, *apatite*, and *sodium silicate phases* are observed and as in water finally *gyrolite*. Similar phases were observed by Byers et al. (1985) with a defense waste glass. The amorphous layer is composed of two basic structures that are morphologically and chemically distinct.

Numerous studies have shown that basalt glasses are appropriate natural analogues for the long-term significance of alteration products and for surface layer morphology (Malow and Ewing 1981, Grambow et al. 1985, Lutze et al. 1985). After initial ion exchange the dissolution of basalt glass becomes congruent till the appearance of secondary phases, which precipitate. The first compounds to be formed in experiments are *aluminium* and *iron hydroxides* (Crovisier et al. 1989b). Then, when silicon concentration increases in solution, *aluminosilicates* form. Other studies (Byers et al. 1985) allow observing the formation of *clays (vermiculite* at 190°C) at high reaction progress (182 days). In natural weathering, the first phases to form constitute a superficial layer or rind called *palagonite* (Honnorez 1972, 1981). Then, *clays* appear, generally followed by *zeolites* (Honnorez 1981, Byers et al. 1985, Grambow et al. 1985, Crovisier 1989, Crovisier et al. 1992a, Le Gal et al. 1999). The palagonite is similar in morphology to the gel formed with nuclear waste glasses and seems to be

formed by precipitation of mineral species having reached their limit of solubility, following the congruent dissolution of glass.

In the case of a sub-glacial palagonitisation (Iceland), the *palagonite* and *intergranular clayey material* have a similar global chemical composition, indicating chemical equilibria. The *intergranular clays* are *nontronite*, *Fe-saponite* or *smectites*. *Zeolites* (*chabazite*, *erionite*, *phillipsite*, *analcime*) and sometimes, *calcite* and *opaline silica* are also observed (Honnorez 1972, 1981, Grambow *et al.* 1985, Crovisier 1989, Crovisier *et al.* 1992a, Le Gal 1999; Le Gal *et al.* 1999). Vapour phase alteration products are (Byers *et al.* 1985) *analcime*, followed by *gyrolite*, and *montmorillonite*. These results present very good similarities with waste glass alteration (Cf. above).

Modelling

Advocat (1991) has used KINDIS to predict the alteration product sequence of R7T7 glass as follows: *hydroxides of iron, clay, hydroxides of Zn and Mn, laumontite, strontianite, chalcedony, calcite, albite* and *zeolites (epistilbite, dachiarite)*. The chemical composition of clay is predicted to change during alteration. The model predicted a faster appearance of zeolites than observed and the representation of the alteration gel by the solid solution of 6 poles of clays was incorrect. Better agreement between predicted clay composition and experimental observations was obtained by Michaux *et al.* (1992) using a solid solution with 9 poles of 2/1 clays. Additionally to the minerals considered above, Durst (1998) defines another solid solution made up of 10 poles, constituted by pure oxides, to represent the gel (amorphous silica, ThO₂, ZrO(OH), LaPO₄, CePO₄, NdPO₄, AmPO₄, UO₂, NpO₂ and PuO₂). The precipitated compounds are: the *gel*, then *gibbsite, clay, kaolinite, rare earths carbonates* and *AmOCO₃OH, strontianite, cesium oxide* and finally *calcite*. The composition of the gel then evolves with the reaction progress. The results obtained are more in adequacy with the experimental results.

The sequence of precipitation of minerals following the dissolution of basaltic glass has been modelled using GLASSOL by Grambow *et al.* (1985) and DISSOL (Fritz 1975, Fritz 1981, Clément and Madé 1981, Tardy and Fritz 1981, Madé *et al.* 1994) by Crovisier (1989), Crovisier *et al.* (1989a), Crovisier *et al.* (1992a).

The model used by Grambow *et al.* (1985) (basalt glass dissolution at 25°C in deionised water) represents the *palagonite* as *nontronite*. The results show that this compound can precipitate as well as *smectite (Fe-saponite)*, and *zeolites (chabazite and phillipsite)*.

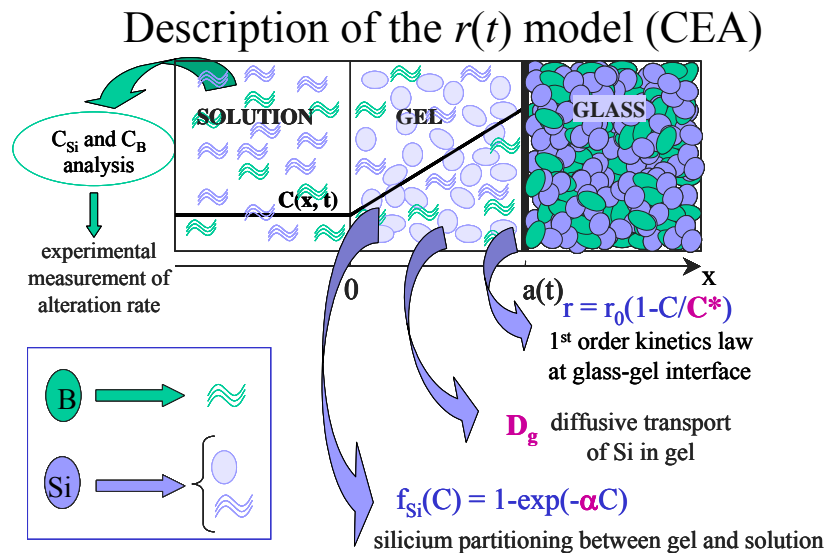
DISSOL (and KINDIS) described the formation of a mixture of T.O.T. clays by a solid solution with 15 poles (Crovisier 1989, Crovisier *et al.* 1989a, Crovisier *et al.* 1992a). The predicted sequence (paragenesis) of phases is *Fe and/or Al hydroxides*, followed by *kaolinite* and *T.O.T. clay minerals*. Then *zeolites (chabazite and clinoptilolite)* form. The evolution of the chemical composition of intergranular clays fits with the observation of altered subglacial basalt glasses from Iceland, especially for the oldest samples.

The accurate match of observations and modelling confirms that the alteration layer remains equilibrated with the chemical variations of the solution, without keeping the memory of the former stages. Nevertheless, in the work of Techer *et al.* (2001) alkali containing secondary phases were predicted to form which are not observed in the experimentally. Thus, many studies have still to be conducted especially to precise the chemical composition of the palagonite in the course of the alteration time.

Some geochemical models allow simulating the kinetic of the glass dissolution (KINDIS, LIXIVER, EQ3/6 and GLASSOL for example) considering precipitation of secondary phases and gel formation. GLASSOL (Grambow 1987) was validated by a large set of experimental data for radioactive and inactive glass SON68 as a function of S/V, temperature, water flow rate in presence or absence of bentonite and iron corrosion products. These modellings are generally in better agreement with experimental results than without mineral precipitation (Bourcier *et al.* 1990). In some cases the precipitation prevents the dissolution rate from dropping to zero irrespective of the progress of the reaction. The final affinity is called “residual affinity” by Grambow (1985) and “contextual affinity” by Advocat *et al.* (1990). Zeolite formation may in some cases even increase the dissolution rate with time.

3.2.1.3 The $r(t)$ model

In this model, the dissolution rate depends on the orthosilicic acid affinity between the glass and the solution (Grambow’s equation). Many assumptions are made by the model (Techer 1999, Techer *et al.* 2000), what leads to the rate equation expressed below (Delage 1992):



with C_v the silicon concentration in the glass, C_{slb} the silicon concentration really released by the glass, C_{int} the silicon concentration at the glass/gel interface and C the silicon concentration in solution

$$r = r_0 \frac{1 - \frac{C}{C^*}}{1 + r_0 \frac{C_{slb} x}{D_g C^*}}$$

with r the dissolution rate, r_0 the initial rate, C the silicon concentration in solution, C^* the total silicon concentration at saturation with respect to the glass, C_{slb} the silicon concentration really released by the glass, x the thickness of the gel layer, and D_g the silicon diffusion coefficient into the gel

The silicon liberated by the glass (C_{slb}) depends on a retention function (f_{Si}) of the silicon in the gel (C_v) and the parameter α :

$$C_{slb} = C_v \cdot (1 - f_{Si}) \text{ and } f_{Si} = 1 - \exp(-\alpha \cdot C)$$

The code LIXIVER (r(t) model) was applied to experimental alteration of basaltic glass (Techer *et al.* 2000) and it was applied to more than 50 experiments with nuclear waste glass performed between 1983 and 2001 for temperatures between 50° and 90°C, pH between 7 and 9, water flow rates between 0 et 1,24 d⁻¹ S/V ratios between 125 and 2000 m⁻¹ (Gin *et al.*, 2001 ; Jégou, 1998 ; Frugier *et al.*, 2001 ; Noguès, 1984 ; Delage, 1992 ; Caurel, 1990 ; Godon, 1988 ; Advocat, 1991 ; Tovina, 1995). The modelling agrees with their experimental results using k₊, D_g, α, and C* as a fitting variables.

LIXIVER does not take into account water diffusion, the real composition and the structure (porosity) of the alteration gel nor the incidence of its composition on the variations of the diffusion coefficient. It is to note that generally the composition of this gel is homogeneous and does not exhibit a gradient other than that of silica. The model is not applicable to cases were silica concentrations in solution are higher than C*.

3.2.1.4 The model GM2001

Grambow and Müller (2001) have modified their initial model (Grambow 1985) by taking into consideration the ionic exchange/water diffusion process and the dissolution of the glassy matrix. Water diffusion is considered both in the short and in the long term. The penetration of water is described by an advection/dispersion/reaction equation, typically used for mass transfer calculation of reactive contaminant transport in porous media:

$$\frac{\delta C_{H_2O,gl}}{\delta t} = D_{H_2O,eff} \frac{\delta^2 C_{H_2O,gl}}{\delta x^2} - U(t) \frac{\delta C_{H_2O,gl}}{\delta x} - k C_{H_2O,gl}$$

with C_{H₂O,gl} the space and time-dependent concentration of free mobile water molecules in the glass, x the distance variable (x = 0 denotes the position of the original glass surface prior to the start of the glass water reaction), D_{H₂O,eff} the effective diffusion coefficient of water molecules in the dray glass, U(t) the time-dependent matrix dissolution rate and k a rate constant describing the potential immobilization of water molecules by the formation of hydroxyl groups attached to the glass network (silanol groups).

The corrosion rate U(t) correspond to all processes which lead to the loss of the glassy state by interaction with water, expressed by the affinity law coupled to the effect of a potentially protective surface gel layer.

In the case of repository conditions the concentration of silicic acid in the groundwater may be considered constant at some distance of dissolving glass surface (m_{Si,CCB}). In that case, constant concentration boundary models (CCB) can be applied, implying a stationary state concentration gradient and thus, the dissolution rate can expresses as:

$$U(T) = \frac{k_+(T)}{\sigma_{glass}} \left(1 - \frac{k_+(T)FS\beta L + \phi D_{Si}(T)m_{Si,CCB}\rho_{sln}}{K_{SiO_2}(T)\phi D_{Si}(T)\rho_{sln} + k_+(T)FS\gamma_{Si}\beta L} \gamma_{Si} \right)$$

with D_{Si} the pore diffusion coefficient of silicic acid in the layer thickness L and porosity ϕ , m_{Si} and $m_{Si,int}$ the molalities of dissolved silica (as H_4SiO_4) in bulk solution and at the glass/solution interface, γ_{Si} the activity coefficient of dissolved silica, β a dimensionless factor characterizing the ratio of total interfacial surface area (including surface roughness) to the cross-sectional surface area perpendicular to mass transport direction, ρ_{sln} the solution density and FS describes the retention of silica in the surface alteration product

The model was then applied to experimental data, using the four parameters (k_+ , K_{SiO_2} , $D_{H_2O,eff}$ and FS) as adaptable in a fit.

Grambow and Müller (2001) have applied this model to the static alteration of nuclear waste borosilicate (WAK glass) at 50°C in deionised water at $S/V = 1000 \text{ cm}^{-1}$ during 100 days. The agreement between the experimental results and the modelling are very good. Furthermore, Grambow and Müller demonstrated that Jégou's results (Jégou 1998), which seemed to refute the first-order rate law, can easily be explained by their model.

3.2.1.5 Conclusions

All of these results help to evaluate the difficulties encountered in the modelling of glass dissolution. Models become more refined; their results more accurate. But numerous progresses have still to be made considering all parameters.

Indeed, the dissolution law depends initially on the affinity between the shortly altered glass (or the gel) and the solution. But rapidly, the dissolution rate depends on the diffusion of elements (mainly silicon) through the gel. The model has thus to render the influence of the gel (influence linked with its thickness, its composition, its porosity...). This rate must take into account the influence of the stability and the solubility of precipitated minerals as well

The literature review has indicated the following shortcomings in existing models, which have been addressed in the GLASTAB project by model development:

- a still still ambiguous understanding of gel formation by condensation and hydrolysis of glass network bonds. Understanding shall be improved by Monte Carlo modelling
- a still inaccurate description of the thermodynamic constraints governing the formation of the gel layer. This has been improved in GLASTAB by solid solution modelling
- an inaccurate description of the effect of porosity evolution on glass dissolution kinetics. This problem has been addressed by either applying the code KIRMAT to glass dissolution or by development of a new code.
- A better overall representation of the glass water reaction scheme.

3.2.2 **MONTE-CARLO MODELLING OF INITIAL GLASS DISSOLUTION REACTION/PORE STRUCTURE, SATURATION AND GEL FORMATION**

3.2.2.1 Visualisation of the pore structure

In experiments, after silica saturation is reached, the leaching of soluble elements goes on. For better understanding this phenomenon, it is interesting to have information about the path by which these elements leach out of the glass. On real glasses, this is

hard to obtain but on molecular simulations like Monte Carlo, this is possible. Therefore, routines have been written in which the particle configuration during the simulations is written regularly down into files. Afterwards these files can be read by the molecular visualisation programme Xmole.

3.2.2.2 Comparison of SCK and CEA versions

In this text, we will only compare the versions of SCK and CEA programmes at the beginning and at the end of the GLASTAB project.

Comparing two Monte Carlo (MC) programmes means comparing the different parts of these programmes. Therefore, we first briefly explain where a Monte Carlo method consists of. Then we will compare each of the different parts as well as the results of the simulations.

A Monte Carlo method starts from an initial configuration. The method consists of repeating the generation (according to some rules) of a 'new' configuration from an 'old' configuration. Once a new configuration is generated (and accepted), it becomes the 'old' configuration for the next generation. For being meaningful from a physical point of view, this sequence of configurations should evolve to thermo-dynamic equilibrium. This is assured by the detailed balance condition:

$$\frac{P(A \rightarrow B)}{P(B \rightarrow A)} = \exp\left(-\frac{E(B) - E(A)}{k_B T}\right)$$

with:

$P(A \rightarrow B)$ the probability to move from state (configuration) A to state B ,

$P(B \rightarrow A)$ the probability to move from state (configuration) B to state A ,

$E(A)$, $E(B)$ the potential energy in the respective states,

k_B the Boltzmann constant,

T absolute temperature.

A standard algorithm of generating new states according to some probability is:

- (1) generate at random a trial configuration from the present configuration,
- (2) calculate the transition probability P from the present to the trial configuration,
- (3) generate a random number R ,
- (4) if $P > R$, accept the trial configuration, else reject the trial configuration
- (5) return to (1)

Alternatives to this algorithm exist.

SCK and CEA start from a similar initial configuration: a 'glass' volume next a to a water volume. The glass is a random configuration of (1) strongly attractive particles (which we call here 'silica'), and (2) particles with weak (approximately zero) bond strength (which we call 'sodium'). Both CEA and SCK now have a programme version allowing three glass components: two types of strongly attractive particles ('silica') and a weakly bonded particle ('sodium'). In both SCK and CEA models, the glass/water surface is initially flat. In the SCK model, all particles move on a

diamond lattice (hence a coordination number of four). At the start of GLASTAB, in the CEA programme the particles were on a cubic lattice (hence the coordination number is six). During GLASTAB, CEA developed a MC programme (which we call CEA-4) on a lattice with coordination number four. For simulating secondary phase formation, SCK developed a programme version allowing a different attraction between precipitated silica and ‘glass silica’.

The initial configuration is not the lowest energy configuration. Depending on the value of

$$J = \left| \frac{\Delta E}{k_B T} \right|$$

(with ΔE the energy of a Si-O-Si bond), the lowest free energy configuration corresponds to a phase-separated system or not. Since glass is a solid, it seems logical to perform only simulations at sufficiently large J values, where phase separation occurs naturally.

What are the common parameters in the CEA and SCK programmes? First, there is the fraction of ‘silica’ in the glass. Second, there is the parameter J , which in a phase-separated system determines (partly in the CEA simulations) the silica solubility. Third, there is also a parameter characterizing the initial silica dissolution rate. Besides, the MC programmes of both institutes also have specific parameters. SCK considers silica diffusion and sodium dissolution. Each of these processes is described by an additional parameter. CEA introduces a parameter E_0 that is called stabilization energy. This parameter is defined by expressing the energy difference between a silica particle in solution and a silica particle in the solid as $E(n) = E_0 + n \Delta E$ with n the number of Si-O-Si bonds in the solid and ΔE the energy of a Si-O-Si bond. In the simulations of SCK, the parameter E_0 is always zero. Apart from differences between the SCK and CEA programmes, there are also differences between the CEA programme at the start of GLASTAB (on a lattice with a coordination number of six) and CEA-4. In CEA-4, instead of the parameter J , three dissolution probabilities and one condensation probability are used. The stabilization energy E_0 is not used anymore either.

The MC programmes of SCK and CEA also differ in the way they are implemented. Detailed balance assures that both programmes should evolve to the same equilibrium state, but it remains silent about most features like e.g. kinetics. CEA uses a kind of Kawasaki dynamics. SCK tries to make silica particles dissolve according to the silica dissolution mechanism proposed by Dove. Other features are: what to do with finite dissolved clusters? Should they remain in the system (SCK), or should they be taken out of the system (CEA)? If yes, what can be considered as a finite dissolved cluster? Should one adapt the time when taking out of the system a finite dissolved cluster? How is time defined? ...

Due to these differences it does not make much sense to compare the present simulation results of SCK and CEA in a quantitative way. Qualitative comparisons are possible, and here both programmes provide similar results. They both show for dynamic tests (simulation tests of course) an increase of the dissolution rate over several orders of magnitude when varying the sodium content of a glass. In static (simulation) tests, the system evolves in both programmes to a stationary state, where the silica solubility is approximately independent on the fraction of sodium in the (pristine) glass. SCK finds that the silica solubility is proportional to $\exp(-2J)$; CEA

does not report results on this matter. SCK observes for static tests that in the evolution towards silica saturation, the instantaneous silica concentration in solution can be higher than the final silica solubility. Although not explicitly mentioned, this seems also the case with some CEA-4 simulations.

3.2.2.3 Conclusions

Monte Carlo models are able to reproduce quantitatively the experimentally observed short term leaching phenomenology for simple glasses: the initial congruent leaching, the formation of gel, of gel cross-link density and a porosity representation, saturation of Si, interpreted by porosity blocking, reduction of release rates of B, Na well after saturation of Si, but related to saturation of Si. Efforts have still to be made on altered layer morphology prediction, on the application of MC to more complex glasses, on the long-term evolution of the gel and long-term dissolution of glass constituents and on the distinction between transport processes for dissolved species (Si) and of reactants (H₂O) in the layer.

3.2.3 **THERMODYNAMIC MODELLING OF GEL FORMATION BY SOLID SOLUTION FORMATION**

The influence of the gel layer on glass dissolution has been taken into account in affinity models. These models were applied only on short-term dissolution and without considering neither the incidence of the gel formation on the chemical composition of the solution nor the incidence of the formation of other secondary products on the dissolution process. The aim of the present study is to simulate the dissolution of glass with the geochemical model KINDIS by taking into account the incidence of the formation of the alteration gel on the chemical composition of the solution.

3.2.3.1 Experimental procedure and results

The two simplified glasses (*glass 1*: Si-Al-B-Na and *glass 2*: Si-Al-B-Na-Ca-Zr) have a chemical composition corresponding to the elemental molar ratios of the French SON68 nuclear glass. Their chemical composition is given in Table 1. The static alteration experiments were performed in pure water at 90 °C (± 1 °C) with two surface area of glass/volume of solution (S/V) ratios: 1 cm⁻¹ and 80 cm⁻¹.

Molar %	B ₂ O ₃	Al ₂ O ₃	SiO ₂	Na ₂ SiO ₃	CaSiO ₃	ZrSiO ₄
Glass 1	0.2003	0.0478	0.5939	0.1580	-	-
Glass 2	0.2003	0.0478	0.5093	0.1579	0.0714	0.0133

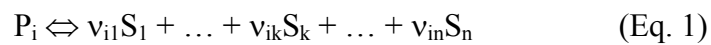
Table 1: Nominal composition of the two studied glasses in % molar oxides meta-silicates

Experimental results showed that the concentrations of boron and sodium increased regularly in solution. The pH values stabilised after 60 days around 9, probably due to the buffer effect of boron. Silicon and aluminium concentrations presented similar behaviours according to the S/V ratio: they increased and then stabilized after 60-90 days. The final dissolution rate of the glasses after 180 days was between 0.03 and 0.001 g/m²d as observed similarly by Jégou C. (1998). The chemical composition of the alteration gel was estimated by three different methods: direct analysis with ASEM and ASTEM, and calculation from solutions composition. The estimation of the gel composition from the analyses of solutions composition assumes that all the boron has been totally released in solution. From this hypothesis, the gel composition has been deduced by the difference between the effective elements release in solution and what this release would have been by the complete glass destruction, for the same boron release. These experimental results were used as a base for comparison to modelling prediction.

3.2.3.2 Solid solution simulation

The simulation of the dissolution of the two simplified glasses was performed by using the geochemical code KINDIS [Made et al. 1990, 1994a, 1994b]. Two kinetic affinity based rate laws were used by the model, one in which only the orthosilicic acid affinity in solution is considered the other for the global affinity model, in which the overall affinity of the glass is considered.

If we consider the equilibrium condition between the end-member P_i and the solution (case of an ideal solid solution) (Eq. 1), its solubility product K_i and its molar fraction x_i express as following (Eq. 1 and 2):



$$K_i = \frac{Q_i}{A_i} = \frac{\prod_k a_k^{v_{ik}}}{x_i} \quad (\text{Eq. 2})$$

with K_i the thermodynamic solubility product of the end-member P_i, Q_i the ionic activity product of the end-member P_i, and a_k the activity of the specie S_k in solution

The sum of the molar fractions of the end-members of the solid solution is equal to unity (ideal solid solution) (Eq. 3):

$$\sum_{i=1}^{i=p} x_i = \sum_{i=1}^{i=p} \frac{Q_i}{K_i} = 1 \quad (\text{Eq. 3})$$

This last relation implies that the end-members are in equilibrium with the solution while their molar fraction is lower than 1. This state of saturation is then greatly different from what it is in the case of a pure end-member (where $x_i = 1$). When considering the solid solution formation, KINDIS model calculates all the Q_i/K_i ratios and their sum. When the sum of the Q_i/K_i ratios reaches the unity, the solid solution precipitates. The composition of the solid solution ensues then directly from the Q_i/K_i ratios. Three types of solid solution, having oxides, hydroxides or metasilicates as end-members, were tested (Table 2). Additionally, three different siliceous end-members were considered: quartz, chalcedony and amorphous silica. The thermodynamic parameters are given in appendix 1.

	Glass 1			Glass 2				
	Si	Al	Na	Si	Al	Na	Ca	Zr
Oxides	SiO ₂	Al ₂ O ₃	Na ₂ O	SiO ₂	Al ₂ O ₃	Na ₂ O	CaO	ZrO ₂
Hydrox.	SiO ₂	Al(OH) ₃	NaOH	SiO ₂	Al(OH) ₃	NaOH	Ca(OH) ₂	Zr(OH) ₄
Meta.	SiO ₂	Al ₂ O ₃	Na ₂ SiO ₃	SiO ₂	Al ₂ O ₃	Na ₂ SiO ₃	CaSiO ₃	ZrSiO ₄

Table 2: End-members of the solid solutions considered in simulation (SiO₂: amorphous silica, chalcedony or quartz).

3.2.3.3 Application of the model

Simulation of silicon content in solution

When considering the affinity of the glass dissolution reaction, silicon concentration in solution is determined by the amount of dissolved glass and by the formation of silicated secondary products, having reached their solubility limit. The thermodynamic stability of these products may thus have a great influence on silicon concentration in solution.

In order to quantify the incidence of the thermodynamic stability of siliceous secondary products, three different siliceous end-members constituting the solid solution representing the alteration gel have been tested: amorphous silica (the less thermodynamically stable), quartz (the most stable) and chalcedony (of medium stability), for both glasses considered. The other end-members are constituted by hydroxides (Table 2), whose solubility constants were reported in Table 3. The experimental values were represented by empty marks. On this Fig. 1, the reaction progress corresponds to boron concentration in solution, since it increases with the alteration time without being reincorporated in secondary products.

For the simplest glass, silicon concentration in solution stabilized close to the curve simulated with quartz when the S/V ratio is small whereas, at high S/V ratio, it stabilized above chalcedony curve. The alteration of the glass 2, which has a more complex composition, led to silicon concentration close to but slightly higher than the one obtained with chalcedony simulation, whatever the S/V ratio.

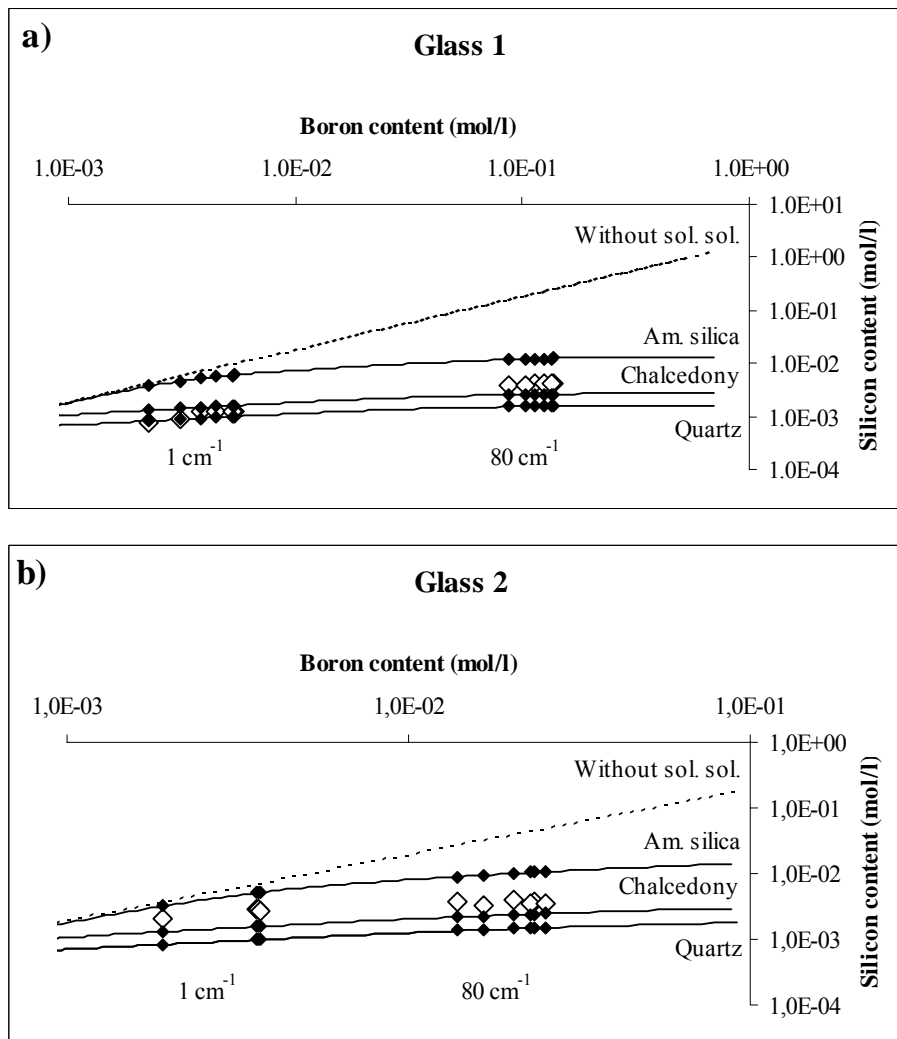


Figure 1: Silicon content versus boron content in solution (mol/l). Experimental values (empty mark) and simulated values (solid mark) with a solid solution having amorphous silica, chalcedony or quartz as siliceous end-member and hydroxides as other end-members (a): glass 1 and b): glass 2).

On Figure 1 were also reported simulated curves obtained considering that no silica containing phase can form and which thus correspond only to the increase of silicon concentration in solution due to glass dissolution. The agreement between experiments and simulation justifies the description of the alteration gel in simulation by considering a total dissolution process followed by an in situ precipitation of the gel at equilibrium with the solution. The good results obtained by using chalcedony as siliceous end-member led to use it in subsequent simulations.

Simulation of gel global composition

Simulated compositions of the alteration gel layer are plotted in Figure 2 (% oxide weight). At low S/V ratio, the composition of the gel varies a little with the reaction progress whereas at high S/V ratio the composition remains constant with increasing reaction progress, whatever the glass considered. The mean compositions of the gel layers are reported in Table 7.

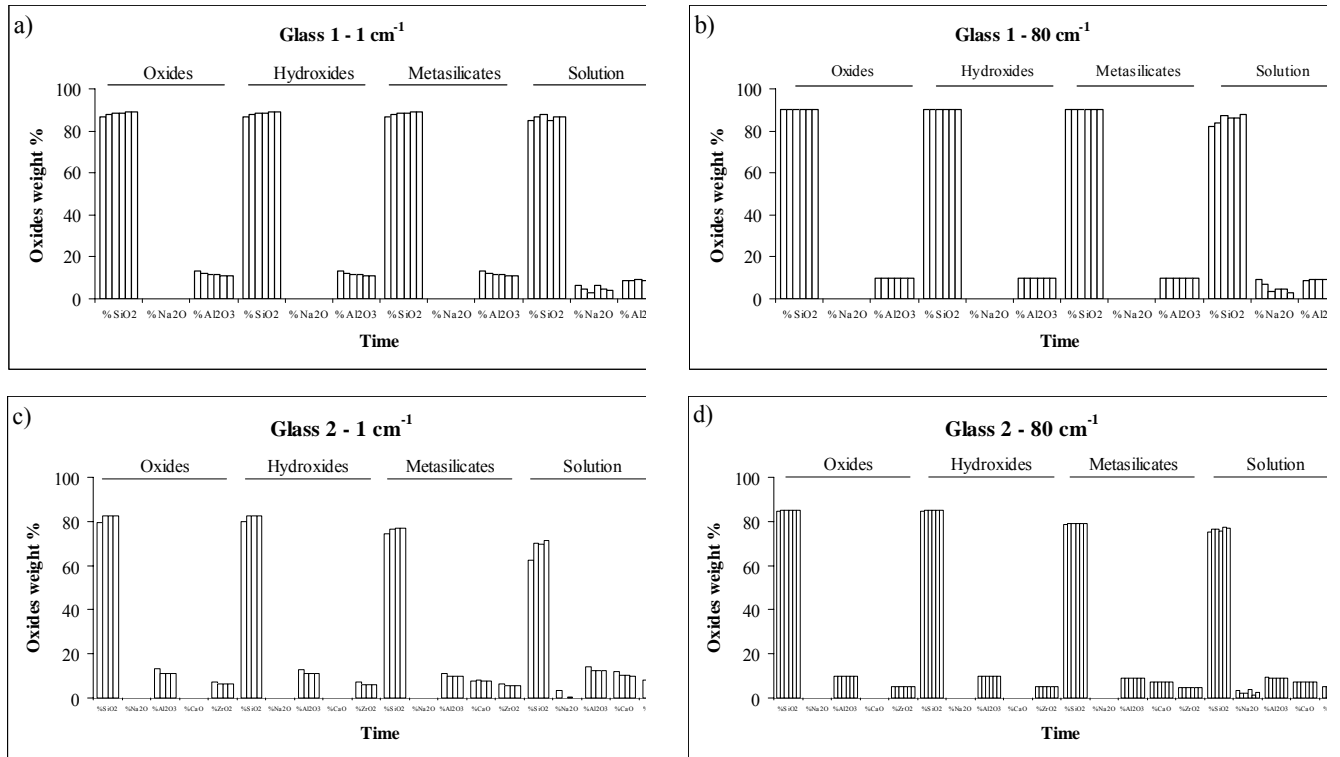


Figure 2: Composition of the simulated and deduced from solution alteration gel (% oxide weight) according to the choice of end-members (oxides, hydroxides, meta-silicates) and the alteration time (from left to right: 30, 60, 90, 120, 150 and 180 days, except for glass 2 at 1 cm⁻¹: 30, 60, 90 and 180 days) (a and b: glass 1, c and d: glass 2).

For the glass 1, the mean composition is very similar for the same S/V ratio whatever the end-members used. The gel composition varies slightly with to the S/V ratio and at high S/V ratio the gel is enriched in silicon and impoverished in aluminium. The effect of end member choice is larger for glass 2. The simulated gel layer composition varies also with S/V ratio as it is the case experimentally. The gel layer is slightly enriched in silicon with increasing S/V ratio and impoverished in aluminium and zirconium as it is observed from experimental solution data.

On the whole, the results obtained by KINDIS model for the calculation of the gel layer composition reflects the main tendencies obtained for the gel layer formed during experiments. Very good agreement is obtained for silicon (80 %), aluminium (99 %) and zirconium (99.9 %), especially at 80 cm⁻¹. The simulation of calcium content is impressive when meta-silicates are used. The main discrepancy between the experimental and the simulated composition of the alteration layer concern essentially to the sodic end-members. The high solubility of sodic end-members considered in this study (Table 3) does not allow their incorporation into the solid solution.

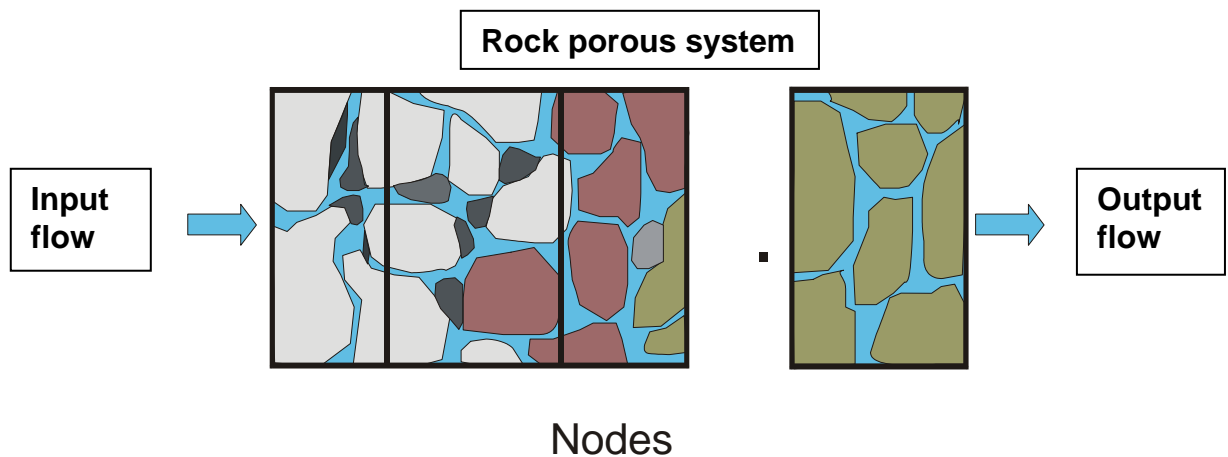
The presence of sodium in alteration gel layer of nuclear glass has been reported in literature (Ricol 1995, Zarembowitch-Déruelle O. 1997). These authors explained the observed Na content by the structure of the gel. Indeed, in the alteration gel layer, Al atoms are likely to have a four-fold coordination (AlO₄⁻) and Zr atoms a six-fold coordination (ZrO₆²⁻) (Ricol 1995). This structure involves excess of charges and thus requires the presence of compensators for the charge balance such as alkaline and alkaline earth elements.

3.2.3.4 Conclusion

The experiments show that the gels formed do not consist of identifiable minerals but amorphous products, not very porous and not easily distinguishable from glass except from their composition. The good agreement observed between simulated and experimental gel layer composition especially for sparingly soluble elements indicates that the hypothesis of a thermodynamic equilibrium of solid solution representation of the gel with the solution is adequate to predict the gel composition. However, a better knowledge of the structures of the gels is certainly necessary, as it allows (a) to refine the model by taking into account notably the structure of the gel (i.e. Na/Al charge balance as it has been done for clays by Fritz (1981) and Tardy and Fritz (1981) and its reticulation process and (b) to predict porosity evolution, necessary to assess transport processes in the gel.

3.2.4 MODELLING OF POROSITY EVOLUTION WITH KIRMAT

The GM2001 model (see review above) uses a diffusion advection equation to describe the coupling of water diffusion/alkali ion exchange and affinity/gel mass transfer controlled glass matrix dissolution, but it does not account for geochemical constraints. This makes it promising to use a coupled geochemical/transport code to simulate the glass water reaction. Such codes typically use as well the diffusion/advection equation, however on macro scale (meters to km) rather than on the nano scale required for glass dissolution simulation. In the GLASTAB project we used the code KIRMAT to simulate glass dissolution. It is a reactive transport or hydro chemical code. The mass transport phenomena through the total connected porosity of a water-saturated porous medium are solved over one spatial dimension (1D).



An explicit or forward time scheme is computed, using the finite difference method to model all the hydrodynamic conditions from the pure advection to pure diffusion. The code is able to quantify the reactive mass transport through a double porosity medium in which the flow porosity (filled with free water) and the diffusion porosity (filled with stagnant water) are considered as two distinct sub mediums. The thermo-kinetic hydro chemical code KIRMAT has been developed from the single reaction path model KINDIS by keeping all its geochemical formulation and its numerical method to solve chemical equations. Solute transport is added to kinetic dissolution and/or

precipitation reactions. The solid solution model developed for KINDIS could as well be applied to KIRMAT. The explicit finite difference scheme requires the maximum time step to be limited by convergence criteria:

3.2.4.1 Mathematical description

Given the following symbols:

- $\overline{\overline{D}}$: hydrodynamic dispersion tensor ($L^2 T^{-1}$)
- D^*_L : coefficient of longitudinal hydrodynamical dispersion ($m^2 T^{-1}$)
- D : coefficient of effective diffusion ($m^2 T^{-1}$)
- m_e : molality of element e (moles per kg H_2O^{-1})
- N_k : set of minerals controlled by the local equilibrium
- N_m : set of minerals controlled by kinetic reactions
- U : Darcy velocity (LT^{-1})
- V_k : molar volume of mineral k ($m^3 T^{-1}$)
- α_L : coefficient of longitudinal dispersivity
- α_{jk} : number of moles of j in mineral k
- Ξ_m : rate of precipitation or dissolution of mineral m per unit of the rock and fluid system
- ϕ'_k : volume fraction of mineral k per volume unit of fluid
- ϕ_g^ω : geochemical flow per unit of total rock volume ($mole L^{-3} T^{-1}$).
- ψ_j total concentration (in mole per water mass or volume) of the j primary aqueous species
- ω flow porosity of the rock control volume

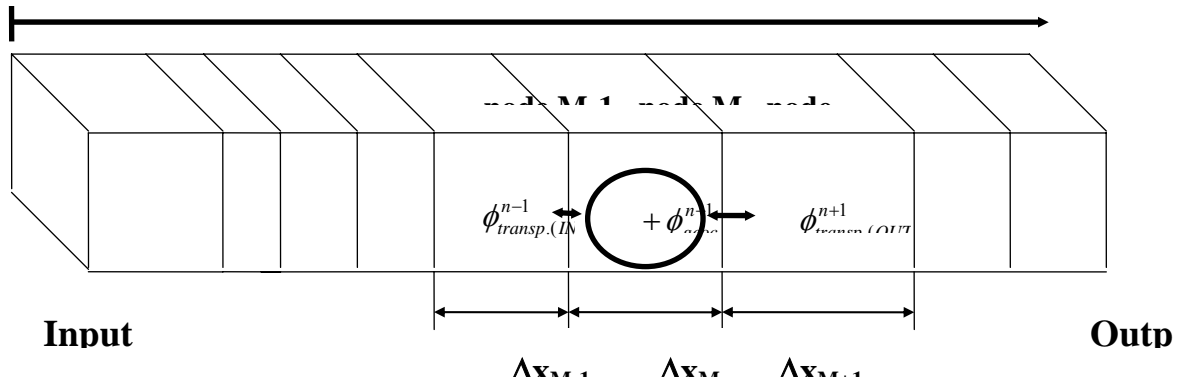
The system to be solved is:

$$\omega \frac{\partial \psi_j}{\partial t} = \text{div}(\overline{\overline{D}} * \overrightarrow{\text{grad}} \psi_j - \psi_j \overrightarrow{U}) + \phi_{g_j}^\omega$$

Rewriting the geochemical flow $\phi_{g_j}^\omega$ in the form of a partial differential in dimension x leads to:

$$\omega \frac{\partial}{\partial t} \left[\psi_j + \sum_{k=1}^{N_k} \alpha_{jk} (V_k)^{-1} \phi'_k \right] = D^*_L \frac{\partial^2 \psi_j}{\partial x^2} - U \frac{\partial \psi_j}{\partial x} + \sum_{m=1}^{N_m} \alpha_{jm} \frac{\partial \Xi_m}{\partial t}$$

At each node we have the following accumulation model:



At time t , accumulation ($\Delta m_e / \Delta t$) in the solution contained in the node M is given by:

$$\frac{\Delta m_e}{\Delta t} = \phi_{transp.(IN)}^{n-1} - \phi_{transp.(OUT)}^{n-1} + \phi_{geoch.}^{n-1}$$

where e represents a chemical element in the solution.

The partial differential equations (see above) are then approximated by finite differences.

3.2.4.2 Code modifications

Originally KIRMAT was designed to simulate a porous medium saturated with a given initial solution. That scheme cannot be used in the case of a glass with a very small porosity. Therefore the code was modified in the following way:

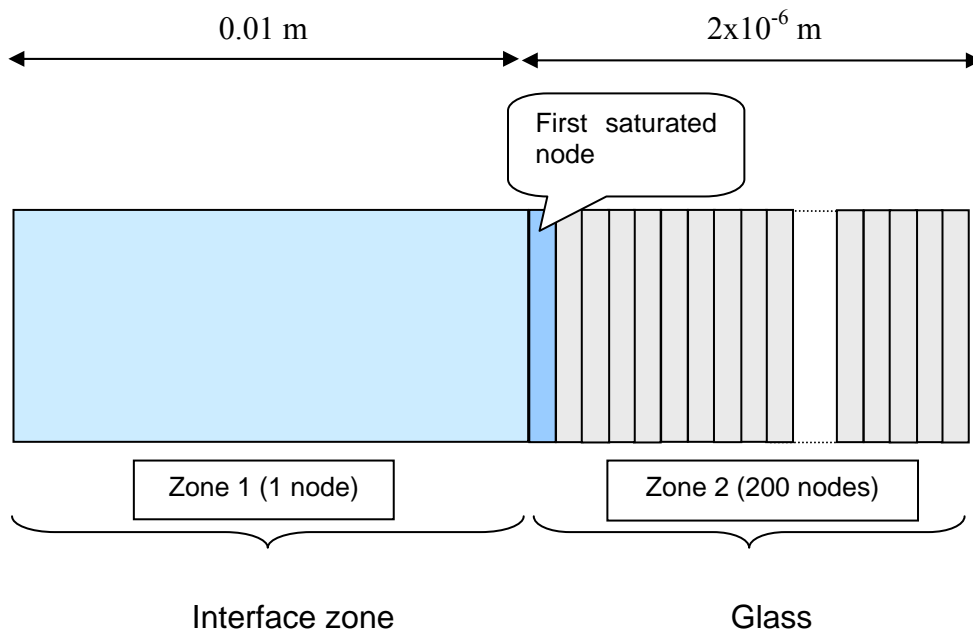
- The user specifies the n first nodes of the system that are to be considered as saturated with an initial given solution. The other $N-n$ nodes are inactive.

At the beginning of a new Δt step, a new node i is considered saturated if:

$(U \cdot \Delta t) + L(init) \geq L(i)$, where $L(i)$ represents the length of the system including node i , $L(init)$ is the initial length of the saturated zone and U is the Darcy's rate.

- Then the new active node is initialized:
 - Total concentrations are equal to that of node $i-1$
 - Aqueous species concentrations are computed by calling the initial equilibrium module and the saturation indexes of minerals and kinetic rates are calculated
 - After node i , a null dispersive flow boundary condition is fixed (Neumann's condition) i.e. as if node i was the end of the system
- After which the new node is included in the common set of active nodes and the process resumes.

3.2.4.3 Description of the simulated system for GLASTAB



The first zone contains one node with a length of 0.01 m. The second zone contains 200 nodes, each node of length 10^{-8} m. Initially only the first zone and the first node of the second zone are saturated with an aqueous solution. The data used for the simulation are:

Transport coefficients:

Parameter	Zone 1	Zone 2
Porosity	0.9	0.01
Permeability (m^2)	10^{-9}	10^{-11}
Coef. of diffusion ($m^2/year$)	0.0315	10^{-15}
Dispersivity (m)	0.01	10^{-8}
Factor of cementation	2	2
Darcy's rate (m/year)	3×10^{-8}	3×10^{-8}

Physical and chemical parameters:

Parameter	Zone 1	Zone 2
Temperature (°C)	90	90
pH	5.9	5.9
pCO ₂	3.02x10 ⁻⁴	1.8x10 ⁻⁵
Total concentrations (moles/kg H ₂ O)		
Al	10 ⁻¹¹	10 ⁻¹¹
Na	10 ⁻⁷	10 ⁻⁷
Ca	10 ⁻¹⁰	10 ⁻¹⁰
Zr	10 ⁻¹³	10 ⁻¹³
B	10 ⁻¹¹	10 ⁻¹¹
Si	10 ⁻¹⁰	10 ⁻¹⁰
C	10 ⁻¹⁰	5x10 ⁻⁷
Cl	10 ⁻¹⁰	10 ⁻¹⁰

Mineralogical composition:

Mineral	Zone 2			
	Molar fraction	Molar volume	Surface reaction (m ²)	Kinetic constant (neutral k ₀)
SiO ₂	.51	22.69	7.93x10 ⁻⁶	0.01
B ₂ O ₃	.2	27.26	3.75x10 ⁻⁶	1.
Al ₂ O ₃	.05	25.58	8.39x10 ⁻⁷	0.01
Na ₂ SiO ₃	.16	128.49	1.39x10 ⁻⁵	1.
CaSiO ₃	.07	39.94	1.96x10 ⁻⁶	0.01
ZrSiO ₄	.01	176.11	1.61x10 ⁻⁶	0.01

Zone 1 contains a single mineral, SiO₂, which can be considered as inactive. It is used as basis for the solid matrix of zone 1.

3.2.4.4 First results

Using the previous parameters, several tests have been made under the assumption that no feed back effects on porosity, permeability, coefficient of diffusion and reaction surfaces of minerals are taken into account.

The results show that after a period of 1 year, the global composition of the solid solution is: Al_{1.001}Si_{1.999}Zr_{0.979}O_{3.96}H_{0.002}. ZrSiO₄ reached the saturation and stopped its dissolution in the nodes representing the glass. Several processes have been tested: formation of the solid solution outside the glass zone, transport of dissolved elements from the glass in the first zone, progression of the solution into the glass. These results show that the code should be able to represent some of the experimental data and could give some indications on the evolution of the leached glass.

A major problem encountered in the simulation tests is the relative low progression in time at given transport parameters, particularly if the overall feed-back of porosity

change, mineral surface area change, permeability change, mass balance at interface of very small and very large cells are to be taken into account. The Δt values are limited by the convergence criteria. Obviously, respecting the convergence criteria has a counterpart: given these conditions, the number of increments needed by KIRMAT to simulate one year of reaction would be 10^7 . The corresponding computer time would be approximately 100 hours on a middle range station (Sun Ultra 10).

Another explanation of the small time paths sometimes used by the code lies with the concentrations of some aqueous species. KIRMAT chooses a Δt that is inversely proportional to the largest of the first derivative variations among all the solute concentrations. It could happen that the concentrations of some complexes species become very low and determine Δt despite the fact that they have little influence in the simulated system.

3.2.5 MODELLING OF POROSITY EVOLUTION BY A PARTICLE TRACKING MODEL

A three dimensional glass dissolution model (RW3D) has been developed based on "particle tracking" and "random walk" mechanism. The glass is considered as a porous medium. The various glass constituents and the water molecules are represented by individual particles with different diffusivities. The particles are exposed to convective movements and to stochastic fluctuations in three dimensions, which account for the dispersion of particle speeds in a porous medium.

The successive position of a given particle in space (coordinates X, Y, Z) and time $t+\Delta t$ is given by the equations

$$\begin{aligned} X(t+\Delta t) &= X(t) + U\Delta t + Z_1 (6D_m\Delta t)^{1/2} \\ Y(t+\Delta t) &= Y(t) + Z_2(6D_m\Delta t)^{1/2} \\ Z(t+\Delta t) &= Z(t) + Z_3(6D_m\Delta t)^{1/2} \end{aligned}$$

where D_m is the molecular diffusion coefficient, and U is the advective water flow rate. Z_1 , Z_2 and Z_3 are uniformly distributed random numbers in the range between -1 and $+1$.

The evolution with the number of iterations n of the propability density function of the positions X and Y of a given partilce is given in Figure 2.

Two model versions were developed: a microscopic and a macroscopic model. Both variants use the same stochastic approach for the mobility of glass constituents but they differ in the chemical representation of glass dissolution. In the model an irreversible exchange between water particles and glass particles is considered. Each diffusing particle has the following characteristics: size, diffusion coefficient, and a term for concentration, indicating which quantity of atoms is fixed on a given water particle. The microscopic model accounts for the three dimensional atomic structure of the glass, using as simplification an orthorhombic structure. The distribution of atoms onto the glass structure is given by the glass composition. For simplicity the composition $\text{Na}_2\text{O}(\text{SiO}_2)_5\text{Fe}_2\text{O}_3$ was used. The distribution of atoms in the glass network was made by a stochastic procedure. This simplification does not take chemical interactions between the atoms of the glass network into account. An example for the glass structure network is given in Figure 3:

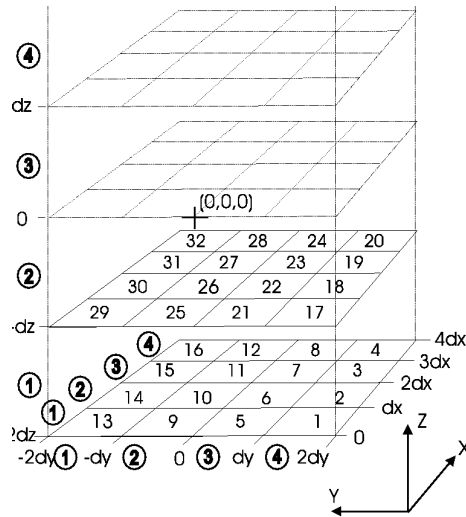


Figure 3: Example of the build-up of a three-dimensional glass network

The macroscopic model considers the glass as a structureless porous medium. The glass structure is not anymore described as a network of atoms but the glass phase is considered as a porous medium of the dimension of micrometers. Chemical reactions with the glass phase are considered by a Langmuir isotherm.

For a simple binary alkali silicate glass the calculated porosity evolution and the corresponding surface concentration profiles for of the outer surface are given in figure 4 as a function of time.

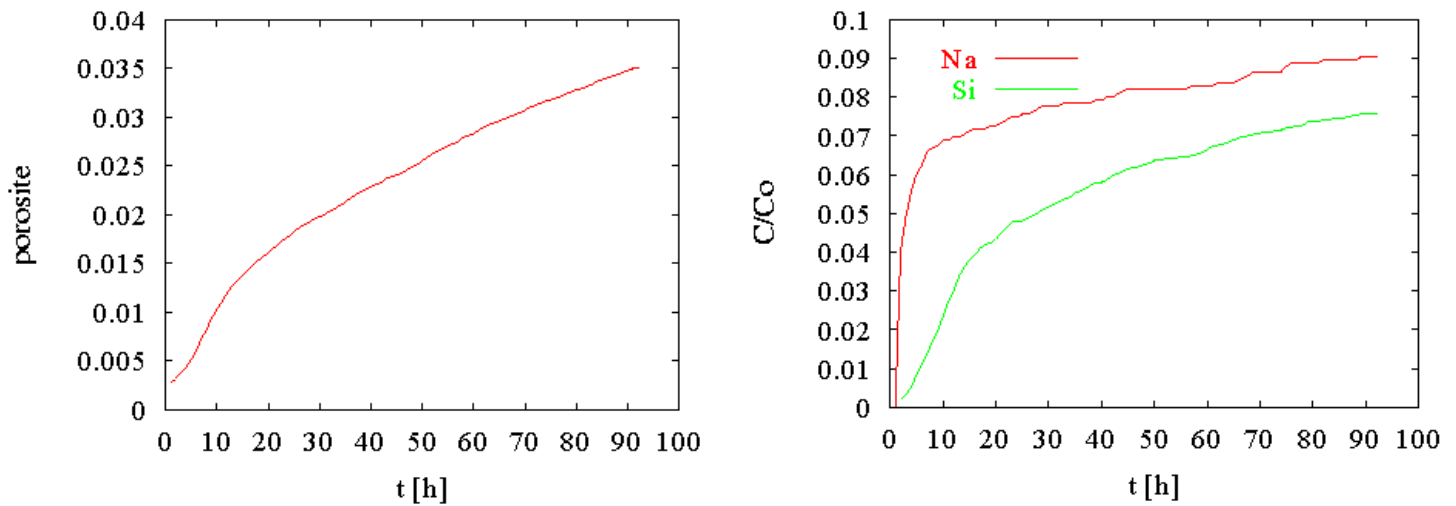


Figure 4: Porosity evolution and concentration profiles at the surface of a binary alkali silicate glass

An application of the code RW3D to experimental data of N. Valle, Thèse 2000 is given in figure 5. The concentration profile of Na in SON68 glass is calculated for 3 month. The fit of the experimental data was done with an apparent diffusion water coefficient of $3.85 \cdot 10^{-19} \text{ m}^2/\text{s}$.

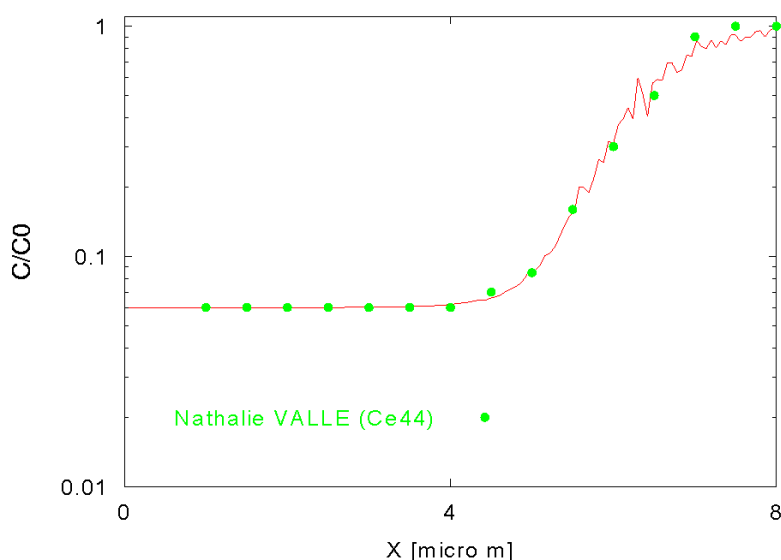


Figure 5: Modelling of concentration profile of Na after 3 month at the surface of SON68 glass and comparison to measured profiles (PhD thesis of N. Vallé)

3.2.6 PARAMETERISATION OF OVERALL KINETIC REACTION SCHEME FOR GLASS DISSOLUTION

The modelling of the overall reaction scheme of glass dissolution is based on the literature review and on the model development provided in this project. The current understanding is sufficient developed to provide a quantitative semi-empirical description of the evolution of reaction rates with time. The overall reaction scheme accounts for the following processes: initial ion-exchange/interdiffusion, hydrolysis of the glass network and release of glass constituents, reduction of release rates either by saturation in solution or by protective gel layer formation and continued long-term corrosion driven by resumption of water diffusion and may be of secondary phase formation. Glass dissolution leads to surface alteration. The following steps can be distinguished: (1) formation an alkali-depleted hydrated glass surface region of few nm, (2) retention of oxyhydrates of sparingly soluble metal ions such as Fe or Al including retention of a small fraction of Si, (3) formation of a gel by increased Si retention, hydrolysis and condensation of silanol groups, and decrease of reaction rate (4) Stabilisation of gel close to saturation, with rates of Si transport in the gel close to zero, (5) continuing water diffusion/ion exchange forming a hydrated glass. There may be a transformation of hydrated glass to gel, if solubility of water in glass is exceeded. The differentiation between the gel and the hydrated glass is of conceptual nature: if water and glass form a solid solution, it is a hydrated glass, if water filled pores are formed, one may speak of the gel. Analytically it is often difficult to distinguish between these two forms of altered glass surfaces.

There is general consensus that the mathematical description of the overall reaction can be realised by a combination of silica transport in a growing gel to a rate law, which is formally similar to a first order rate law. While the present project provides clear evidence for water diffusion and alkali-ion exchange as a long-term relevant

process, due to its low rate and the fast decrease with time, water diffusion is probably not a process of importance for long-term prediction, but it is a critical process, which needs to be taken into account when using experimental data for the paramétrisation of glass corrosion models used for performance predictions. Since water diffusion until now is only included in one of the kinetic reaction scheme models (GM2001), it is clear that there exist still large uncertainties in the paramétrisation of the models. Nevertheless, there is general agreement of the principal parameters to consider.

The important parameters to quantify this rate law are the forward rate of reaction, k_+ , the silica retention factor f_{si} for the gel, the diffusion coefficient D_g of dissolved silica in gel, an (empirical or thermodynamically justified) stability constant for Si-saturation in solution C^* and a long-term rate r_{fin} .

These parameters are sufficient to derive a conceptual model. An assessment of model uncertainties related to different paramétrisation approaches is outside of the scope of the GLASTAB project. It is subject of the concerted action GLAMOR, which assesses as well the significance of saturation constant in first order law and the parameterisation of long-term Si-diffusion in the transition to final rate.

The forward-rate constant k_+ depends primary on pH and on temperature (Figure 6). This dependency is very well known. Activation energies E_a for nuclear waste and basaltic glass are similar. The choice in the numerical value constant is only of low significance for glass performance assessment for European repository concepts, if static conditions can be assured, but it may be of importance in the case of presence of large quantities of clay accelerating glass corrosion rates until the forward rate is reached.

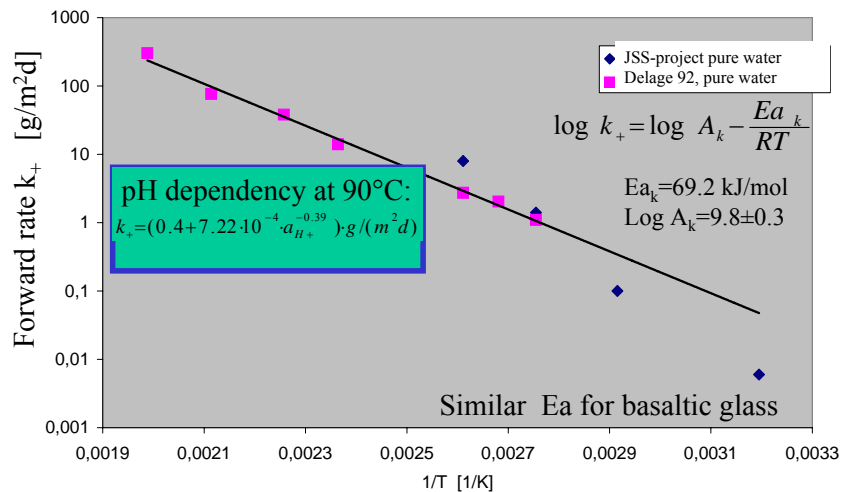


Figure 6. pH and temperature dependency of the forward-rate constant k_+ .

The second parameter, the saturation constant for Si, C^* controls the rate of hydrolysis at the glass-gel interface. As discussed in the literature review, there is a long history about C^* : recently it is considered in the $r(t)$ model only a fitting parameter but it is in GM2001 and most other cases considered as a thermo-dynamical constant controlling an equilibrium between the glass surface and the solution but this does not imply that this intrinsic glass parameter, since glass surface composition is not constant with time. For a large series of tests performed in the last 20 years at 90°C in pure water, Figure 7 gives the experimentally measured Si concentrations,

both in units normalised to the Si inventory in the glass and in units of molality, and a comparison of these data with the normalised concentration of boron in solution. All data are expressed as a function of “normalised time” which here is the product of the S/V ratio and time. The data are of different sources obtained for a very large range of S/V values between 10 and 500000 m⁻¹ are coherent: for normalised times shorter than about 100 d/m corrosion rates are governed by the forward rate and congruent leaching of B and Si (indicated by equal normalised concentrations) is observed. For longer normalised times, B and Si data deviate more and more. In the parameterisation considering water diffusion, this deviation is considered as resulting from Si saturation in solution (achieved at about 0.001 molal H₄SiO₄), the continuous release of B would be interpreted as being governed by water diffusion and the continuous Si release would be governed by pH and ionic strength changes. In the very long term, a final rate of 0.0005 g·m⁻²·d⁻¹ can be achieved. In the parameterisation ignoring water diffusion, if one would have to choose a single Si-saturation value, it would have to be assumed that silica saturation in bulk solution will not even be achieved until a molality of 0.01 is reached. Deviation of Si and B data are explained by Si retention in the gel and reduction of B release rates are an effect of transport limitations in the gel. In other words, Si concentrations at the gel/glass interface are close to the saturation value, while low silica concentrations are encountered in bulk solution.

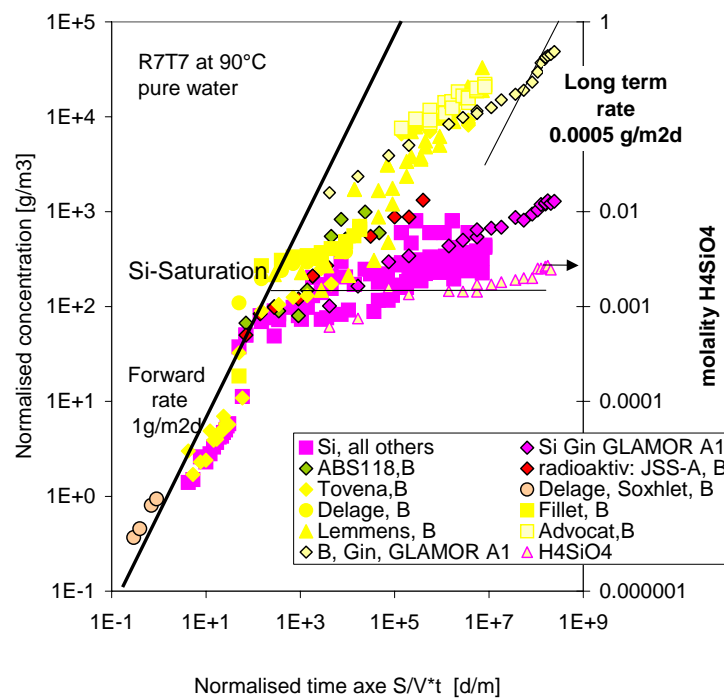


Figure 7: Si and B concentrations (normalized) as a function of normalised time for different static leaching tests performed by a variety of authors with SON68 glass in pure water at 90 °C for S/V ratios ranging between 10 and 500 000 m⁻¹.

However, for the paramétrisation ignoring water diffusion (the $r(t)$ model), C^* is only a fit parameter. Hence different sets of data in figure 7 will have different C^* value. A documentation of the dispersion of C^* values is given in figure 8. As can be seen, the C^* values obtained for the $r(t)$ model depend strongly on S/V ratios and on temperature. Most of C^* values are between 10 and 100 ppm, that is within one order of magnitude. The values over 100 ppm correspond to extreme leaching condition. From a general point of view, C^* variations for the paramétrisation of the $r(t)$ model are more limited than the D_g variations (see below).

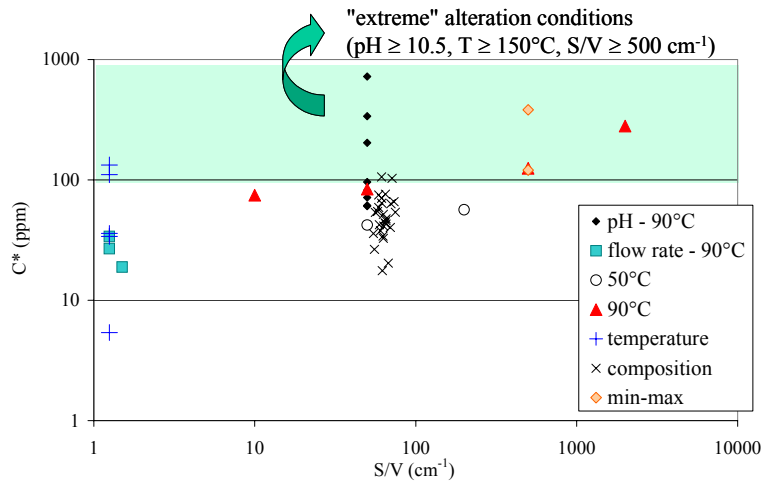


Figure 8. Silica saturation parameter C^* for parameterisation of the $r(t)$ model as a function of leaching conditions.

Silica saturation constants C^* for the GM2001 model show as well some scatter, but most of this can be explained as a function of pH, temperature and ionic strength. Only via these variables, S/V may influence saturation concentrations. An example for the pH dependency is given in Figure 9.

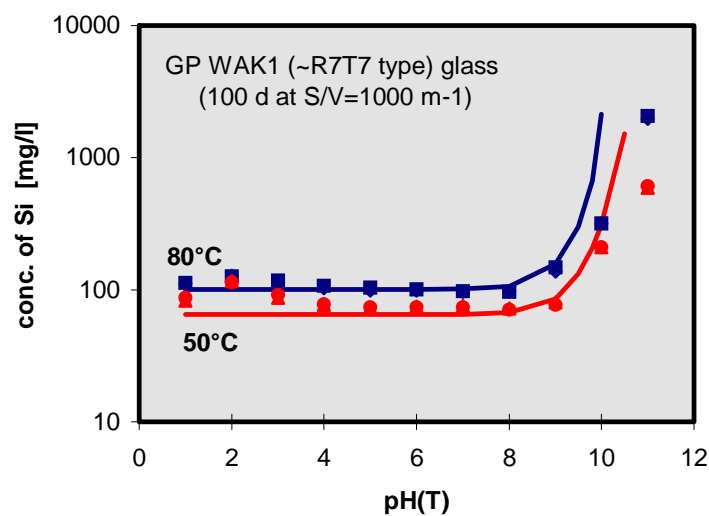


Figure 9. Comparison of calculated and measured saturation concentration for the glass GP WAK 1 as a function of time and temperature.

The temperature dependency (corresponding experimental data are not shown here) at infinite dilution is described according to the equation

$$\log K_{\text{SiO}_2, \text{glass}}(T) = \log K_{\text{SiO}_2, \text{glass}}^o + \frac{\Delta H_{\text{SiO}_2, \text{glass}}^o}{2.303 \cdot R} \left(\frac{1}{T^o} - \frac{1}{T} \right)$$

with $\log K_{\text{SiO}_2, \text{glass}}^o = -3.07 \pm 0.5$ and $\Delta H_{\text{SiO}_2, \text{glass}}^o = 12.4 \pm 4$ kJ/mol. Saturation constants C^* can be obtained from this relations using standard procedures for activity coefficient correction and for correction of hydrolysis of orthosilicic acid with pH. For pH values > 9.5 (see figure 9) experimental C^* values are lower than calculated ones.

The distribution of diffusion coefficients of silica in the gel is given in figure 10. For the $r(t)$ model variations of up to 8 orders of magnitude are encountered with S/V being the key variable influencing the D_g . Temperature, pH and glass composition effects are less important. In contrast, for the parameterisation of the GM 2001 model, there is no dependency on S/V .

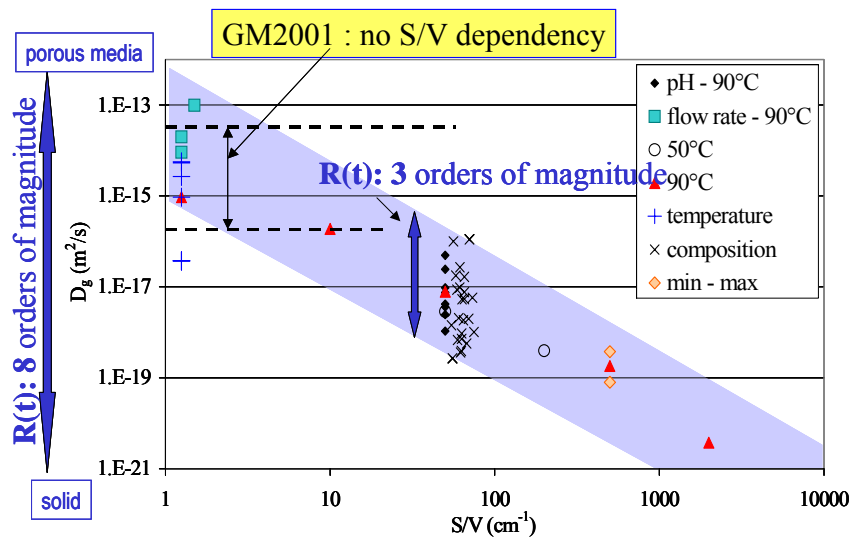


Figure 10: Dependency on leaching conditions of diffusion coefficient for silica transport in the gel layer D_g

Saturation and protective layer effects only explain the rate drop with time and with environmental conditions as it is observed in most static and dynamic tests. However, both the GM2001 and the $r(t)$ model would predict long-term reaction rates lower than any rate ever measured in the laboratories. There is however clear evidence that long-term corrosion rates do not approach a value of zero, but a small final rate remains.

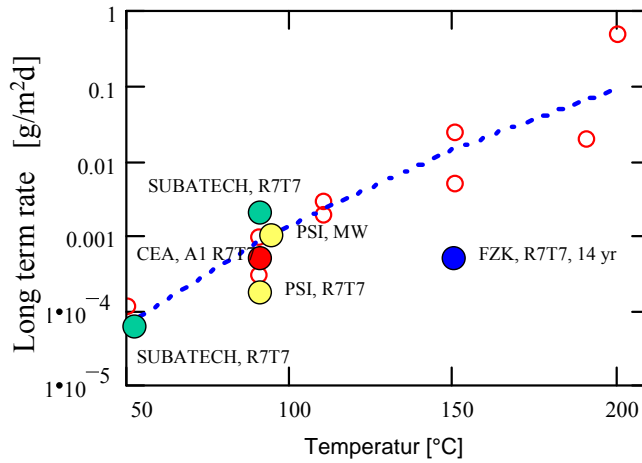


Figure 11: Final reaction rates observed in various static long-term glass corrosion tests

$$\Delta H_{\text{SiO}_2, \text{glass}}^{\circ} = 12.4 \pm 4.0 \text{ kJ/mol}$$

Final rate values of different studies are compiled in Figure 11 as a function of temperature. They are described by the equation

$$\log r_{\text{fin}} = \log A_{\text{fin}} - \frac{Ea_{\text{fin}}}{RT}$$

with $\log A_{\text{fin}} = 8.75 \pm 0.35$ and an activation energy of 61 kJ/mol, similar to the activation energy for the forward rate constant.

As a general rule one can say that final glass corrosion rates are at least a factor of 1000 lower than the forward rate. The rate controlling process is still poorly understood. One possible explanation is that the kinetics of formation of secondary phases drives glass corrosion.

Finally, for the model GM2001, one needs as well the parameterisation for the diffusion coefficient of water molecules in the glass. Figure 12 compares the coefficients observed in the present project with those observed by other authors for other glasses and a large range of temperatures.

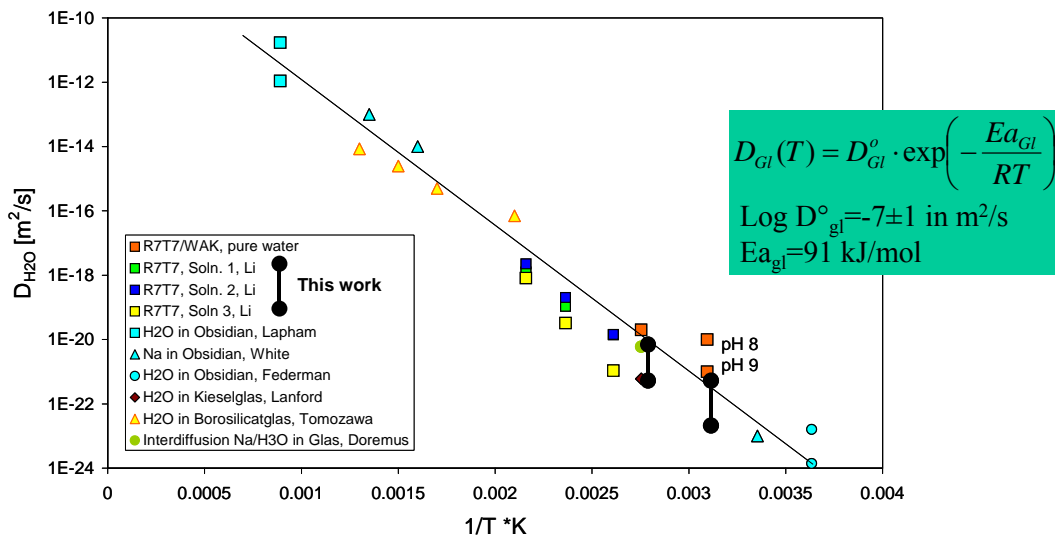


Figure 12: Comparison of diffusion coefficients for water molecules in glass with literature values

3.2.7 CONCLUSIONS

There is now a very good phenomenological description of the processes controlling glass dissolution kinetics and secondary phase formation. Surface layer compositions and their evolution with time can be predicted by assuming establishment of a thermodynamic equilibrium between a solid solution representation of the gel and the bulk solution, but the structure of the gel cannot be assessed by this means. Structural data are important to assess the transport properties of the gel. Predictions of structure evolution have been pursued by Monte Carlo techniques. Models were developed to assess transport porosity evolutions, but the models were either too complicated to obtain calculation results in reasonable times (KIRMAT) or they were only applied to binary silicate glasses (RW3D). More work is necessary in this area.

The kinetic reaction scheme of glass corrosion can be described quantitatively by two models: the $r(t)$ and the GM2001 model. The fundamental mathematical concepts of the two models are similar but in GM2001 also water diffusion into the glass after silica saturation is considered. Inclusion or exclusion of water diffusion is probably of minor importance for long-term corrosion, which is governed by the final reaction rate, but it is very important for deriving long-term relevant leach data from experimental observation. In fact, entire different parameter sets and parameter dependencies on environmental variables are obtained for the two models if water diffusion is included or not.

3.2.8 REFERENCES

- Aagaard P. and Helgeson H. C. (1982) Thermodynamic and kinetic constraints on reaction rates among minerals and aqueous solutions. I. Theoretical considerations. *American Journal of Science* **282**, 237-285.
- Advocat T. (1991) Les mécanismes de corrosion en phase aqueuse du verre nucléaire R7T7. Approche expérimentale. Essai de modélisation thermodynamique et cinétique. PhD Université Louis Pasteur, pp213.
- Advocat T., Chouchan J. L., Crovisier J. L., Guy C., Daux V., Jégou C., Gin S., and Vernaz E. (1998) Borosilicate nuclear waste glass alteration kinetics : chemical inhibition and affinity control. *Scientific Basis for Nuclear Waste Management*, XXI, 63-70.
- Advocat T., Crovisier J. L., Fritz B., and Vernaz E. (1990) Thermokinetic model of borosilicate glass dissolution: contextual affinity. *Scientific Basis for Nuclear Waste Management*, XIII, 241-248.
- Advocat T., Jollivet P., Crovisier J. L., and del Nero M. (2001) Long-term alteration mechanisms in water for SON68 radioactive borosilicate glass. *Journal of Nuclear Materials* **298**(1-2), 55-62.
- Aja S. U., Wood S. A. And Williams-Jones A. E. (1995) – The aqueous geochemistry of Zr and the solubility of some Zr-bearing minerals – *Applied Geochemistry* – **10**, 603-620.
- Babushkin, V. I., Matveyev, G. M. and Mchedlov-Petrosyan, O. P. (1985) - Thermodynamics of silicates – *Ed. Springer-Verlag, Berlin*, 459p.

- Berger G., Claparols C., Guy C., and Daux V. (1994) Dissolution rate of a basalt glass in silica-rich solutions: implications for long-term alteration. *Geochimica et Cosmochimica Acta* **58**(22), 4875-4886.
- Bourcier W. L., Carroll S. A., and Phillips B. L. (1994) Constraints on the affinity term for modeling long-term glass dissolution rates. *Scientific Basis for Nuclear Waste Management*, *XVII*, 507-512.
- Bourcier W. L., Peiffer D. W., Knauss K. G., McKeegan K. D., and Smith D. K. (1990) A kinetic model for borosilicate glass dissolution based on the dissolution affinity of a surface alteration layer. *Scientific Basis for Nuclear Waste Management*, *XIII*, 209-216.
- Byers C. D., Jercinovic M. J., Ewing R. C., and Keil K. (1985) Basalt glass: an analogue for the evaluation of the long-term stability of nuclear waste form borosilicate glasses. *Scientific Basis for Nuclear Waste Management*, *VIII*, 583-590.
- Carroll S. A., Bourcier W. L., and Phillips B. L. (1994) Surface chemistry and durability of borosilicate glass. *Scientific Basis for Nuclear Waste Management*, *XVII*, 533-540.
- Caurel J., Vernaz E., and Beaufort D. (1990) Hydrothermal leaching of R7-T7 borosilicate glass (nuclear waste glass). *Scientific Basis for Nuclear Waste Management*, *XIII*, 309-318.
- Clément A. and Madé B. (1981) DISSOL, EVAPOR et EQUIL. Trois modèles de simulation sur ordinateur des interactions entre les eaux naturelles et les minéraux. Institut de Géologie, pp20.
- Crovisier J. L. (1989) Dissolution des verres basaltiques dans l'eau de mer et dans l'eau douce. Essai de modélisation. PhD Université Louis Pasteur, pp253
- Crovisier J. L., Advocat T., Petit J. C., and Fritz B. (1989a) Alteration of basaltic glass in Iceland as a natural analogue for nuclear waste glasses : geochemical modelling with DISSOL. *Scientific Basis for Nuclear Waste Management*, *XII*, 57-64.
- Crovisier J. L., Atassi H., Daux V., Honnorez J., Petit J. C., and Eberhart J. P. (1989b) A new insight into the nature of the leached layers formed on basaltic glasses in relation to the choice of constraints for long-term modelling. *Scientific Basis for Nuclear Waste Management*, *XII*, 41-48.
- Crovisier J. L., Fritz B., Grambow B., and Eberhart J. P. (1985) Dissolution of basaltic glass in seawater: experiments and thermodynamic modelling. *Scientific Basis for Nuclear Waste Management*, *IX*, 273-280.
- Crovisier J. L., Honnorez J., Fritz B., and Petit J. C. (1992a) Dissolution of subglacial volcanic glasses from Iceland: laboratory study and modelling. *Applied Geochemistry Supplement* **1**, 55-81.
- Crovisier J. L., Vernaz E., Dussossoy J. L., and Caurel J. (1992b) Early phyllosilicates formed by alteration of R7T7 glass in water at 250°C. *Applied Clay Science* **7**(1-3), 47-57.
- Curti E., Crovisier J.-L., Karpoff A.-M. and Munier I. (in preparation) - Long-term glass alteration of two simulated nuclear waste glasses (MW and SON68): kinetics and geochemical results.(2004)
- Daux V., Guy C., Advocat T., Crovisier J.-L., and Stille P. (1997) Kinetic aspects of basaltic glass dissolution at 90°C : role of aqueous silicon and aluminium. *Chemical Geology* **142**(1-2), 109-126.

- Delage F. (1992) PhD thesis, Université Montpellier II
- Durst P. (1998) Etude de la mobilité des produits de fission et des éléments transuraniens lors de l'altération d'un verre de confinement des déchets radioactifs. DEA, Physique et Chimie de la Terre, Université Louis Pasteur, pp29
- Fritz B. (1975) Etude thermodynamique et modélisation des réactions entre minéraux et solutions. Application à la géochimie des altérations et des eaux continentales. Sciences Géologiques. Université Louis Pasteur, **41**, pp152.
- Fritz B. (1981) Etude thermodynamique et modélisation des réactions hydrothermales et diagénétiques. Sciences Géologiques. Université Louis Pasteur, **65**, pp197.
- Gauthier A., Le Coustumer P., Motelica M., and Donard O. F. X. (2000) Real time alteration of a nuclear waste glass and remobilization of lanthanide into an interphase. *Waste Management* **20**(8), 731-739.
- Gin S. (1996) Control of R7T7 nuclear glass alteration kinetics under saturation conditions. *Scientific Basis for Nuclear Waste Management, XIX*, 189-196.
- Gin S., Jollivet P., Mestre J. P., Jullien M., and Pozo C. (2001) French SON 68 nuclear glass alteration mechanisms on contact with clay media. *Applied Geochemistry* **16**, 861-881.
- Gong W. L., Wang L. M., Ewing R. C., Vernaz E., Bates J. K., and Ebert W. L. (1998) Analytical electron microscopy study of surface layers formed on the French SON68 nuclear waste glass during vapor hydration at 200°C. *Journal of Nuclear Materials* **254**(2-3), 249-265.
- Grambow B., "Influence of Saturation on the Leaching of Borosilicate Nuclear Waste Glasses", *Glastechn. Ber.*, **56**, 566-571 (1983)
- Grambow B. and D.M. Strachan. "Leach Testing of Waste Glasses under Near Saturation Conditions." *Mater. Res. Soc. Symp. Proc.* **26**, 623-34 (1984)
- Grambow B. (1985) A general rate equation for nuclear waste glass corrosion. *Scientific Basis for Nuclear Waste Management, VIII*, 15-27.
- Grambow B., M.J. Jercinovic, R.C. Ewing and C.D. Byers. "Weathered Basalt Glass : A Natural Analogue for the Effects of Reaction Progress on Nuclear Waste Glass Alteration" *Mat. Res. Soc. Symp. Proc.* **50**, 263-72 (1986)
- Grambow B., H.P. Hermansson, I.K. Björner, H. Christensen and L. Werme, "Reaktion of Nuclear Waste Glass with slowly flowing Solutions", *Advances in Ceramics*, **20**, 465-474 (1986)
- Grambow B. and Müller R. (2001) First-order dissolution rate law and the role of surface layers in glass performance assessment. *Journal of Nuclear Materials* **298**, 112-124.
- Guy C. (1989) Mécanismes de dissolution des solides dans les solutions hydrothermales déduits du comportement de verres basaltiques et de calcites déformées. PhD Université Paul Sabatier, pp188.
- Helgeson H. C., Delany J. M., Nesbitt H. W. and Bird D. K. (1978) – Summary and critique of the thermodynamic properties of Rock-forming minerals – *American J. Science* – **278-A**, 1-220.
- Honnorez J. (1972) La palagonitisation : l'altération sous marine du verre volcanique basique de Palagonia (Sicile). Vulkaninstitut Immanuel Friedlaender, Birkhäuser Verlag, **9**, pp131.

- Honnorez J. (1981) The aging of the oceanic crust at low temperature. In *The Sea* (ed. C. Emiliani), Wiley Interscience, 525-587.
- Jégou C. (1998) Mise en évidence expérimentale des mécanismes limitant l'altération du verre R7T7 en milieu aqueux. Critique et proposition d'évolution du formalisme cinétique. PhD Université de Montpellier, pp224.
- Jégou C., Gin S., and Larché F. (2000) Alteration kinetics of a simplified nuclear glass in an aqueous medium : effects of solution chemistry and of protective gel properties on diminishing the alteration rate. *Journal of Nuclear Materials* **280**, 216-219.
- Knauss K. G., Bourcier W. L., McKeegan K. D., Merzbacher C. I., Nguyen S. N., Ryerson F. J., Smith D. K., Weed H. C., and Newton L. (1990) Dissolution kinetics of a simple analogue nuclear waste glass as a function of pH, time and temperature. *Scientific Basis for Nuclear Waste Management, XIII*, 371-381.
- Le Gal X. (1999) Etude de l'altération de verres volcaniques du Vatnajökull (Islande). Mécanismes et bilans à basse température. PhD Université Louis Pasteur, pp153
- Le Gal X., Crovisier J.-L., Gauthier-Lafaye F., Honnorez J., and Grambow B. (1999) Meteoric alteration of Icelandic volcanic glass: long-term changes in the mechanism. *Comptes Rendus de l'Académie de Sciences, Paris - Série IIa: Sciences de la Terre et des Planètes* **329**(3), 175-181.
- Leturcq G., Berger G., Advocat T., and Vernaz E. (1999) Initial and long-term dissolution rates of aluminosilicate glasses enriched with Ti, Zr and Nd. *Chemical Geology* **160**(1-2), 39-62.
- Linard Y. (2000) Détermination des enthalpies libres de formation des verres borosilicatés. Application à l'étude de l'altération des verres de confinement de déchets radioactifs. PhD Université Paris VII, pp. 265.
- Linard Y., Advocat T., Jegou C., and Richet P. (2001a) Thermochemistry of nuclear waste glasses: application to weathering studies. *Journal of Non-Crystalline Solids* **289**(1-3), 135-143.
- Linard Y., Yamashita I., Atake T., Rogez J., and Richet P. (2001b) Thermochemistry of nuclear waste glasses: an experimental determination. *Journal of Non-Crystalline Solids* **286**(3), 200-209.
- Lutze W., Malow G., Ewing R. C., Jercinovic M. J., and Keil K. (1985) Alteration of basalt glasses: implications for modelling the long- term stability of nuclear waste glasses. *Nature* **314**(6008), 252-255.
- Madé B., Clément A. and Fritz B. (1990) – Modélisation cinétique et thermodynamique de l'altération : le modèle géochimique KINDIS - *Comptes Rendus de l'Académie des Sciences, Paris – Série IIa: Sciences de la Terre et des Planètes* – **310**, 31-36.
- Madé B., Clément A., and Fritz B. (1994) Theoretical approach and modelling of the dissolution and precipitation of minerals under kinetic control. *Water Rock Interactions, 7th, Rotterdam*, 101-105.
- Madé B., Clément A. and Fritz B. (1994a) – Modeling mineral/solution interactions : the thermodynamic and kinetic code KINDISP – *Computers & Geoscience* – **20**, 31-36.
- Madé B., Clément A. and Fritz B. (1994b) – Modélisation thermodynamique et cinétique des réactions diagénétiques dans les bassins sédimentaires – *Revue de l'Institut du Pétrole* – **49**, 9, 1347-1363.

- Malow G. and Ewing R. C. (1981) Nuclear waste glasses and volcanic glasses : a comparison of their stabilities. *Scientific Basis for Nuclear Waste Management, III*, 315-322.
- McGrail B. P., Ebert W. L., Bakel A. J., and Peeler D. K. (1997) Measurement of kinetic rate law parameters on a Na-Ca-Al borosilicate glass for low-activity waste. *Journal of Nuclear Materials* **249**(2-3), 175-189.
- McGrail, B. P., J. P. Icenhower, and E. A. Rodriguez, “Origins of Discrepancies Between Kinetic Rate Law Theory and Experiments in the Na₂O-B₂O₃-SiO₂ System” MRS (2001a)
- McGrail, B.P., D.H. Bacon, J.P. Icenhower, F.M. Mann, R.J. Puigh, H.T. Schaeff, S.V. Mattigod, “Near-field performance assessment for a low-activity waste glass disposal system: laboratory testing to modeling results”; *J. Nucl. Mater.* 298 (2001b) 95-111
- Michaux L., Mouche E., Petit J.-C and Fritz B. (1992) – Geochemical modelling of the long-term dissolution behaviour of the French nuclear glass R7T7 – *Applied Geochemistry* – **Suppl. 1**, 41-54.
- Oelkers E. H. and Gislason S. R. (2001) The mechanism, rates and consequences of basaltic glass dissolution: I. An experimental study of the dissolution rates of basaltic glass as a function of aqueous Al, Si and oxalic acid concentration at 25°C and pH = 3 and 11. *Geochimica et Cosmochimica Acta* **65**(21), 3671-3681.
- Parker V. B., Wagman D. D. and Evans W. H. (1971) – Selected values of chemical thermodynamic properties. Tables for alkaline earth elements (elements 92 through 97 in the standard order arrangement) – *NBS Technical Note* – **270-6**, pp106.
- Paul A. (1977) Chemical durability of glasses; a thermodynamic approach. *Journal of Material Sciences* **12**, 2246-2268.
- Ricol S. (1995) – Etude du gel d’altération des verres nucléaires et synthèse de gels modèles - *Thesis of the University Pierre et Marie Curie, Paris VI* – pp177.
- Rieber C. (1999) Etude théorique et modélisation de l’altération et de la formation de phases minérales complexes considérées comme des solutions solides généralisées. DEA, Physique et Chimie de la Terre, Université Louis Pasteur, pp. 28.
- Robie R. A., Hemingway B. S. and Fisher J. R. (1979) – Thermodynamic properties of minerals and related substances at 298.15 K and 1 Bar (10⁵ Pascals) pressure and at higher temperatures – *Geological Survey Bulletin* – **1452**, pp456.
- Robie R. A. and Hemingway B. S. (1995) - Thermodynamic properties of minerals and related substances at 298.15 K and 1 Bar (10⁵ Pascals) pressure and at higher temperatures – *U. S. Geological Survey Bulletin* – **2131**, pp461.
- Shock E. L. and Helgeson H. C. (1988) – Calculations of the thermodynamic and transport properties of aqueous species at high pressures and temperatures : Correlation algorithms for ionic species and equation of state predictions to 5 kb and 1000°C – *Geochimica et Cosmochimica Acta* – **52**, 2009-2036.
- Shock E. L., Helgeson H. C. and Sverjensky D. A. (1989) – Calculations of the thermodynamic and transport properties of aqueous species at high pressures and temperatures : Standard partial molal properties of inorganic neutral species – *Geochimica et Cosmochimica Acta* – **53**, 2157-2183.

- Shock E. L., Sassani D. C., Willis M. and Sverjensky D. A. (1997) – Inorganic species in geologic fluids : Correlations among standard molal thermodynamic properties of aqueous ions and hydroxide complexes - *Geochimica et Cosmochimica Acta* – **61**, 5, 907-950.
- Tardy Y. and Fritz B. (1981) An ideal solid solution model for calculating solubility of clay minerals. *Clay Minerals* **16**, 361-373.
- Techer I. (1999) Apports des analogues naturels vitreux à la validation des codes de prédiction du comportement à long terme des verres nucléaires. PhD Université de Montpellier, pp206.
- Techer I., Advocat T., Lancelot J., and Liotard J.-M. (2000) Basaltic glass : alteration mechanisms and analogy with nuclear waste glasses. *Journal of Nuclear Materials* **282**, 40-46.
- Techer I., Advocat T., Lancelot J., and Liotard J.-M. (2001) Dissolution kinetics of basaltic glasses : control by solution chemistry and protective effect of the alteration film. *Chemical Geology* **176**, 235-263.
- Vernaz, É.Y. “Estimating the lifetime of R7T7 glass in various media” C. R. Physique 3 (2002) 813–825
- Wagman D. D., Evans W. H., Parker V. B., Halow I., Bailey S. M. and Schumm R. H. (1968) – Selected values of chemical thermodynamic properties – Tables for the first thirty-four elements in the standard order of arrangement – *NBS Technical Note* – **270-3**, pp264.
- Wallace R. and Wicks G. (1983) Leaching chemistry of defense borosilicate glass. *Scientific Basis for Nuclear Waste Management*, VI, 23-28.
- Werme L.O., I. Björner, G. Bart, H.U. Zwicky, B. Grambow, W. Lutze, R. Ewing, C. Magrabi; "Chemical Corrosion of Highly Radioactive Borosilicate Nuclear Waste Glass under Simulated Repository Conditions", *J. Mater. Res.*, **5** (5) (1990) pp. 1130-46
- Zarembowitch-Déruelle O. (1997) – Etude in situ de la couche d'altération de verres – *Thesis of the University Pierre et Marie Curie, Paris VI* – p.186.

Appendix 1

Thermodynamic parameters calculation

According to Paul (1977), the glasses were considered as a solid solution of oxides and metasilicates (Table 1). Their solubility constant was calculated from the free enthalpy of formation of their components (Table 1 and Table 3). The LogK values at 90 °C were estimated by the Van't Hoff relation.

Dissolution equations	Log K _{90°C}	ΔG _{diss, 90°C}	References
SiO _{2am} + 2H ₂ O ⇌ H ₄ SiO ₄	-2.25	3.75	Helgeson et al. (1978)
SiO _{2chalcedony} + 2H ₂ O ⇌ H ₄ SiO ₄	-2.96	4.92	Helgeson et al. (1978)
SiO _{2quartz} + 2H ₂ O ⇌ H ₄ SiO ₄	-3.19	5.30	Helgeson et al. (1978)
H ₄ SiO ₄ ⇌ H ₃ SiO ₄ ⁻ + H ⁺	-8.95	14.87	Fritz B. (1981)
Na ₂ O + 2H ⁺ ⇌ 2Na ⁺ + H ₂ O	56.39	-93.71	Helgeson et al. (1978), Shock E (1997)
CaO + 2H ⁺ ⇌ Ca ²⁺ + H ₂ O	26.56	-44.13	Helgeson et al. (1978)
B ₂ O ₃ + 3H ₂ O ⇌ 2B(OH) ₃	5.08	-8.45	Robie R. A., (1979) Shock E. L (1989)]
Al ₂ O ₃ + 5H ₂ O ⇌ 2Al(OH) ₄ ⁻ + 2H ⁺	-24.54 -7.78	40.79	Robie R. A., et al. 1979, 1995 Helgeson et al. (1978), Babushkin et al (1985)
ZrO ₂ + 2H ₂ O ⇌ Zr(OH) _{4aq}		12.92	Aja et al. (1995)
NaOH ⇌ Na ⁺ + OH ⁻	6.87	-11.41	Robie et al. 1995
Ca(OH) ₂ + 2H ⁺ ⇌ Ca ²⁺ + 2H ₂ O	18.63	-30.96	Wagman D. D., et al. (1968) Parker et al. (1971)
Al(OH) ₃ + H ₂ O ⇌ Al(OH) ₄ ⁻ + H ⁺	-12.51 -11.85	20.78	Fritz, B. (1981) Babushkin et al (1985)
Zr(OH) _{4c} ⇌ Zr(OH) _{4aq}		19.70	Aja et al. (1995), Shock E.L. et al. (1988)
Na ₂ SiO ₃ + 2H ⁺ + H ₂ O ⇌ 2Na ⁺ + H ₄ SiO ₄	17.75	-29.49	Paul, A. (1977), Robie et al. 1995
CaSiO ₃ + 2H ⁺ + H ₂ O ⇌ Ca ²⁺ + H ₄ SiO ₄	8.83 -13.53	-14.68	Paul A.(1977) Helgeson et al. 1978, Babushkin et al (1985)
ZrSiO ₄ + 4H ₂ O ⇌ Zr(OH) _{4aq} + H ₄ SiO ₄		22.49	Aja et al. (1995) Shock E.L. et al. (1988)

The solubility constant of the two glasses were calculated as follow, using chalcedony as siliceous end-member: LogK_{glass 1, 90°C} = 0.39 and LogK_{glass 2, 90°C} = 0.97. These

values can be compared to the logK value of a simplified Si-Na-B glass measured experimentally by Linard *et al.* (2001). Their results indicated a $\text{Log}K_{90^\circ\text{C}} = 0.89 \pm 0.34$, which is of the same magnitude.

3.3 Glass corrosion in near-field conditions

The work packages related to the different topics are listed in the table below.

TOPIC	WORK PACKAGES	PARTNER
Integral experiments.	WP4-1, WP4-3, WP4-6, WP4-7, WP4-8	CEA, SCK.CEN
Study of near-field materials	WP4-4, WP4-5	SCK.CEN

3.3.1 INTRODUCTION

This chapter is devoted to the study of the corrosion behaviour of HLW glass in contact with near-field materials. The scope is limited to the effects of clay and of metallic corrosion products. The clay is either host rock clay (boom clay) or backfill clay (FoCa7 bentonite).

In previous European (and other) research programmes, it was already demonstrated that the presence of clay can have a clear impact on the glass dissolution mechanisms and -rate.

The main processes can be represented as a number of serial and parallel processes (Fig. 1).

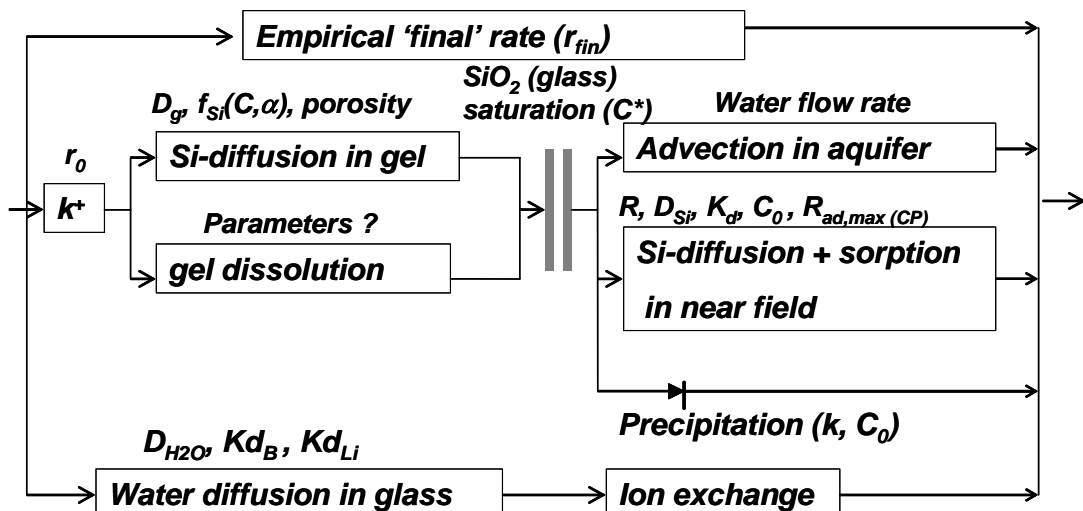


Figure 1: Overview of processes involved in glass dissolution in near-field conditions. The main parameters used to describe the mechanisms are shown as well.

The presentation in **Figure 1** is limited to mechanism and parameters that are considered in the current European models, developed to simulate glass dissolution in near-field conditions (Lixiver, the SCK•CEN lifetime model, GLADIS). Most processes presented in Figure 1 occur also in absence of near-field materials. The presence of such near-field materials (clay, metallic corrosion products, or other, with or without direct contact with the glass) will have an impact through (1) Si-diffusion and sorption in that material, (2) changes in the chemical equilibria in the (interstitial) solution, which may lead to specific precipitation processes, or even to specific values for C^* (depending on the interpretation of this parameter), (3) the rate of gel dissolution. This chapter is therefore devoted mainly to these three processes. The potential effect of clay on r_0 and on radionuclide concentrations is also discussed

Specific experiments were performed within GLASTAB to focus on these processes. This includes (1) the study of near-field materials (WP4-4, WP4-5), (2) integral experiments (WP4-1, WP4-3, WP4-6, WP4-7, WP4-8), and (3) geochemical and Monte Carlo modelling of glass/clay interactions (WP5-6, WP5-7). Certain experiments were performed in conditions similar to those expected *in situ* after the thermal stage. The results of these tests can be considered as a demonstration of *in situ* behaviour. Detailed description of experiments and results are given in the Annex.

3.3.2 EXPERIMENTAL RESULTS AND DISCUSSION

3.3.2.1 Effect of near-field materials on the initial dissolution rate r_0

The initial dissolution rate r_0 is a function of pH and temperature. If the other, downstream processes presented in **Figure 1** provide a sufficient slow-down of Si transport, the long-term effect of r_0 on the glass dissolution rate will be small. For conservative glass life time calculations, however, a constant initial dissolution rate can be assumed. In that case, the life time will be proportional to r_0 , making it an important parameter.

The considered models do not take into account a possible influence of near-field materials on the initial dissolution rate r_0 . Nevertheless, some data exist that suggest that there may be a direct impact. More specifically, *in situ* tests in boom clay with PAMELA glass SM513 had previously shown that the dissolution rate can be higher than the initial dissolution rate expected for this glass. Therefore, it is necessary to confirm the r_0 obtained in tests in pure water by tests in the presence of clay.

The initial dissolution rates of glasses SON68 and SM539 at 30 °C were estimated in the tests of WP4-6, where glass coupons were in contact with solid boom clay at 30 °C for durations up to 580 days. The pH in the interstitial clay water is not exactly known, but probably close to the *in situ* pH of 8.2. Linear regression of the coupon mass losses in the first year resulted in an average dissolution rate of 0.010 " 0.007 $\text{gm}^{-2}\text{d}^{-1}$ for glass SON68, and 0.012 " 0.009 $\text{gm}^{-2}\text{d}^{-1}$ for glass SM539 (**see Fig. 1**).

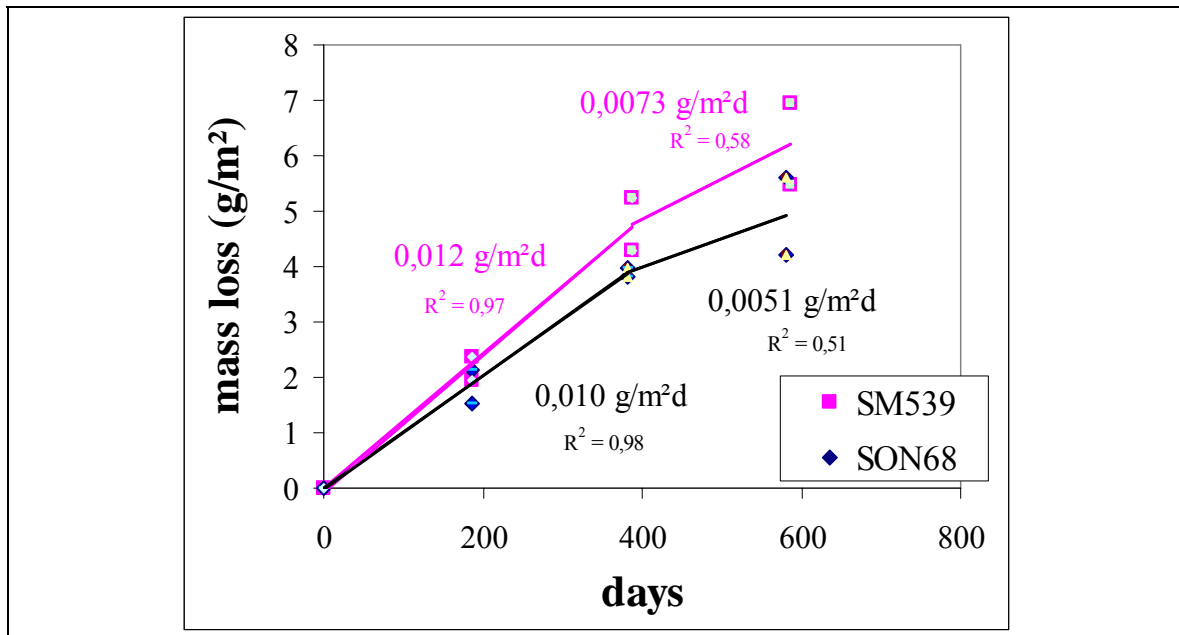


Figure 1: Mass losses for glass SM539 and SON68 in contact with boom clay at *in situ* density, at 30 °C.

The mentioned uncertainty is expressed as a 95 % confidence interval. The average dissolution rate in the first year is close to the previously estimated initial dissolution rate of $0.0075 \text{ gm}^{-2}\text{d}^{-1}$, although the rates that were observed in these tests should be lower than the initial rate as defined in the first order rate law, because the initial Si concentration in the clay water is different from zero. In similar *in situ* tests, Si concentrations were in general $> 10 \text{ mg/l}$ [FR]. If this is true also for the tests of WP4-4, and assuming that $C^* = 10^{-3.01} \text{ M} = 27 \text{ mg/l}$, the rate initially measured is theoretically $(1-10/27) \times r_0 = 0.63 \times r_0$. Previous short term tests have however shown that the initial rate in the presence of clay is close to the initial rate measured in absence of clay, in spite of high initial Si concentrations. This seems to be the case for the tests of WP4-4 also. Although this is problematic w.r.t. the validation of the first order rate law in the presence of clay, we will – for the time being – consider that the rates measured in solid boom clay are an estimation of the initial dissolution rate.

Uncertainty on the obtained rates

The 95 % confidence interval on the rates mentioned higher does not include possible systematic bias. The most important source of such bias may be the mentioned effect of Si in the initial solution. Because the value is similar to the one obtained in media without clay, we can assume that it is independent of the medium.

Conclusion:

The initial dissolution rate of SON68 (and SM539) has been determined in realistic disposal conditions (30 °C, high-density clay).

3.3.2.2 Si diffusion and sorption in the near field

Many potential near-field materials are able to immobilise Si in some way. The exact mechanisms are in general not well known. Previous experiments with FoCa7 clay have suggested that the immobilization consists of a first stage, interpreted as sorption, and a second stage, interpreted as precipitation. The Si sorption and

diffusion properties of boom clay and FoCa7 clay were determined in several types of experiments in the GLASTAB programme (WP4-4 and WP4-5).

In WP4-4, experiments were performed to measure the Si sorption behaviour of boom clay at room temperature in conditions where the clay water solution is *oversaturated in Si* w.r.t. the clay (i.e. high Si concentration). This experiment allows measuring the total Si sorption capacity of the clay, as can be expected near the HLW package. Within WP4-5, the sorption (and diffusion) behaviour of Si was measured for FoCa7 clay, in conditions where the clay water is *close to Si saturation* w.r.t. the clay (i.e. low Si concentration). This is the situation expected at larger distance from the HLW package.

In the experiment with high Si concentration (WP4-4), clay water was equilibrated with SON68 frit, and then led through a cell, filled with boom clay, at 25-30 °C. The difference in Si concentration at the inlet and outlet of the cell allows calculating how much Si is immobilized by the clay as a function of time. After correction for outliers, the total short term sorption capacity was estimated at 1.8 mg Si/ g clay. The average Si concentration in the test with boom clay was 96 mg/l. This corresponds to a K_d of 0.019 m³/kg, which is close to the K_d values between 0.019 and 0.026 m³/kg obtained by batch sorption tests with ³²Si at Si concentrations estimated < 30 mg/ []. This good agreement suggests that the Si-sorption can be described by the measured K_d for Si concentrations up to 100 mg/l, this is for the Si concentration range that we can expect *in situ*. The short term sorption capacity measured in boom clay is somewhat lower than the sorption capacity of FoCa7 clay, for which, at 25 °C, a total sorption of 2.6 mg/g was observed, corresponding to a K_d of about 0.034 m³/kg []. In the latter experiments, it was observed that temperature had not much influence on K_d . It is likely that this is also the case for Boom clay, although this was not shown by experiments. The total sorption of silica measured in these tests is in equilibrium with the Si in solution. It is likely that, for higher Si concentrations, more Si will be immobilized, but because the range > 100 mg/l Si was not investigated, this cannot be confirmed experimentally.

The experiment with Si concentrations close to equilibrium (WP4-5) was of the pulse-injection type. By means of a pressure gradient, a flow of (Boom) clay water is forced through a core of compressed FoCa7 clay at 25°C. When the system is at equilibrium, a pulse of ³²Si is injected at the inlet of the cell. The ³²Si peak then starts to migrate through the clay core. At the end of the test, the clay core is analysed to determine the ³²Si diffusion profile and to fit the corresponding sorption and diffusion parameters. An experiment with FoCa7 was stopped 753 days after the ³²Si injection. The values determined for the sorption- and diffusion parameters, and a comparison with the values measured previously for boom clay at *in situ* density are presented in Table I.

	FoCa7	Boom clay
Retardation factor R	(109/0.4=) 273	100 - 300
Distribution coefficient K_d	$((273-1)*0.4/1.5=)$ $0.073 \text{ m}^3 \text{ kg}^{-1}$	$0.025 - 0.075 \text{ m}^3 \text{ kg}^{-1}$
Apparent diffusion coefficient ¹ D_{app}	$4 \times 10^{-14} \text{ m}^2 \cdot \text{s}^{-1}$	2×10^{-13} and 7×10^{-13} $\text{m}^2 \cdot \text{s}^{-1}$

Table I: Migration parameter values for Si in FoCa7 clay at 25 °C and comparison with similar data for boom clay

It appears that the results for R and K_d are close to the maximum estimations for boom clay. This may be due to the large specific surface area of the FoCa7 (430 m²/g, compared to 44 m²/g for boom clay), and/or to the presence of an important fraction of goethite (and hematite) in FoCa7, which can offer more sites for Si sorption. These results are qualitatively in agreement with the smaller K_d measured for boom clay in WP4-4, compared to the K_d for FoCa clay. Because more Si is sorbed per gram of FoCa7 clay, D_{app} is lower, implying that Si moves slower through the clay than in boom clay. The fact that D_{app} is lower than for boom clay suggests that the pore diffusion coefficient (D_p) is smaller. This may be linked to the diameter of the pores (the swelling FoCa7 can contain more interfoliar water). The SCK•CEN life time model (based on the first order rate law, combined with Si diffusion in the clay) predicts faster glass dissolution when D_{app} is smaller. Therefore, we expect a shorter glass life time in the presence of FoCa7 clay than in the presence of boom clay. The exact life time predictions will depend of course on the details of the model and the values given to the other parameters.

Remark: the K_d values estimated from ³²Si percolation tests in boom clay at *in situ* density are higher (up to 0.075 m³/kg) than the 0.019 m³/kg estimated from tests in more diluted systems, like the tests of WP4-4 or previous batch sorption tests. This may be due to partial dissolution of clay in the more diluted systems, leading to a decrease of sorption site density.

Conclusion: Si sorption is somewhat larger for FoCa7 than for boom clay, and (at least for boom clay) probably linear up to (at least) 100 mg/l Si. The value of K_d depends on the experimental method. Because the tests in solid boom clay are more realistic, we propose to use the values in Table I as reference.

3.3.2.3 Precipitation

Based on glass mass losses and surface analyses, it has been observed that the mass of Si, dissolved from glass coupons in clay slurries, divided by the mass of clay, is often higher than the short term sorption capacity of ~ 2 mg Si per gram of clay. This suggests that a remaining Si fixation (precipitation) mechanism exists in boom clay. Also from a principal point of view, it is likely that long-term precipitation occurs,

¹ Distinction is made between the apparent diffusion coefficient (D_{app}), the effective diffusion coefficient D_{eff} , and the pore diffusion coefficient D_p , with the following definitions: $D_{app} = D_{eff}/\eta R$, $D_{eff} = \eta D_p$, $D_{app} = D_p/R$ (η = clay porosity, R = retardation factor).

because the equilibrium Si concentration of many potential secondary phases is lower than the solubility of the glass. We therefore must assume that long-term precipitation will most probably occur, although it may be (very) slow. One of the objectives of the experiment of WP4-4 was to see if a remaining Si fixation rate could be demonstrated in boom clay. The results reveal, however, no clear evidence for such long-term Si fixation mechanism (Fig. 2).

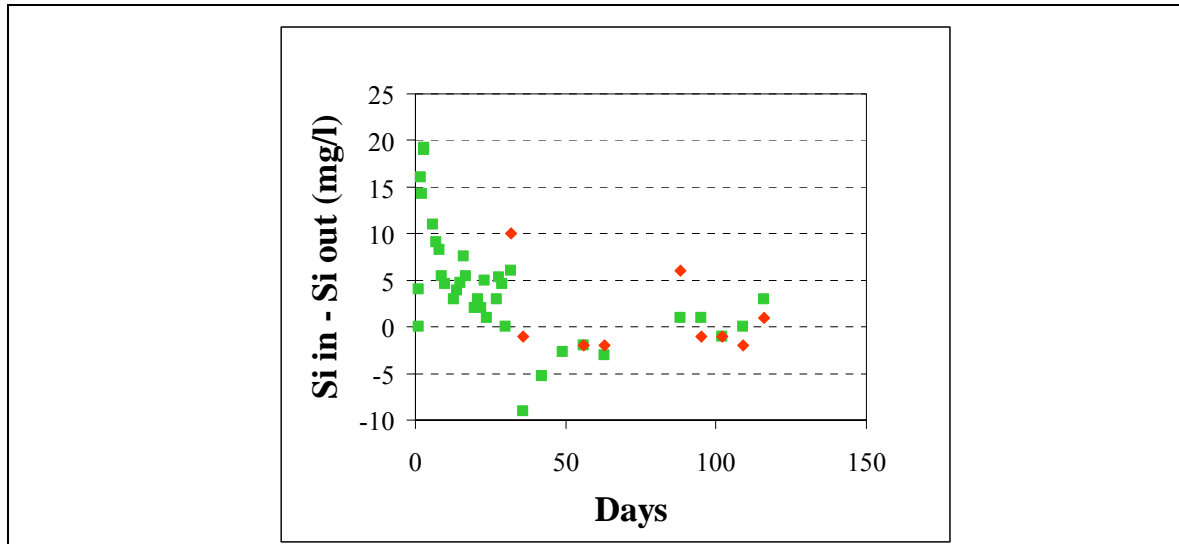


Fig. 2: Net Si sorption ($S_{i_{inlet}} - S_{i_{outlet}}$) on boom clay as a function of percolated clay water volume. Green squares represent unfiltered samples; red diamonds represent ultra-filtered samples (YM30). The long-term net sorption (precipitation) is close to 0 mg/l.

Indeed, in Figure 2, the long-term net sorption of Si is close to 0 mg/l. A potential small remaining sorption would anyway be hidden by the low reproducibility of the tests (probably due to clay instability). In [Gin, 2001], a remaining Si fixation rate was observed for FoCa7, but data are available only for the relatively short term (32 days or less). This means that there is still no direct evidence that a remaining Si fixation rate exists on the long term in boom clay or FoCa7.

Indications about the relevance of precipitation were also given by the experiment of WP4-6, where a coupon of ^{32}Si doped glass was corroded at 90 °C in contact with solid boom clay for 391 days. At the end of the test, the ^{32}Si diffusion profile in the clay was measured. The ^{32}Si released by the glass, had migrated over a distance of more than 25 mm. If released Si precipitates, this is more likely near the glass surface than at larger distance. Precipitation would hence result in a sudden decrease of the ^{32}Si profile near the glass surface. This is clearly not observed. This implies again that Si precipitation was not important in the considered timescale and geometry.

As already mentioned, precipitation (secondary phase formation) is nevertheless likely from a thermodynamic point of view. This was investigated by geochemical modelling with PHREEQC (WP5-6) for dissolution of glass SON68 in boom clay. In a first step, the equilibria in the pure boom clay – boom clay water system were studied. Previous models had the important drawback that the observed clay water composition was explained with phases that were not observed in the clay. Within GLASTAB, the model was improved to overcome this problem. An assemblage of minerals (approximating the real composition of boom clay) was defined in such a way that the chemical composition of an aqueous phase in equilibrium with these

minerals is similar to the chemical composition of the real boom clay interstitial clay water. A first part of the model consists of a multi-site pH-dependent cation exchange model to describe the functional group capacity of boom clay organic matter. Next, this cation exchange model together with different sets of minerals was used to calculate an equilibrium solution composition. Two sets of minerals ((1) quartz, kaolinite, calcium, K-Feldspar and NaMontmorillonite, or (2) quartz, kaolinite, calcium, illite and NaMontmorillonite) resulted in equilibrium concentrations of Al, Ca, K, Mg, Na and Si close to the observed concentrations. All included minerals are observed *in situ*. For *in situ* clay, quartz gives only a slight underestimation of the observed Si concentrations, so this phase is proposed as the one imposing Si solubility. In diluted, heated clay slurries however, Si concentrations are much higher, and amorphous SiO₂ seems to control Si concentrations. At 90 °C, the silica concentrations are so high (200-300 mg/l), that they cannot even be explained by amorphous SiO₂. No explanation was found for these high Si concentrations.

In the next step, these models were used to predict the nature and amounts of secondary phases that may form upon dissolution of SON68 in boom clay. Three types of experiments were modelled: SON68 – distilled water, SON68 – synthetic clay water, and SON68 – synthetic clay water – boom clay (experiments from the previous EC programme). For the two first systems, three approaches were tested to describe the measured concentrations of Si, Na, Al, Ca, Mg (only in second system) and pH:

- Congruent glass dissolution with precipitation of pure secondary phases
- Congruent glass dissolution with precipitation of a secondary gel phase described by an ideal solid solution model
- Incongruent glass dissolution with precipitation of a secondary gel phase, both described by an ideal solid solution model.

All three model approaches resulted in different minerals to describe the measured concentrations at the three different temperatures (40, 90, and 150 °C). However, the models with a solid solution needed less mineral phases compared to the pure mineral model. Since at lower reaction progress, Al is preferentially included in a secondary phase compared to Ca and at larger reaction progress Ca precipitation increases, a sequence of different minerals with different Ca:Al(:Si) ratio's must be defined in the pure mineral model (in which the stoichiometric coefficients are constant). This problem is circumvented using a solid solution model. In addition, the different minerals in the solid solution models for the different temperatures are mainly due to different solubilities at a given temperature. For example, the temperature dependence of the solubility of quartz (as defined in the thermodynamic database) is not able to describe the measured Si-concentration at the three temperatures. Therefore, solubilities of SiO₂, CaSiO₃, Al(OH)₃ and MgSiO₃ in a solid solution model were adapted for each temperature to fit the measured concentrations. The fitted temperature dependence of these solubilities is then used in other systems. For example, the fitted temperature solubility of SiO₂ based on the distilled water system was successfully applied to describe the measured Si concentrations in the synthetic interstitial clay water system.

The simulation for the SON68 – synthetic interstitial water – boom clay system (tests from the previous EC programme) was based on a congruent glass dissolution model with precipitation of pure secondary phases and the boom clay pore water model from the previous paragraph. Since the measured Si-concentrations were as high as in the boom clay – synthetic interstitial clay water, amorphous SiO₂ was included in the

model to control the Si concentration. As mentioned in section 2.2, Si sorption is likely also at Si concentrations > 100 mg/l (until equilibrium is reached). Nevertheless, the adsorption of Si on the clay was neglected in the model. The most striking simulation result is that the multisite cation exchange complex determines significantly the concentrations of Na, Mg and Ca. For Na, beside the cation exchange complex, no additional secondary mineral is required to describe its concentration. An acceptable description of the measurements was obtained by including amorphous SiO_2 , calcite, a pure Al-phase and a Mg:Si phase in the model. In the future, this data set will be further analyzed using the two other model approaches and, eventually, including Si sorption.

Conclusion:

There is indirect evidence for long-term precipitation of Si, and geochemical calculations suggest a number of potential secondary phases. The experiments performed within GLASTAB nevertheless show that these processes will be observed only in long-term experiments.

3.3.2.4 Gel dissolution

In water without solids with a Si sorption capacity, the gel dissolution rate is assumed to be small. In other words, glass dissolution is iso-volumetric, meaning that the gel/water interface does not retreat. Hence, models used for glass dissolution in pure water do not have to include gel dissolution kinetics. In the presence of clay (or other Si sinks), this may not be the case any more. Evidence for this was given in previous programmes, but also the tests of WP4-4 (GLASTAB) lead to this conclusion. Indeed, tests with SON68, exposed to boom clay for 382 days at 30°C resulted in a mass loss of 3.97 g/m²day (3.83 g/m²day for the duplicate), this corresponds to a dissolved layer thickness (d_{cg}) of 1.4 μ , assuming congruent dissolution. If dissolution would effectively be congruent, then we would not observe a surface layer on the sample. The SIMS analyses show however that the thickness of the depleted layer on the coupon surface (L) is 0.1 μ . So we must assume that the dissolution is at least partially selective. If we assume that the gel/clay interface does not retreat at all, then we would observe a layer that is at least 1.4 μ thick (if the density of the layer is half the density of the pristine glass, it would be 2.8 μ). Because in reality, we only see a layer of 0.1 μ , we must conclude that the dissolution was predominantly congruent. The gel/clay interface has probably retreated by $\sim (1.4-0.1) = \sim 1.3$ μ . Similarly, the test with inactive SON68 in boom clay at 90°C resulted in a calculated dissolved layer of 33 μ after 1 year, whereas the SIMS analyses showed a layer of only 10 μ . So here also, we must assume gel dissolution.

Laboratory tests were performed in comparable conditions for WP7 of CORALUS, with dried boom clay, and with the Praclay mixture (65 % FoCa7, 30 % sand, 5 % graphite). In this case, the coupon mass losses were estimated, based on the experiments of WP4-4 of GLASTAB. The glass mass losses with the Praclay mixture is expected to be somewhat lower than in the dried boom clay, but the impact should be relatively small. The results are presented in Table II. Here also, the difference between the calculated (d_{cg}) and observed layer thickness (L) suggest that the gel was partially dissolved, with retreat of the gel/clay interface.

	Medium	d_{cg} (μm)	L (μm)
WP4-4, 30°C, 1 year	boom clay	1.4	0.1
WP4-4, 90°C, 1 year	boom clay	33	10
WP7 (CORALUS), 30°C, 2 years	boom clay	1.8 – 2.4 (estimated) ²	1 " 0.5
WP7 (CORALUS), 90°C, 1 year	boom clay	33 – 78 (estimated) ³	50 - 60
WP7 (CORALUS), 30°C, 2 years	Praclay mixture	1.8 – 2.4 (estimated)	<0.25
WP7 (CORALUS), 90°C, 1 year	Praclay mixture	33 – 78 (estimated)	70 " 0.5
WP7 (CORALUS), 30°C, 2 years	FoCa7 + frit	?	~50 nm
WP7 (CORALUS), 90°C, 1 year	FoCa7 + frit	?	0.1-0.2

Table II: Comparison of (1) the thickness of the dissolved layer assuming congruent dissolution, based on mass loss (d_{cg}) and (2) the thickness of the altered layer actually observed (L)

Similar results from previous *in situ* tests with very high mass losses ($> 2000 \text{ g m}^2$ after 7.5 years at 90 °C) and yet relatively thin surface layers, also suggest that the gel/clay interface effectively retreats, at least in contact with fresh clay. It is possible that the difference between d_{cg} and L is due to the fact that layers on the glass surface in contact with fresh clay are very brittle, and that they are lost when the sample is retrieved. In that case, one could argue that the gel/clay interface has actually not moved. However, if the layers are indeed very brittle, it is unlikely that they constitute a barrier for further glass dissolution. So, for a general description of glass dissolution, this layer is equivalent to an inert layer. On the other hand, the gel could transform into secondary minerals. These may act as a sink for glass constituents (leading to long-term dissolution), or they may be inert w.r.t. glass dissolution. At this moment, it is not clear if the dissolved gel layer should be treated as a sink (equivalent to a clay layer) or as an inert layer. It is however clear that it should not be treated as a protective layer.

In contact with Si-saturated clay, gel dissolution seems not important. For WP4-4, and for WP7 of CORALUS, tests were performed with SON68 (and SM539) in contact with a mixture of FoCa-clay and SON68 glass frit, at 30°C (and 90°C). The observed surface layers were very thin (Table II), but comparison with mass losses is not

² Extrapolation of mass loss for SON68 in BC at 30°C of WP4-4.

³ The lower boundary is given by the mass loss for inactive SON68 in boom clay after 1 year at 90 °C in WP4-4. This was lower than expected (92 g.m^{-2}), and may therefore not be representative. The higher boundary is based on the dissolution rate of the ³²Si doped glass, which was estimated at 215 gm^{-2} , based on accumulated ³²Si release.

possible (due to broken coupons and/or problems with water saturation of the clay). Similar tests in more diluted clay media have however shown that very low mass losses (close to zero) are obtained in contact with Si saturated clay. Therefore, we can assume that glass dissolution will finally become iso-volumetric in Si saturated clay. We could not demonstrate this (so far) with the GLASTAB experiments in high-density clay, though.

No attempt was made to describe the gel dissolution kinetics or to parameterize the process.

For lifetime calculations, we propose to consider a first stage with congruent dissolution, lasting until Si saturation of the clay, and a second stage with selective dissolution.

The stability of the gel in integrated conditions was studied further in WP4-1 (tests with SON68 in the presence of metal corrosion products, clay and percolating water), and WP4-3 (tests with SON68 in compacted FoCa7 clay with siliceous additives).

Conclusions: In contact with fresh (Boom or FoCa7) clay, gel dissolution is likely. It is not certain if it is due to complete dissolution or rather to embrittlement. For glass dissolution modelling, it should be treated as an inert layer or as a layer of clay (or secondary minerals).

In Si saturated clay, glass dissolution is probably iso-volumetric.

3.3.2.5 Modelling of the integrated system

Specific models have been developed to describe glass dissolution in contact with Si sinks like (certain) clays and metallic corrosion products. Most frequently used within the EC are Lixiver (France), GLADIS (Switzerland) and the SCK•CEN lifetime model (Belgium). Formerly, the GLASSOL code (Germany) was also used for this purpose. The results of the experiments of WP4-4 at 30°C in boom clay have been compared with Lixiver predictions made for SON68 in contact with (dried) boom clay, in the frame of WP7 of CORALUS⁴. This can be considered as a validation exercise. The results are presented in [Figure 4](#).

⁴ Moreover, within WP7 of CORALUS, predictions were made with Lixiver for the two other media investigated in CORALUS, i.e. the Praclay mixture, and FoCa7 with SON68 glass frit.

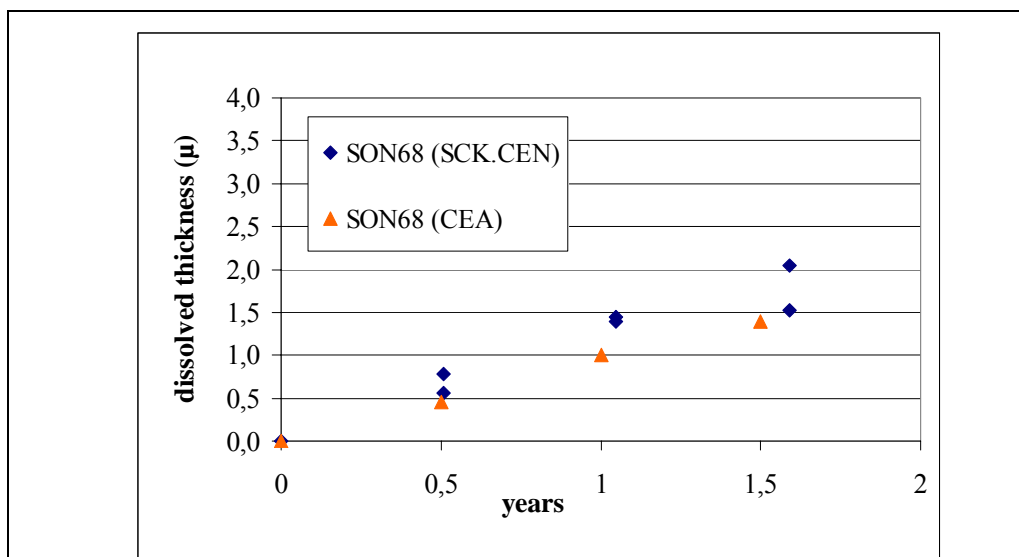


Figure 4: Comparison of results obtained for WP4-4 and predictions for similar conditions with Lixiver.

Although the absolute difference between predictions and observations is small for these short durations⁵, extrapolation to the long term using the same parameter values may lead to much larger differences. Apart from the model concept, the discrepancy between model and measurement may be due to the selected parameter values. More specifically, we expect an influence of r_0 , which was set at $0.0075 \text{ gm}^{-2}\text{d}^{-1}$ instead of the $0.01 \text{ gm}^{-2}\text{d}^{-1}$ observed in WP4-4, the relatively large value chosen for D_p ($10^{-10} \text{ m}^2\text{s}^{-1}$, whereas values between $2 \cdot 10^{-10}$ and $2 \cdot 10^{-11}$ can be derived from Table II) and the relatively low value for K_d ($0.018 \text{ m}^3\text{kg}^{-1}$, whereas values between 0.025 and $0.075 \text{ m}^3\text{kg}^{-1}$ can be found in Table II). With adapted values for these parameters, the fit with the experimental results would probably be better. So because relatively good fits can be obtained with independently measured parameter values, the main remaining question is related to the validity of the model concept. More specifically, it is not clear if the first order rate law is valid in the presence of solid clay. Indeed, in several experiments in the presence of clay, relatively high glass dissolution rates have been observed in spite of high Si concentrations in solution (see also section 2.3). This cannot be explained with the reaction scheme presented in Figure 1, unless we use a very high value for C^* . Moreover, Lixiver does not take into account gel dissolution, which is nevertheless likely in these experiments.

Even if the models are able to reproduce short term experiments, some modifications may be necessary to use them for extrapolations. It is, *e.g.* advisable to include Si precipitation in the extrapolation models, although this process is not well quantified. Precipitation can be included explicitly, but because the process is badly known, this is probably equivalent to adding a ‘black box’ constant final rate.

⁵ There is a slight underestimation by Lixiver, in spite of the fact that it does not take into account the effect of an initial background Si concentration of probably $>10 \text{ mg/l}$. If it would take this into account, the initial rate would be 0.37 % lower than currently predicted (see section 2.1), and the predicted dissolved thicknesses would then be only about half the observed thicknesses.

Conclusions:

Lixiver can be used to simulate relatively well the observed glass dissolution. Remaining uncertainties are related mostly to conceptual uncertainties.

3.3.2.6 Determination of radionuclide concentrations at the glass-clay interface

Radionuclide concentrations were determined at the glass-clay interface in WP4-7 (Np, Tc) and in WP4-8 (Se, Sn, Zr, Pd), to see if steady state values are reached, which can be used as input for performance assessment studies.

Np and Tc concentrations

The objective of the experiments was to gain more insight in the importance of redox potential on the Np and Tc concentrations in FoC7a-clay, which is considered as an oxidising medium, unless reducing agents are added. The experimental programme consisted of static leach tests at 40°C with glass SON68, doped with ⁹⁹Tc and ²³⁷Np performed in a FoCa7-clay/real clay water slurry made reducing by addition of 2.5 % pyrite and Fe coupons. The interpretation focussed on the determination of the mobile Np and Tc concentrations in the leachates obtained by ultra filtration over membranes of 100 000 MWCO and on the analysis of the activity of Np and Tc associated to the clay.

Good reducing conditions were obtained by addition of Fe coupons to the leach tests. This induced very low Np and Tc concentrations in the leachates, while most of the activity of Np and Tc was found associated to the clay. The remaining Np and Tc activity is distributed in the leachates and on the Fe coupons. The activity of Np and Tc found on the FoCa7 clay increases slightly as a function of time while their activity in the real clay water remains stable. The results obtained from two series of tests showed good reproducibility. The Np and Tc activity sorbed on the Fe coupon is also stable with time. In terms of molar concentrations in the leachates, even with the high Tc and Np weight % in the glass (0.12 wt% and 0.33 wt% respectively), the Np and Tc concentrations in the clay water are very low, about 1.6×10^{-10} M for Np and 3×10^{-10} M for Tc. In a previous programme, Np and Tc concentrations of respectively 6×10^{-8} M and 10^{-6} M were measured in the leachates of tests under comparable conditions (FoCa7-clay), but in absence of pyrite or iron coupons. The presence of Fe coupons in the FoCa7-clay is expected to induce the reduction of Np(V) to Np(IV) and Tc(VII) to Tc(IV). Indeed, except in highly reducing conditions, Tc exists as pertechnetate ion (TcO_4^-) which is highly soluble and for which no significant sorption on clay is expected. The Np and Tc concentrations measured in these tests are lower than the Np and Tc concentrations expected from the solubility of $\text{Np}(\text{OH})_4$ or $\text{TcO}(\text{OH})_2$, the solubility limiting solid phase expected for Np(IV) and Tc(IV) under reducing conditions ($S = 5 \times 10^{-9}$ M and $S = 10^{-8}$ M respectively). Once formed, $\text{Np}(\text{OH})_4$ and $\text{TcO}(\text{OH})_2$ can precipitate or sorb on the clay material. Np and Tc are found to be precipitated or sorbed to a great extent on the FoCa7-clay. If sorption could be *a priori* considered as the main mechanism affecting their concentrations in the leachates, the fact that the concentrations in solution are stable as a function of time, while the activities found on the clay increase, could involve also a precipitation process. Affected by precipitation reactions, the distribution ratios of Np and Tc which are very high are thus more like "apparent" distribution coefficients. However, because the solubility limits of $\text{Np}(\text{OH})_4$ and $\text{TcO}(\text{OH})_2$ are not exceeded, other solubility limiting solid phases should be considered. A combination of both mechanisms is highly probable. Nevertheless, the redox potential is the main

parameter affecting the concentrations of the radionuclides. We conclude that, under reducing conditions, FoCa7-clay as a backfill material, contributes to the retention of the radionuclides in the near-field, whatever is the kind of mechanism. The Np and Tc concentrations are even lower than the far-field solubilities determined through migration experiments or used in performance assessment. This should be taken into account when considering the behaviour of Np and Tc in the far-field.

Se, Sn, Zr, Pd concentrations

The experimental programme consisted of leach tests at 40°C with glass SON68 doped with stable isotopes of Se, Zr, Sn, and Pd and performed in a test medium consisting of a mixture of boom clay and near-field materials (FoCa7 clay and metallic corrosion products). Inactive isotopes were used and the leachates were measured by ICP-MS after ultra filtration over membranes of 10 000 and 100 000 MWCO.

To make the distinction between the amount of inactive isotopes leached from the glass and the elements already present in the medium, it was necessary to determine the background concentration of these elements in the solid and the liquid fraction of the starting medium (without glass). These values were then compared with the maximum amount of each element which could come from the glass. The amount of Se and Zr is much more important in the background medium than in the whole glass while for Pd and Sn, we have the reverse situation. The results from the leach tests show that the concentration of Se is stable with time and corresponds to the background concentration of Se in the medium. This is not surprising as the amount of Se in the medium is much more important than in the glass. The Se concentration is relatively high and we expect selenate to be present in the tests but we have no confirmation of the Se speciation. The Sn concentrations are stable with time and correspond also to the background concentration. However, after one year, a slight decrease is observed. Whether this is due to the uncertainty on the measurement or to a real decrease is still not clear. Anyway, the dissolution of the glass does not increase the overall Sn concentration. The evolution of the Pd and Zr concentrations is slightly different. Their concentrations seem to increase first as a function of the time because of the Pd and Zr coming out from the glass to decrease back to their background concentration for the longer test durations. The increase of the Pd and Zr concentrations in the beginning of the tests is certainly due to the formation of colloidal Pd(II) and Zr(IV) hydroxide particles. So even if the glass dissolution has an influence on the concentrations measured in solution, this is only a short-term effect. It can be concluded that the Se, Sn, Zr and Pd concentrations are not significantly higher than their background concentrations. The final steady-state concentrations are given in **Table III**.

[Zr]	5.5×10^{-9} mol/l
[Pd]	9.4×10^{-9} mol/l
[Sn]	4.2×10^{-9} mol/l
[Se]	2.5×10^{-7} mol/l

Table III: Final steady-state concentrations at the glass – near-field interface

Furthermore, there is no difference in concentration level after ultra filtration through 10 000 or 100 000 MWCO membranes indicating that all these elements are probably in the form of small inorganic colloids. The near-field concentrations of Sn, Pd and Zr are even lower than the far-field concentrations measured in migration experiments and the far-field solubilities used in PA except for the Se concentrations. This is expected as the behaviour of Se is more complex due to its redox sensibility as a function of the existing redox conditions of the tests.

Conclusion:

For the immobilisation of radionuclides in the near field, the redox condition of the backfill clay is probably the dominant factor. For elements which occur also as natural isotopes in the near field, the glass dissolution does not increase the natural background concentrations, except possibly for Se.

3.3.3 CONCLUSIONS

The conclusions that can be drawn from the experiments and the modelling work performed in the frame of the GLASTAB project are the following:

- The initial dissolution rate of SON68 (and SM539) has been determined in realistic disposal conditions (30 °C, high density clay)
- There is now direct evidence that fresh Boom clay has a sorption capacity for Si. This capacity is somewhat smaller than for FoCa7. There are indications that the Si sorption can be described well by a K_d in the Si concentration range relevant to disposal conditions (and at slightly basic pH). The GLASTAB project also provided detailed migration parameters values for FoCa clay,
- There is indirect evidence for long-term precipitation of Si, and geochemical calculations can suggest a number of potential secondary phases. The experiments performed within GLASTAB nevertheless show that these processes will be observed only in long-term experiments. Such mechanism does apparently not prevent a strong decrease of the glass dissolution rate. Indeed, very low dissolution rates can be obtained in the presence of clay, when the clay is saturated with Si.
- In contact with fresh (Boom or FoCa7) clay, gel dissolution is likely. It is not certain if it is due to complete dissolution or rather to embrittlement. For glass dissolution modelling, it should be treated as an inert layer or as a layer of clay (or secondary minerals). In Si saturated clay, glass dissolution is probably isovolumetric and dominated by selective leaching.
- As far as radionuclides are concerned, it has been shown that the redox effects are very important for determining the RN concentrations in the near-field, and that the type of clay is not so important if the conditions are reducing. For elements which occur also as natural isotopes in the near field, the glass dissolution does not increase the natural background concentrations, except for Se.
- Lixiver can be used to simulate relatively well the observed glass dissolution. Remaining uncertainties are related mostly to conceptual uncertainties.

The remaining problems are related to the contradiction between the high dissolution rate despite a high Si concentration, to the gel dissolution kinetics, to the relevant mass of bentonite and its effect on the final rate, and to the effect of Si-additives on the waste disposal considered as a whole. Because of the specific effects of clay (or other Si sinks), glass dissolution in concentrated clay seems fundamentally different from glass dissolution in water or in diluted clay suspensions.

3.4 Retention behaviour of actinides and lanthanides in gel/solution systems

The work packages related to the different topics are listed in the table below.

TOPIC	WORK PACKAGES	PARTNER
Co-precipitation	WP1-4, WP1-5	FZK
Sorption	WP1-7, WP2-6	FZK, IReS, CEA
Modelling	WP2-5, WP5-3	IReS, CGS

3.4.1 INTRODUCTION

The oxidation state of an element is its most important property regulating its behaviour upon complexation, precipitation, (ad)sorption and true colloid formation. Tetravalent elements may easily form true colloids with major hydroxide anions of solutions and, in the long term, insoluble crystalline hydroxides precipitate. By contrast, the crystalline minerals formed between the major and strongest ligands in waters, i.e. hydroxide and carbonate anions, and pentavalent (or trivalent) elements are more soluble. These elements are likely to be mobile (except under specific conditions, for example, due to formation of insoluble M^{3+} -phosphate phases) particularly in the form of aqueous carbonate complexes. It is necessary to identify and model the sorption processes – co-precipitation, ion exchange, adsorption – that compete against aqueous carbonate complexation in relevant systems.

The major processes to be considered for predicting accurately the behaviour of Ln and An during corrosion of HLW glasses are (i) aqueous complexation, (ii) precipitation/(co)dissolution, (iii) sorption, (iv) true colloid formation. The contribution of each process to element behaviour depends on the specific physico-chemical conditions (Eh, pH, pCO_2 ...) prevailing in the system, which determine the stable oxidation state of redox-sensitive elements and the nature and amount of aqueous and surface ligands. The formation of surface alteration gels (and clays) along HLW glass corrosion results *a priori* in high amounts of surface hydroxyl ligands (and of ion exchange sites). The questions remain on the nature of the gel surface sites, on their strength and on their relative contribution – compared to other sorption/precipitation processes – in the retardation of Ln/An migration under the relevant physico-chemical conditions.

To answer these questions, it has been necessary to investigate the behaviour of relevant elements under a wide range of physico-chemical conditions and in gel (+glass)/solution systems of growing complexity.

3.4.2 STUDIES PERFORMED DURING THE GLASTAB PROJECT

The different topics, and their objectives, are presented below.

- Topic 1 – Gaining basic knowledge on adsorption/precipitation of Ln/An
 - *Topic 1.1: Precipitation* - The objective is to determine the maximal attainable solution concentrations of fission products, U and Th during long-term corrosion of HLW glass in dependence of pH, and the possible solubility-limiting solid phases.
 - *Topic 1.2: Adsorption of Np(V) and Eu on synthetic alumina gels and Al-/Fe-silicate gels* - The objectives are determining (i) thermodynamic data for surface complexation (i.e. the affinity order) of trivalent and pentavalent elements on strong sites (aluminols) of gels and (ii) the effect of the composition and the structure of silicate gels on their sorptive surface properties.
- Topic 2 – Identifying/modelling (ad)sorption processes of actinides and lanthanides on glass alteration gels
 - *Topic 2.1: Modelling adsorption of Np(V) and Am(III) on the glass alteration gel SON68* – The objectives are determining (i) the surface properties of the gel and (ii) consistent sets of surface reactions and parameters to describe experimental data on the adsorption of Np and Am in dependence of pH, i.e. predictive models of An adsorption on the complex glass alteration gel.
 - *Topic 2.2: Studying the sorption behaviour of Am(III) in presence of the gel layer of pre-corroded, inactive HLW glass GPWAK1 in water and brines* – The objectives are studying the effect of sorption on the retardation of trivalent elements in complex glass/gel/solution systems in dependence of pH and under a wide range of conditions by (i) acquiring data on Am added to pre-corroded glass/(carbonated) water, NaCl and MgCl₂ solution systems and (ii) assessing the homological behaviours of Ln³⁺ initially present in the glass and of Am³⁺ added to solutions.
- Topic 3 – Studying the release/uptake of Ln/An during leaching of doped gels

The objectives are (i) acquiring data on dissolved element concentrations along the leaching of Am-doped, Np-doped and Pu-doped gels, under different redox conditions, in presence of carbonates and (ii) identifying possible solubility-limiting phases and/or sorption processes.

The work packages related to the different topics are listed in the table below.

TOPIC	WORK PACKAGES	PARTNER
1.1.	WP1-4 and WP1-5	FZK
1.2.	WP2-6 (-2, -3, -5) and WP2-5 (-1 to -5, -7)	IReS
2.1.	WP2-6 (-4, -6) And WP2-5 (-6)	IReS
2.2.	WP1-7	FZK
3.	WP2-7 (-1 to -4)	CEA

3.4.3 RESULTS

The studies performed in GLASTAB provided valuable insights into the retention/migration behaviour of lanthanides and actinides in gel/solution systems. We propose here sorption and precipitation reactions that may account respectively for the short-term and the long-term retardation behaviour of the relevant elements, in dependence of pH and other key parameters, from simple gel/solution systems to complex alteration gel/carbonated solution systems.

On the one hand, basic knowledge has been gained (topic 1):

- on the precipitation processes likely to govern, in the long-term, the solubility of relevant elements in glass/gel/solution systems,
- on the adsorption processes on silicate gels, likely to contribute to the short-term retardation of relevant elements in gel/solution systems:
 - on the affinity order of trivalent and pentavalent elements for strong gel surface sites,
 - on the influence of the gel structure on its adsorption properties.

On the other hand, significant progress has been made towards better understanding and modelling of sorption processes in complex element/gel/solution systems (topic 2). The studies led to:

- providing predictive models for the surface complexation (adsorption) of Am and Np(V) on the SON68 silicate glass alteration gel,
- identifying the strong (ad)sorption effect for trivalent elements in complex (glass)/gel/solution systems under specific conditions, and the influence of aqueous carbonates on the effect.

Finally, experiments of leaching of doped Np-, Pu- and Am-gels, in presence of carbonated solutions (topic 3) provided information on the relative contribution of sorption/precipitation processes of An and Ln in the control of solution concentrations of elements along gel leaching, under oxidizing and reducing conditions.

3.4.3.1 Precipitation processes and long-term element solubility

Results of the experiments performed with solutions obtained by glass dissolution and acid solutions containing the elements in soluble form are described in detail in Annex 1. Co-precipitation experiments were performed with the objective to determine the maximal attainable solution concentrations of fission products, U and Th during long-term HLW glass corrosion, and to find out the solid phases controlling the solution concentrations of the various elements.

Aqueous concentrations of elements and solubility-limiting phases

Co-precipitation experiments with the solutions obtained by dissolution of the HLW glass GP WAK1 in highly acid (HCl) and highly basic (NaOH) media (WP1-4) and the acid solutions containing the elements in soluble form (WP1-5) were finished by detailed evaluation of the concentration curves for soluble and less soluble elements in dependence on pH at 80, 50 and 23 °C.

The concentrations of the soluble elements (alkalis, alkaline earths) diminish only slightly with increasing pH up to 9.5. Except Mg, its concentration decreases strongly above pH 7. Regarding the less soluble elements, in both types of solutions lowest solubility was found for the tetravalent elements Th and Zr, then follow with increasing solubility Fe, Al, U and REE and finally, with the lowest solubility Ni and Mn. To find out the solid phases controlling the solution concentration, the pH-dependent concentration curves of various elements were compared with the solubility data of their pure solid phases from literature. It could be shown that the solubility data of $\text{Th}(\text{OH})_4$, AmOHCO_3 (homologue for Y, La, REE), schoepite ($\text{UO}_3 \cdot 2\text{H}_2\text{O}$) and also of gibbsite ($\text{Al}(\text{OH})_3$) and MgCO_3 agree quite well with the concentrations of the respective elements in the solutions (Fig. 1). Therefore, it appears that the concentrations of most elements in the super-saturated solutions studied are controlled by such pure solid phases. In contrast to the gel layer of HLW glasses developed during glass corrosion tests, nearly no retention or sorption effect of the dissolution residues was observed, e.g., for U and REE ions. However, even if the glass dissolution residues would have similar sorption properties like the gel layer on HLW glasses, the sorption effect would not be detectable. In the high concentrated solutions all surface sites in the residues would be occupied immediately because of the high excess of metal cations. No clear differences could be found between the results obtained at 80°C and those at 50°C. With proceeding sampling time a shift to lower concentrations by up to a factor of 10 after 150 days was found at corresponding pH values. At ambient temperature the concentrations of, e.g., U and Nd begin to decrease at higher pH than in the rest of the precipitation tests and run clearly inside the stability range of schoepite and AmOHCO_3 , respectively. With proceeding time, the concentrations of U and Nd diminish and approximate more the solubility limit of the named solid phases, but still remain inside their stability range.

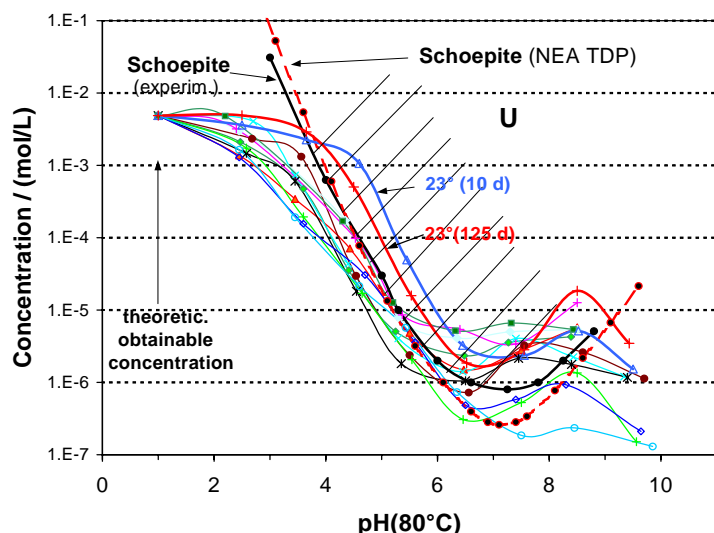


Figure 1: Concentrations of U in the solutions from the co-precipitation tests at 23 and 80 °C and the solubility data of schoepite

Analyses of the precipitates

The formed precipitates and residues were analysed by XRD and SEM/EDX. The XRD pattern of all residues show only few and weak diffraction peaks. Some of the weak peaks could be related to molybdates with powellite structure (CaMoO_4 , NaREEMoO_4) and to oxides and hydroxides of the less soluble elements (CeZrO_2 , ZrO_2 , Fe(OH)_3). The crystalline amount may range below about 2 % and, therefore, the precipitates can be considered as largely amorphous. SEM/EDX analyses revealed that in most samples of the precipitates small tetragonal crystals of Powellite (CaMoO_4) exists, with and without REE. Further crystalline BaCrO_4 and hexagonal Cs-molybdate was found. But most precipitates consist of very fine-grained powders composed of various combinations of elements with low solubility (Th, Ti, Zr, Al, Fe Cr and Mo).

Conclusions

The experiments show that the final concentrations of most elements in the super-saturated solutions obtained by glass dissolution or containing the elements in soluble form are controlled by precipitation of pure solid phases such as Th(OH)_4 , AmOHCO_3 (homologue for Y, La, REE), schoepite ($\text{UO}_3 \cdot 2\text{H}_2\text{O}$). The experiments show nearly no retention or sorption effect of the dissolution residues. Most precipitates consist of fine-grained powders composed of various combinations of elements with low solubility (Th, Ti, Zr, Al, Fe Cr and Mo).

3.4.3.2 Influence of (ad)sorption processes on short-term element retardation

The sorption experiments of actinides and lanthanides performed on gels were designed:

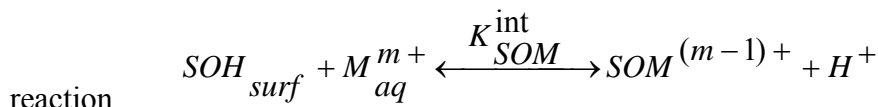
- either to gain basic knowledge on the adsorption processes on silicate/alumina gels (affinity order of An for strong sites of gels, influence of the gel structure ...) to be applied to modelling adsorption on alteration gels,
- or to confirm/infirm the sorption effect on short-term An and Ln retardation in complex gel/solution systems.

The results obtained on the sorption of the relevant elements on gels are presented here for systems of growing complexity.

Relative affinities of trivalent and pentavalent elements for strong sites of gels

Aim and description of the study – The aim was providing thermodynamic data for the binding of trivalent and pentavalent elements at aluminol sites on alumina gel, to be used for describing adsorption on complex Al-silicate alteration gels (cf. III.2.2. and III.3.3). We used a synthetic alumina gel. We performed titration experiments of the gel surface as well as experiments on electrolyte counter-ions sorption. We performed batch sorption experiments at 298K, taking pH as the main solution parameter. The experimental results were analyzed with the diffuse layer model to derive adsorption intrinsic constants.

Surface complexation reactions and related constants – The surface complexation



was applied to describe the pH-dependence of NpO_2^+ and Eu^{3+} adsorption onto the aluminol sites (Fig. 2) gel and to derive the related constants. The constants are reported in Figure 3 plotting the intrinsic DLM adsorption constants on ferrihydrite or Al-oxides in literature versus the hydrolysis constant of elements. Our data are consistent with the general trend reported in literature of increasing adsorption constant values with increasing hydrolysis constant values.

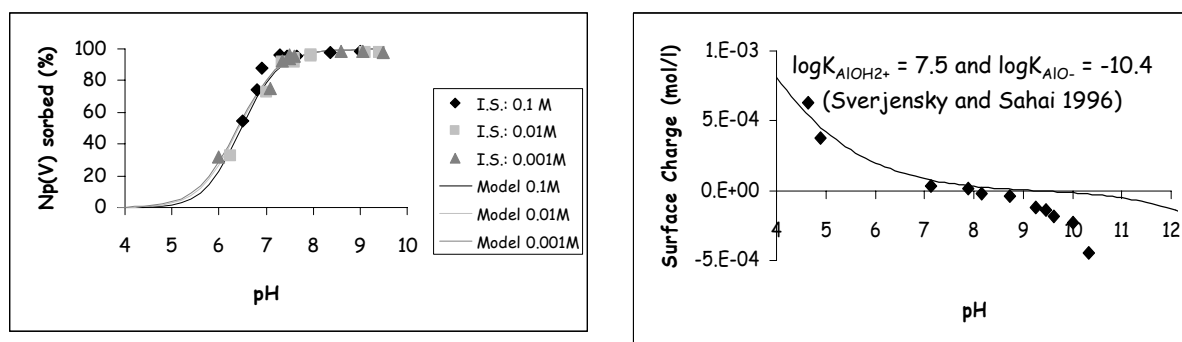


Figure 2: Experimental results on the pH dependence of: (left) the adsorption of $0.5 \mu\text{M}$ Np(V) on 1 g.l^{-1} alumina gel in NaCl solutions at different ionic strength, (right) the surface charge on alumina gel (5 g.l^{-1}) in 0.001 NaCl solutions (specific surface area of the gel: $80 \text{ m}^2.\text{g}^{-1}$).

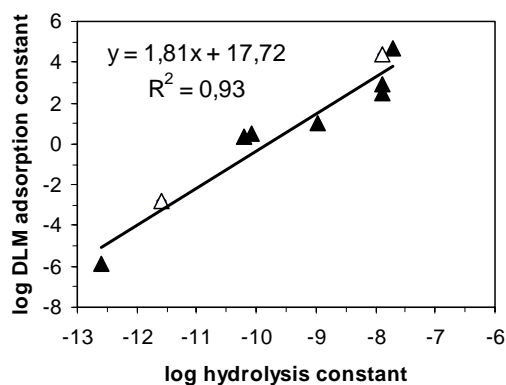


Figure 3: Intrinsic DLM adsorption constant of element reported in the literature (black) or in this study (open) for Fe- or Al-oxihydroxides against hydrolysis constant of element.

Conclusions – Considering the high affinity of trivalent elements for strong aluminol sites, it is to be expected strong adsorption effect on gels, provided aluminol sites on gels are accessible to aqueous ions. Adsorption may be efficient retardation process competing against carbonate aqueous complexation of Am^{3+} or Ln^{3+} . By contrast, the adsorption effect for Np(V) may be much lower, particularly in presence of aqueous carbonates.

Influence of the structure of silicate gels on their adsorptive properties

Aim and description of the study - The aim was understanding and modelling the adsorption of Np(V) on aluminosilicate and ferri-silicate gels having different Si/M molar ratios (M: Al^{3+} or Fe^{3+}). We focused on clarifying the effect of the Si/M molar ratios of the gels on their structure and surface properties. We synthesized Na-silica gel and various Na-Al-silicate ($4 < \text{Si} / \text{Al} < 10$) and Na-Fe-silicate ($2 < \text{Si} / \text{Fe} < 10$) gels (called “gels A”). We studied gel sub-samples (called “gels B”) washed at acidic pH to remove residual Na. The structure and surface properties of the gels was studied by several methods. The sorption of Np(V) was measured under a wide range of pH and chemical conditions. The macroscopic data were analyzed with the DLM considering additive binding of Np(V) at the silanol and ferrinol or aluminol surface sites. The work is described in detail in (Del Nero et al., accepted).

Surface charge of the gels - The surface charge characteristics of the aluminosilicate gels are explained by (i) disordered aluminosilicates with Al in tetrahedral position (ii) poorly-polymerized silica and (iii) accessory aluminium (hydr)oxides. This results in predominant negative Si-O sites on all the Al-silicate gels. Most of our results the ferri-silicate gels display the structure of synthetic amorphous silico-ferric precipitates (Si atoms in tetrahedral cavities and Fe atoms in octahedral sites). However, the striking experimental feature is that adsorption of counter-ions reveals all the ferri-silicate gels brought in solutions display similar surface charges with predominant negative Si-O sites. So, the surface characteristics of the ferri-silicate gels may evolve in contact with solutions due to adsorption of silicate anions at ferrinol sites and/or to formation of silica gel coatings.

Aluminosilicate gels/ Np(V) - The adsorption of Np(V) is independent on the aqueous neptunyl concentration and slightly dependent (Fig. 4, gels A) or independent (gels B) on the gel Si/Al ratio. The acidic washing of gels leads to decreasing Np(V) adsorption at acidic/near-neutral pH, mainly due to the polymerization of the silica(te) phases. The key parameter controlling Np(V) adsorption at near-neutral pH is the concentration of surface silanols i.e. the polymerization state of the aluminosilicate phases. At basic pH, adsorption is due to trace amounts of aluminol sites.

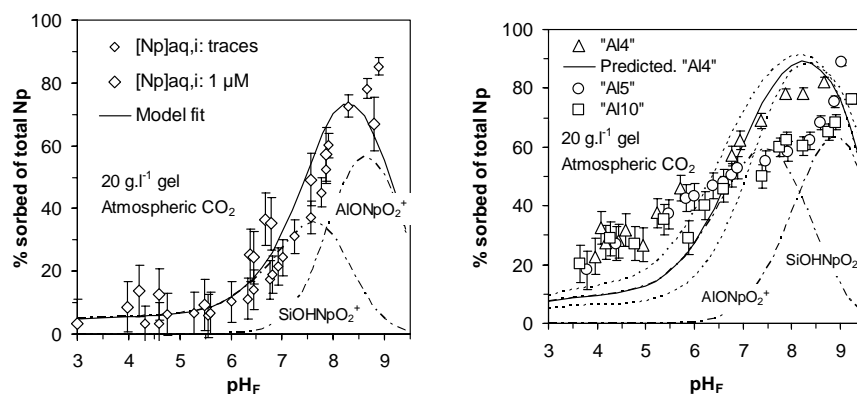


Figure 4: (a) Np(V) adsorption on the silica gel "Al-Si" as function of pH at different Np concentrations ($Np_{aq,i}$), and DLM adsorption curves as $\sum Np$ surface species (fit), $Si - OHNpO_2^+$ and $Al - ONpO_2^0$; (b) effect of the gel Si/Al molar ratio on the adsorption of Np(V) on gels A, and predicted DLM adsorption curves for Al4 as $\sum Np$ surface species, $Si - OHNpO_2^+$ and $Al - ONpO_2^0$

Ferrisilicate gels/Np(V) - The dependence of Np(V) sorption on the gel Si/Fe molar ratio is unexpectedly weak (Fig. 5). The adsorption is unaffected by the acidic washing procedure. Modelling shows that these findings are consistent with similar surface properties of the ferri-silicate gel samples brought in contact with solutions.

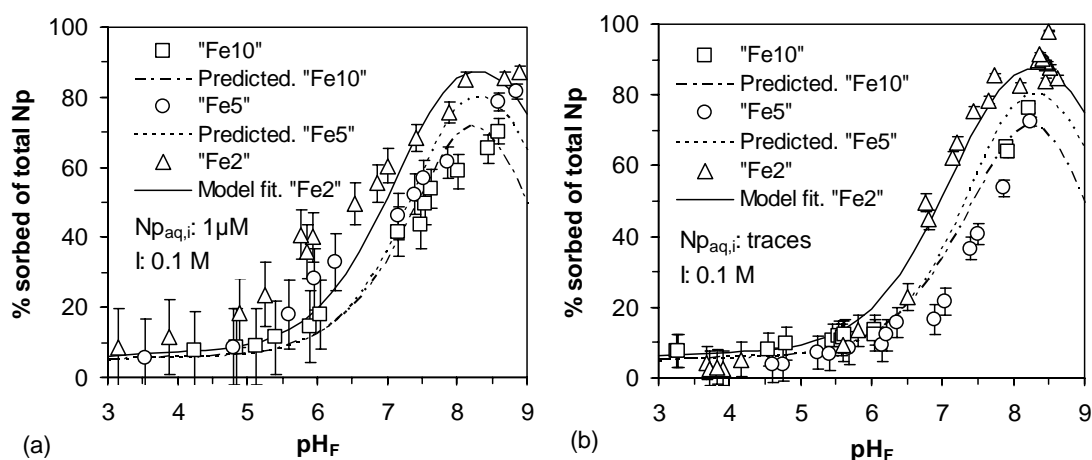


Figure 5: Effect of the gel Si/Fe molar ratio on adsorption of Np(V) on 20 g.l⁻¹ gels A as function of pH, under atmospheric CO₂, at different $Np_{aq,i}$ and fitted/predicted DLM adsorption curves as $\sum Np$ surface species

Conclusions - Our study shows that the Np(V) adsorption on Fe- and Al-silicate gels is controlled by the structure of the gels rather than by their Si/Fe or Si/Al bulk molar ratio.

The key parameter controlling the adsorption of Np(V) on alumino-silicate gels at near-neutral pH is the concentration of surface silanols i.e. the polymerization state of the phases. Modelling suggests that surface aluminols at trace concentration level control Np(V) adsorption at basic pH. So the scavenging capability of alumino-silicate gels

towards Np(V) is expected to be affected by the polymerization of the silica(te) chains at near-neutral pH and by the saturation of the high-affinity sites at basic pH.

The structure of these ferri-silicate phases should ensure the occurrence of high-affinity surface ferrinols on the gels. However, their solubility affects their surface characteristics. The release of silicate anions upon dissolution leads to the decrease of the concentration of the surface ferrinols by silicate anions adsorption and/or by formation of silica gel coatings. This has implications on the prediction of the retention capability of ferri-silicate gels as barriers to the Np(V) migration. However, unlike for the aluminosilicate gels, the structure of the ferri-silicate gels seem to prevent fast re-organizations of the material surfaces upon leaching which would dramatically affect the Np(V) adsorption.

A predictive model of Np(V) and Am(III) adsorption on the gel SON68

Aim and description of the study - The aim was to provide consistent sets of surface reactions and parameters to model the adsorption of Np(V) and Am(III) in dependence of pH on the glass alteration gel SON68. We took into account knowledge acquired in Sections III.2.1 and III.2.2. Experimental data were acquired on the surface charge of gel, on the ion exchange capacity of gel and on the adsorption of Np(V) ($Np_{aq,i} = 10^{-7}$ M, 10^{-6} M and 10^{-5} M; $T = 298$ and 363 K) (Advocat et al., 2001) and of Am(III) at trace concentration levels. The DLM surface complexation model was used.

The surface charge of gel reflects the presence of high-affinity sites - The titrations experiments were consistent with (i) $[SiOH]_{surf}/[MOH]_{surf}$ ($M = Fe^{3+}$ and Al^{3+}) ratio lower than 5 and (ii) with the dissolution of amorphous aluminium hydroxides during experiments ($pH_{PZC} = 7.8$). The ion exchange capacity of the gel (measured by the method of Cs exchange) indicated a high permanent charge (0.1 mmol.g^{-1}) probably due to Al for Si substitutions in the gel lattice.

Adsorption of Np(V) - The following conservative assumptions on the gel surface parameters were made to describe the Np(V) macroscopic sorption (see Section III.2.2):

- The ferrinol sites are occupied by silicate anions, released by gel dissolution.
- Al is mainly in tetrahedral position in the gel and AlOH surface groups on aluminium hydroxides are present at trace concentration level.
- The ratio $[SiOH]_{surf}/[AlOH]_{surf}$ is taken equal to 20 ($[SiOH]_{surf}/[AlOH]_{surf} > Si/Al$ bulk gel).

The surface complexation reactions used for binding at silanol and aluminol sites are those given in Annex 2. The assumptions led to a reasonable description of Np(V) adsorption at the highest Np concentrations (Fig. 6a). Modelling suggested that experimental sorption at the high $Np_{aq,i}$ reflects predominant SiOH groups, whereas Np binding mainly occurs on the “trace” surface aluminols. Assuming a $[SiOH]_{surf}/[MOH]_{surf}$ ($M = Fe^{3+}$ and Al^{3+}) ratio lower than 5 would have resulted in over-predicting the Np(V) uptake. The adsorption at low aqueous neptunyl concentrations clearly reflects the occurrence of low amounts of very high-affinity sites on the gel, that exist beside the AlOH groups (ZnOH etc.).

Adsorption of Am(III) - The same conservative assumptions on the gel surface parameters as those used for Np(V) were made to model binding of Am on the aluminol sites on gel SON68. Figure 6b shows the simulated Am(III) adsorption curves using values of DLM adsorption constants equal to 4.2 and 2.5 (values for Eu^{3+} on alumina

determined in this study, [Section II.2.1](#), or applied to Am^{3+} by Rabung et al. 2000, respectively). The sorption of Am is reasonably described at near-neutral/basic pH by binding at the trace aluminol sites, whereas the discrepancy between simulated and experimental sorption at acidic pH may be due to ion exchange at permanent charged sites of gels (and/or adsorption at other surface sites).

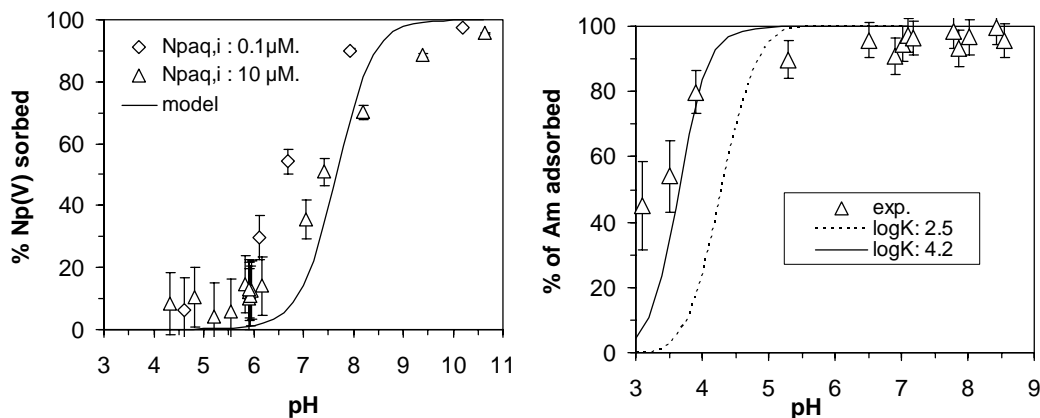


Figure 6: Adsorption on 4 g/L gel SON68 (specific surface area = $180 \text{ m}^2/\text{g}$) of (left) Np(V) at different $N_{\text{paq},i}$ concentrations and of (right) Am(III) at trace concentration level; and DLM simulated adsorption curves (see text).

Conclusion – We provided surface parameters for the gel SON68 based on conservative assumptions regarding the accessibility of the high – affinity ferrinol and aluminol surface sites on gel (see [Section III.2.2](#)). Applying these conservative assumptions and the surface complexation reactions and constants determined in simple gel/solution systems resulted in a reasonable description of the pH-dependent Am and Np(V) adsorption on SON68. Modelling suggested that binding of Am and Np on gel is mainly due to trace amounts of high-affinity sites under our experimental conditions. It is expected that conditions leading to saturation of the high-affinity sites at trace concentration levels on gel SON68 (increasing An aqueous concentrations, decreasing the gel specific surface area ...) may reduce significantly the scavenging properties of this alteration gel towards An.

Identification of the (ad)sorption effect on the behaviour of trivalent elements in specific glass/gel/solution systems

Description and aim of the study - In order to quantify the sorption effect on the retention of metal ions, sorption tests were performed using pre-corroded, simulated HLW glass GP WAK1 as substrate. In previous tests, the retention of Eu (homologue element for trivalent actinides), Th (homologue for Pu(IV), U(IV) and Np(IV)) and U(VI) was investigated in water and brines as a function of pH (Luckscheiter and Kienzler, 2001). In water, the sorption behaviour of these elements show a strong dependence on pH and the distribution ratios (R_s , see below) reflect the different charge of the three ions. The R_s values are highest for Th, followed by the R_s values of Eu, which are lower by about a factor 10 and finally those of U(VI) which are the lowest. The results of these sorption tests show clearly that the alteration layer on the glass surface has a strong effect on the retention of the three elements. To demonstrate that the sorption behaviour of Eu is representative for homologue trivalent actinides, additional

sorption tests were performed with Am^{241} in water as well as in brines. In the presented results, the determined distribution ratios R_s for Am between pH 2 and 10 are compared to the respective R_s values of Eu. The work is described in detail in [Annex 3](#) (Luckscheiter and Nesovic, submitted).

Presentation of the results - Results of the sorption experiments are given in the figures in terms of R_s (L/kg) values as a function of pH ($R_s = \text{Am}_{\text{sorb}}/\text{Am}_{\text{sol}} \times V/m$; Am_{sorb} = amount of Am sorbed, Am_{sol} = Am concentration in the solution, V = solution volume, m = mass of alteration layer). The mass of the surface layer m was calculated from the normalized mass loss of boron minus the normalized mass loss of Si, multiplied by the surface area of the glass powder and corrected for an assumed layer density of 2 g/cm^3 . R_s values were calculated for filtered and ultra-filtered solution samples to check for colloid formation. At pH values above 5, Am-bearing colloidal particles were detected in all sorption tests in water. The Am concentrations in the 450 nm filtered solution samples and above all in the unfiltered samples were much higher than in the ultra-filtered solutions (1.8 nm). The respective R_s values are included in [Figure 1](#) to illustrate the colloidal effect. The Am concentrations in the ultra-filtered solutions of 10^{-10} to 10^{-11} mol/L are far below the stability region of AmOHCO_3 (cr) or $\text{Am}(\text{OH})_3$ (am), the stable solid phases under these conditions. Compositional EDS analyses of the filter residues revealed that the Am-bearing colloids mainly contain silica. Therefore, the colloids may consist of detached fine gel-layer particles containing sorbed Am.

Comparing the behaviour of Am and Eu in water - Distribution ratios (R_s) of Am at 80°C for three starting concentration of 10^{-9} , 10^{-8} and 7×10^{-8} mol/L as a function of the pH after 10 days contacting time are shown in [Figure 7](#). The sorption edges are shifted slightly to higher pH values with increasing starting concentration. This is an effect of the non-constant pH in the solutions, especially during the first sorption test at the lowest starting concentration. In the last test, the changes in pH (about one unit per day at pH 3 to 5) were much lower than in the previous tests. Therefore, the R_s values determined at the highest starting concentration are more reliable. A concentration dependency of the R_s values can be excluded as with Eu, at much higher concentrations of 10^{-6} up to $5 \cdot 10^{-4}$ mol/L Eu, very similar R_s values were determined ([see Fig. 8](#)). [Figure 8](#) shows a comparison of the distribution ratios of Am with those of Eu, determined in previous tests, at various starting concentrations. Despite the relatively large scattering of the data points, it is quite evident that the sorption behaviour of Am is nearly identical with the behaviour of Eu. As shown by the previous sorption tests with Eu, at constant pH the sorbed concentration is about proportional to the solution concentration. Therefore, the sorption behaviour of Eu and Am can be described by a Nernst/Langmuir isotherm.

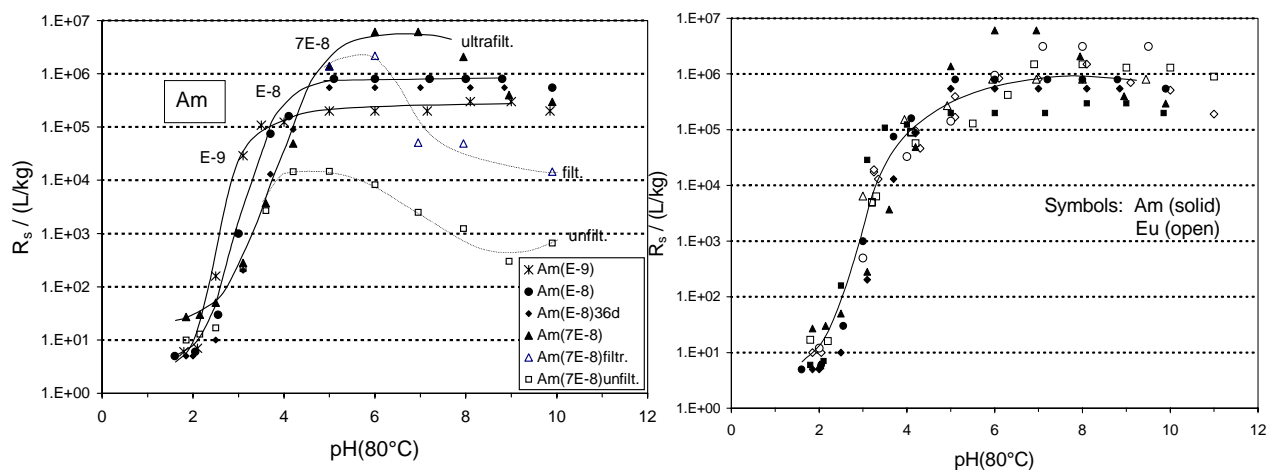


Figure 7 (left): Distribution ratios R_s of Am on pre-corroded HLW glass in water at 80 °C.

Figure 8 (right): Comparison of the distribution ratios R_s of Eu and Am in water at 80 °C.

The strong dependence of the R_s values on the pH may be explained by a surface complexation reaction of Me(III) ions with the alteration layer. For the modelling calculations described by Luckscheiter and Kienzler (2001) only the SiOH surface complex was regarded, as about 80% of the gel layer consists of SiO₂, two sites/nm² and only one sorption site species were assumed. As shown by modelling, the sorption data obtained from Eu and Am can best be described by the formation of a bidentate surface complex: $2 \equiv \text{SiOH} + \text{Me}^{3+} \leftrightarrow (\equiv \text{SiO})_2\text{Me}^+ + 2\text{H}^+$.

Effect of carbonate ligands - Above pH 7, the distribution ratios determined at the highest starting concentration decrease again (Figs. 7-8). This effect may be related to the formation of anionic carbonate complexes, because the solutions are in contact with air.

Am in brines - The sorption edges of Am in the NaCl brine at 80°C in comparison with the sorption edge of Eu at the starting concentration of 10⁻⁴ mol/L are shown in Fig. 9. Again, the distribution ratios of Am agree quite well with the R_s values of Eu. Like for Eu, the R_s values of Am are lower than in water and are independent of the starting concentrations. The sorption of Am and Eu in the MgCl₂ brine between pH 2 and 6.5 is shown in Fig. 10. Compared to the behaviour in water and NaCl brine, also shown in the figure, the distribution ratios of Am and Eu in the MgCl₂ brine are much lower. After an initial sharp rise at low pH, the R_s values rise slowly up to pH 6.5. Like in water and NaCl brine, the distribution ratios of Am and Eu are rather similar. The low retention of Eu and Am in MgCl₂ brine can be explained by competition of Mg²⁺ ions which occupy the sorption sites in the gel layer because of their high excess. A further, reasonable explanation for the lower sorption could result from the formation of clay-like Mg silicates, a common alteration product to form in the gel layer. Due to the formation of, e.g., smectite-type clays a decrease in pH is typical for glass corrosion experiments in Mg-rich solutions. The sorption tests with smectite clays, described in Annex 3, reveal a rather low sorption of Am and REE onto the clay below pH 6.

The desorption of Ce and Nd - During precorrosion of the glass and the sorption tests, Nd and Ce (as well as other REE) are leached out from the glass. From the Nd and Ce concentrations in the solution, „desorption“ coefficients (R_d) can be calculated. These R_d data of Nd and Ce included in Fig. 9 correspond quite well with the R_s data of Am and Eu. Consequently, the retention of REE and Am found in corrosion experiments can be

explained by sorption onto the alteration layer of the glass. (A corresponding agreement between the R_s values of Am/Eu and the R_d values of Ce /Nd was found in the sorption tests in water as well as in $MgCl_2$ brine).

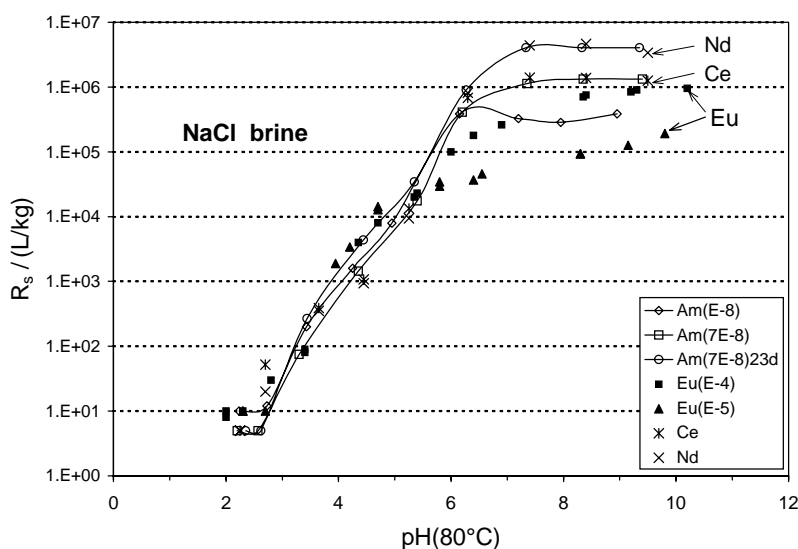


Fig. 9: Distribution ratios R_s of Am (curves) and Eu (solid symbols) in 5.5 M NaCl brine at 80 °C and „desorption“ coefficients R_d of Ce and Nd (crosses).

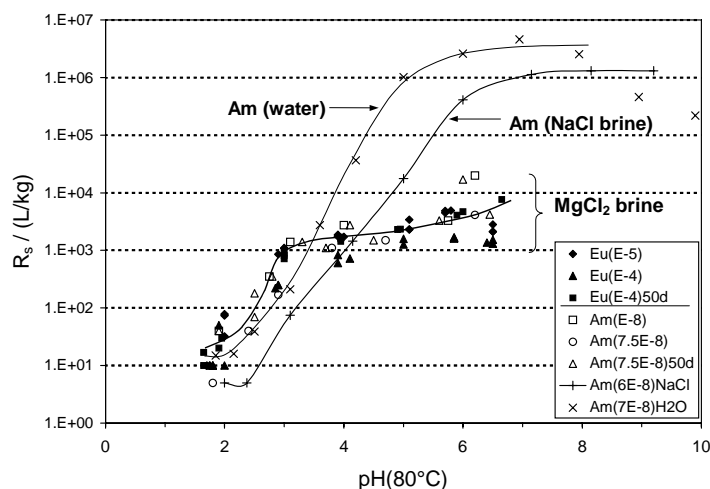


Fig. 10: Distribution ratios R_s of Am and Eu in 5 M $MgCl_2$ brine at 80 °C as well as the sorption edges of Am in water and NaCl brine.

Conclusions - The results of the sorption studies with Eu and Am in water and brines using pre-corroded glass as substrate show (i) the strong sorption effect of the gel layer on trivalent element in water and (ii) clear evidence that the sorption behaviour of Eu is representative for trivalent actinides. The R_s values decrease at high pH (> 7) is related to the formation of anionic carbonate complexes competing sorption. The „desorption“ coefficients R_d determined from the Ce and Nd concentration leached out from the glass in water and brines correspond quite well with R_s values of Am and Eu. Consequently,

the retention of REE and trivalent actinides found in long-term glass corrosion experiments can be explained by sorption on the alteration layer.

The distribution ratios R_s of Am decrease considerably if aqueous solutions contain high Mg concentrations. The low sorption in 5 M $MgCl_2$ brine can be explained by competition of the Mg^{2+} ions which occupy the active sites in the gel layer because of their high excess.

From the poor sorption of REE and Am on natural smectite (and synthetic, fine-grained „smectite“) below pH 6, the conclusion can be drawn that the much stronger sorption on the gel layer of corroded glass surfaces at low pH is not necessarily caused or influenced by the formation of clay-like minerals in the gel. In case of clay minerals, at low pH (< 6) ion exchange is the dominating retention mechanism for Eu and Am. The strong increase of the sorption above pH 6 onto clays is explained by chemisorption on the broken, unsatisfied bonds on edges of the layer silicates. The sorption properties of the gel layer reflect actually a specific structure („gel structure“) and complex composition of the gel with a high number of active sites. In the gel of the glass various sorption sites may exist besides $\equiv SiOH$, $\equiv AlOH$, $\equiv FeOH$, $\equiv ZrOH$, etc. are known to act as much stronger surface ligands than silica (the molar ratios of Al, Fe and Zr to Si in the glass are 0.06:0.03:0.006:1). Therefore, Eu(III) surface complexes in the porous gel may be formed at low pH (> 2.5). Moreover, the elemental composition of the gel varies with pH as less soluble elements - at high pH even Mg and Ca- are increasingly retained. As a consequence, the pH dependent sorption of Eu(III) may be partially caused by the gel composition varying with pH.

Conclusions: Influence of the physico-chemical conditions on the sorption of actinides and lanthanides on gels

Basic knowledge has been acquired on adsorption processes likely to intervene in short-term retardation of actinides and lanthanides in silicate gel/solution systems:

- trivalent elements have very high affinity for surface sites of gels such as the aluminol sites, as compared to pentavalent neptunium;
- the structure of a silicate gel determines its sorptive properties and the accessibility of high-affinity aluminol and ferrinol surface sites, rather than the bulk Si/Al or Si/Fe bulk gel ratio.

Thus, the physico-chemical conditions of gel formation, which influence the structure of the forming “gel” alteration layer at the glass/water interface, also determine the retardation capacity of the alteration layer towards relevant elements. Actually, it has been shown that, whatever the Al or Fe composition of a silicate gel-formed at low temperature and at near-neutral pH- the predominant surface sites are the silanol sites. The ferrinol and aluminol sites are poorly accessible and are present at trace level concentration. These conclusions on the influence of the gel structure on its sorptive properties are relevant for the glass alteration gel SON68. Experimental and modelling studies using SON68 suggest predominant low-affinity silanol sites, whereas adsorption of Np(V) and Am is mainly due to trace amounts of high-affinity aluminol (ferrinol) sites, under the investigated conditions. Assuming the ratio $[SiOH]_{surf}/[AlOH]_{surf}$ (or $[FeOH]_{surf}$) is equal to the ratio Si/Al (Fe) of bulk gel may lead to over-predicted sorption. It is expected, particularly for Np(V), that conditions leading to the saturation of the trace high-affinity sites reduce significantly the scavenging properties of SON68 towards An (i.e. increasing the solution concentrations of An or of competing cations,

decreasing the gel specific surface area ...). We provide consistent sets of surface parameters and binding reactions and constants to predict the effect of key parameters on the uptake of Am and Np(V) by gel SON68.

The influence of physico-chemical conditions on the sorption of trivalent elements on a gel layer on precorroded inactive HLW glass GPWAK1 is also well illustrated here. There is a strong sorption effect of the gel layer on Am and Eu added in water or in NaCl contacting solution at acidic and near-neutral pH. This is attributed to the specific structure („gel structure“) and complex composition of the gel with a high number of active sites, rather than to the secondary formation of clay minerals. In the gel of the glass various sorption sites may exist besides $\equiv \text{SiOH}$, $= \text{AlOH}$, $= \text{FeOH}$, $\equiv \text{ZrOH}$, etc. are known to act as much stronger surface ligands than silica (the molar ratios of Al, Fe and Zr to Si in the glass are 0.06:0.03:0.006:1). In the presence of carbonate ligands (at $\text{pH} > 7$) and/or of high aqueous concentrations of sorbing element (e.g. Mg in the sorption studies of Am and Eu in brines) the sorption effect is reduced, and the uptake of the trivalent element by the alteration gel layer is significantly decreased. These conclusions on the influence of chemical conditions on the sorption of trivalent elements added to alteration gel layer/solution suspensions are relevant for the behaviour of trivalent elements during glass corrosion. The retention behaviour of REE and trivalent actinides during glass corrosion can be explained by sorption on the alteration layer, as desorption data for Ce and Nd leached out from the glass in water and brines correspond actually quite well with sorption values of Am and Eu on pre-corroded glass.

3.4.3.3 Leaching of doped gels

Gels formed by fully alteration at 300°C of α -doped SON68 glasses have been leached at 50 °C and 44 cm^{-1} under oxidizing medium ($E_h \sim +150$ mV) and reducing medium ($E_h \sim -250$ mV). The aim of these experiments was to measure the dissolution rate of gels and to get experimental data on the actinides sorption/precipitation behaviour during leaching. The Am-doped gel leads to pH of leachates 0.5 unit lower than ones measured with Np and Pu-doped gels. It is due to α -radiolysis of air present above the solution in the reactor.

Gel dissolution rates

Since 1 day of leaching, the gels dissolution is highly non-congruent. Assuming silicon as tracer of gels dissolution, the experiments lead to an average dissolution rate of $4.4 \cdot 10^{-5} \text{ g} \cdot \text{m}^{-2} \cdot \text{d}^{-1}$. In general, Am-doped gel dissolution rates are higher than for the other gels. Actually, this phenomenon can be explained either by a direct α -radiolysis of the silicate network of gel, either by a S/V ratio higher for the Am-doped gel (factor 2) than for the Np,Pu-doped gels. About 35 and 50 % of Np are trapped in the gel during their dissolution respectively under oxidizing and reducing medium while this percentage is more than 90 % for Pu and Am. The rare earth elements La, Ce, Nd have similar behaviour during leaching.

Actinide concentrations in leachates

Actinides concentrations in leachates are roughly constant versus time and depend on the E_h value of the leachate. The Np solution concentrations are about $3 \cdot 10^{-7} \text{ mol} \cdot \text{l}^{-1}$ under oxidizing medium and $5 \cdot 10^{-8} \text{ mol} \cdot \text{l}^{-1}$ under reducing medium. Similar effect is observed for plutonium: Pu concentrations are of about $4 \cdot 10^{-9}$ and $10^{-9} \text{ mol} \cdot \text{l}^{-1}$ under oxidizing and

reducing medium, respectively. Dissolution/equilibrium modelling tests show that the solubility of Nd may be controlled by the pure phase NdOHCO_3 (Fig. 11a) for the durations lower than 6 months. On the reverse, no pure phases seem to control the solubility of the actinides (see Fig. 11b for americium). Inclusion of phosphate compounds in modelling can not reproduce the Nd and Am leachate concentrations, either. Possible explanations for the concentrations of actinides in the leachates are sorption on gel surface or/and co-precipitation in solid solutions.

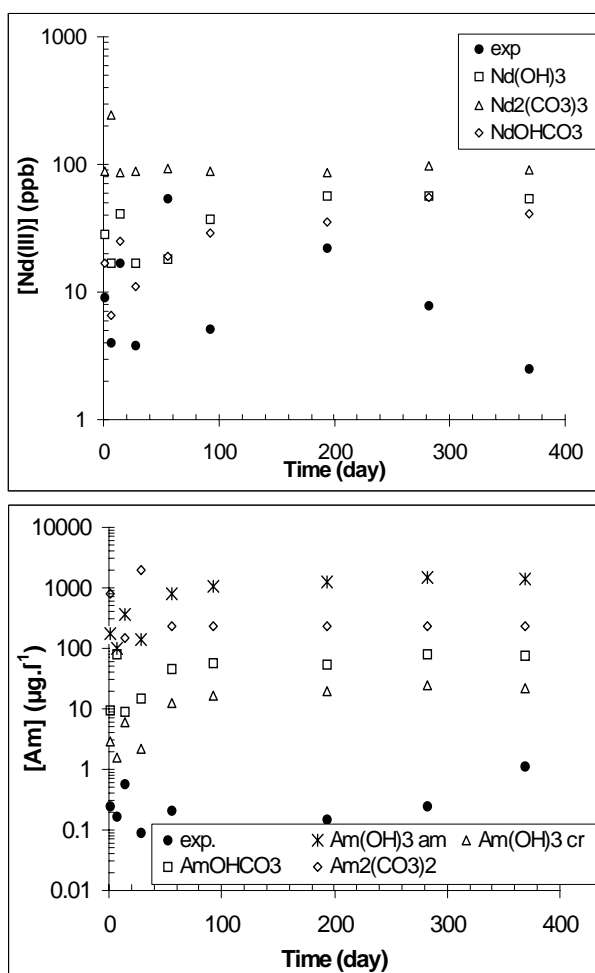


Fig. 11: Experimental and calculated solubility of (a) (left) Nd for three solid compounds during Np-doped gel leaching under oxidizing medium and (b) (right): Am for four solid compounds during Am-doped gel leaching under oxidizing medium

3.4.4 CONCLUSIONS ON THE RETENTION BEHAVIOUR OF AN AND LN IN (GLASS)/GEL/SOLUTION SYSTEMS

The studies performed in GLASTAB have led to identifying, in some specific systems, the retention mechanisms of Ln and An. The complementary fundamental studies on precipitation/adsorption led to proposing reactions for better prediction, in the specific systems, of the retention behaviour of relevant elements. But, the main contribution to the field of An and Ln retention in gel (+ glass)/solution systems is the clear illustration of the influence of the physico-chemical conditions and of the element oxidation state on the predominant mechanism and on its efficiency for element retardation.

Precipitation processes are likely to control the maximal solution concentrations of relevant elements (Th, Am, Ln and U) at very long-term glass corrosion. The final concentrations of most elements in super-saturated solutions obtained by glass dissolution in highly acid (HCl) and highly basic (NaOH) media or containing the elements in soluble form are controlled by precipitation of pure solid phases such as $\text{Th}(\text{OH})_4$, AmOHCO_3 (homologue for Y, La, REE), schoepite ($\text{UO}_3 \cdot 2\text{H}_2\text{O}$). The experiments show nearly no retention or sorption effect of the dissolution residues. Most precipitates consist of very fine-grained powders composed of various combinations of elements with low solubility (Th, Ti, Zr, Al, Fe Cr and Mo).

Sorption processes intervene in the retention behaviour of trivalent An and Ln during glass corrosion. The sorption effect of pre-corroded glasses on trivalent elements, identified for Am and Eu added to pre-corroded glass suspensions, is relevant for the behaviour of trivalent elements during glass corrosion. The “desorption” data of Ce and Nd leached out from the glass in water and brines correspond indeed quite well to sorption values of Am and Eu on pre-corroded glass.

The influence of physico-chemical conditions on the sorption effect of pre-corroded glass/gel layer on trivalent elements is well illustrated. The sorption effect is strong for Am and Eu added to water or to NaCl solutions contacting the pre-corroded glass, at acidic and near-neutral pH. This is attributed to the specific structure („gel structure“) and complex composition of the gel with a high number of active sites, rather than to the secondary formation of clay minerals. In the gel of the glass various sorption sites may exist besides $\equiv \text{SiOH}$. $\equiv \text{AlOH}$, $\equiv \text{FeOH}$, $\equiv \text{ZrOH}$, etc. are known to act as much stronger surface ligands than silica (the molar ratios of Al, Fe and Zr to Si in the glass are 0.06:0.03:0.006:1). It is suggested that the pH-dependence of trivalent elements sorption may also result from the pH-dependent nature and composition of the gel layer, as less soluble elements are incorporated with pH. The presence of carbonate ligands (at $\text{pH} > 7$) and/or of high solution concentrations of sorbing cations (e.g. Mg in the sorption studies of Am and Eu in MgCl_2 brines) leads to a significant decrease of trivalent element uptake. The Mg concentration effect may alternatively be explained by the formation of Mg-silicates in the system, with ion exchange becoming the predominant sorption process (lower efficiency than surface complexation).

The physico-chemical conditions of gel formation, which influence the structure of the forming “gel” alteration layer at the glass/water interface, also determine the retardation capacity of the alteration layer towards relevant elements. Whatever the Al or Fe composition of silicate gels -formed at low temperature and at near-neutral pH- the predominant surface sites are the weak silanol sites. The strong ferrinol and aluminol sites are poorly accessible and are present at trace level concentration. These conclusions on the influence of the gel structure on its sorptive properties are relevant for the glass alteration gel SON68. Adsorption in dependence of pH on the gel SON68, for Np(V) and Am at low aqueous concentrations, is mainly due binding at high-affinity sites (aluminol and/or ferrinol) present at trace level concentration, despite the high Al and Fe concentrations of bulk gel. It is expected that physico-chemical parameters controlling the saturation of the trace aluminols, such as element solution concentration and/or solution concentrations of other sorbing cations, etc., are crucial parameters influencing the efficiency of SON68 towards actinide retardation (particularly towards neptunyl ions which display low affinity for gel surface sites compared to trivalent elements). We provide sets of surface parameters and binding reactions and constants to be used to predict the effect of chemical parameters on the adsorption of Np(V) and Am(III) on aluminosilicate and ferri-silicate gels as well as on the alteration gel SON68, using very

conservative approach. But further studies are necessary before applying the binding reactions and constants proposed here to adsorption on other alteration products in glass/solution systems (i.e. clays which have more distinct surface properties than gels) or to compacted systems.

Finally, experiments of leaching of doped gels formed at high temperature illustrate the importance of An/Ln sorption processes on gels in the short- and mid-term (= year) retention behaviour of relevant elements, as well as the influence of physico-chemical conditions on the sorption efficiencies. No pure phases seem to control the solubility of the actinides and lanthanides (except NdOHCO₃ for Nd). The general trend of retention order for Pu, Am, and Np follow the general sorption trend: An(IV) > An(III) ≥ Ln(III) > An(V) (for tetravalent elements, precipitation of insoluble phases might also intervene in the experiments). So redox conditions obviously play crucial role on retention of the redox-sensitive elements. Nevertheless, more work is needed to fully characterize the different sorption processes (co-precipitation, adsorption ...) that may succeed during mid-term and long-term leaching of complex gels, because predominant processes are obviously dependent on the secondary phases formed i.e. again, on the physico-chemical conditions.

3.4.5 PUBLICATIONS

Advocat T., Jollivet P., Crovisier J.L. and Del Nero M. (2001): Long-term alteration mechanisms in water for SON68 radioactive borosilicate glass, J. Nucl. Mat., 298, 55-62.

Del Nero, M., Assada, A., Madé, B., Duplâtre G.: Np(V) adsorption on synthetic aluminosilicate and ferri-silicate gels, accepted for publication in Chem. Geol.

Luckscheiter, B., Nesovic, M.: Sorption behaviour of Am on precorroded HLW glass in water and brines, submitted paper.

Luckscheiter, B., Kienzler, B.: Determination of sorption isotherms for Eu, Th, U and Am on the gel layer of corroded HLW glass. J. Nucl. Mater. 298, 155 (2001).

3.5 Performance calculations: long-term glass package behaviour under integral conditions

The work packages related to the different topics are listed in the table below.

TOPIC	WORK PACKAGES	PARTNER
Literature review, critical review	WP5-1, WP6-2	CEA, SUBATECH ?XXX
Operational modelling	WP3-4	CEA
Performance calculation	WP5-2, WP5-4, WP5-5, WP5-6	
PA exercices	WP5-8	Nagra
Overall view of glass performance	WP6-1	All partners

The aim of all the scientific knowledge presented in the previous chapters is to ensure the reliability of performance assessment (PA) of glass source term in disposal conditions. To do this, this knowledge has to be somehow integrated into the codes used in PA exercices. This can be done either explicitly, for example by using in the

models the dependence of initial rate with temperature, or implicitly, for example by neglecting the actinide retention in the gel layer, although this retention is an important phenomena. In this case, a conservative assumption is made in the model.

The first step is the building of “operational models”, dealing with the glass package only, that have to be coupled in a second step with models of disposal environment in order to make performance calculations. So, this chapter presents firstly the characteristics of operational models, and secondly an example of performance assessment and of sensitivity analysis that can be done with PA code.

3.5.1 OPERATIONAL MODELLING OF GLASS SOURCE TERM

3.5.1.1 Operational modelling versus scientific modelling

The table below details the differences between scientific and operational modelling.

	Scientific modelling	Operational modelling
Objective	To improve the scientific knowledge. To get a better understanding of the phenomena. To quantify the phenomena.	To calculate the glass source term. To perform sensitivity analysis.
Modelled function	Glass alteration kinetics, gel composition, etc.	Quantity of altered glass (or RN released) as a function of time and disposal conditions.
System considered	Known glass surface area in a controlled/known environment.	Glass package in disposal conditions.
Criteria to assess the quality of the model	Good agreement between experimental results and modelling results (realistic model).	Simple, robust, parameterised, uncertainties checked and known, more or less conservative depending on the choice of the model.
Use	Used for testing the validity of a hypothesis, or for quantifying a parameter, or to dimension an experiment.	Used for predictive calculation, with a preliminary choice of dominant phenomena, hypotheses, numerical values and associated uncertainties.

3.5.2 PERFORMANCE ASSESSMENT: SENSITIVITY ANALYSIS ON GLASS DISSOLUTION RATE AND ASSESSMENT OF BARRIER FUNCTION OF ALTERED GLASS WITH A PERFORMANCE ASSESSMENT MODEL CHAIN

The aim of this work consists in coupling an operational model of glass alteration to a model of near- or far-field, in order to get an overall view of glass performance in disposal conditions. In the frame of the GLASTAB project, this work has been done with a model developed by Nagra.

3.5.2.1 Introduction

Recently, a safety assessment was carried out for the planned Swiss repository for spent fuel, vitrified high-level waste and long-lived intermediate level waste (Nagra, 2002). The model chain, developed for that purpose, is used to illustrate the role of the glass source term, investigated in the present GLASTAB project, within the multi barrier system of a repository. In particular, the sensitivity of the glass barrier performance on the dissolution rate and a potential barrier effect by radionuclide sorption and solubility limitation in the altered glass is assessed.

3.5.2.2 Swiss concept for the disposal of vitrified high-level waste

For a detailed description of the repository layout and the safety assessment carried out, we refer to the corresponding safety report (Nagra, 2002) and references therein. Here, only the main features are outlined.

The steel flasks containing the vitrified waste are planned to be placed into massive carbon steel containers which will be emplaced into horizontal tunnels in the opalinus clay host rock. The tunnels will be backfilled with bentonite pellets to form a compacted buffer between canister and host rock after water saturation.

The following barriers are taken into account in the model chain used for safety assessment calculations:

- the steel canister (a lifetime of 10 000 years is assumed)
- the glass (source term of radionuclides after canister breaching by slow dissolution)
- the bentonite (solubility limitation and chemically retarded diffusive transport of radionuclides)
- the opalinus clay (chemically retarded diffusive transport of radionuclides)
- the biosphere.

For the present study the biosphere is not explicitly considered. To allow a comparison between the different release rates mentioned below, the latter are scaled with biosphere dose conversion factors representing steady state conditions in the reference case biosphere. Calculations are performed for one canister containing COGEMA glass.

3.5.2.3 Representation of the glass dissolution in the model chain

The safety assessment model simplifies glass dissolution. It assumes a constant glass dissolution rate. A transient phase, during which the protective gel layer is formed and silica "saturation" conditions are reached, is not considered. For the reference case a final rate of $7 \times 10^{-5} \text{ kg m}^{-2} \text{ a}^{-1}$ was used. As a pessimistic case, however, the initial glass dissolution rate of $4 \times 10^{-2} \text{ kg m}^{-2} \text{ a}^{-1}$ was used and the calculations were complemented with an optimistic rate of $7 \times 10^{-7} \text{ kg m}^{-2} \text{ a}^{-1}$. The resulting glass-matrix dissolution rates, i.e., the fractions of the initial glass mass dissolved per year, are shown in [Figure 1](#). The intersection of a curve with the time axis is equal to the total glass lifetime under the corresponding dissolution rate.

The glass block is represented by a number of equal spheres with a total initial surface area of 15 times the surface of the block. The factor of 15 takes into account a surface area increase due to fracturing of the block. Please note that the glass lifetime is

inverse proportional to this factor (as to the glass dissolution rate). A variation of this factor between e.g. 5 and 50 has therefore a small influence on the glass lifetime compared to the influence of the assumed variation of the glass dissolution rate.

For the reference case the sensitivity on the geometrical representation of the glass was evaluated. In one case the glass block was represented by a plate which corresponds to a constant surface area during the whole lifetime of the glass. In a second case the glass was represented by a cylinder with the same initial surface area, i.e. 15 times increased compared to the glass block. It is evident from [Figure 1](#) that the way how the glass block is geometrically represented is not very important for its lifetime.

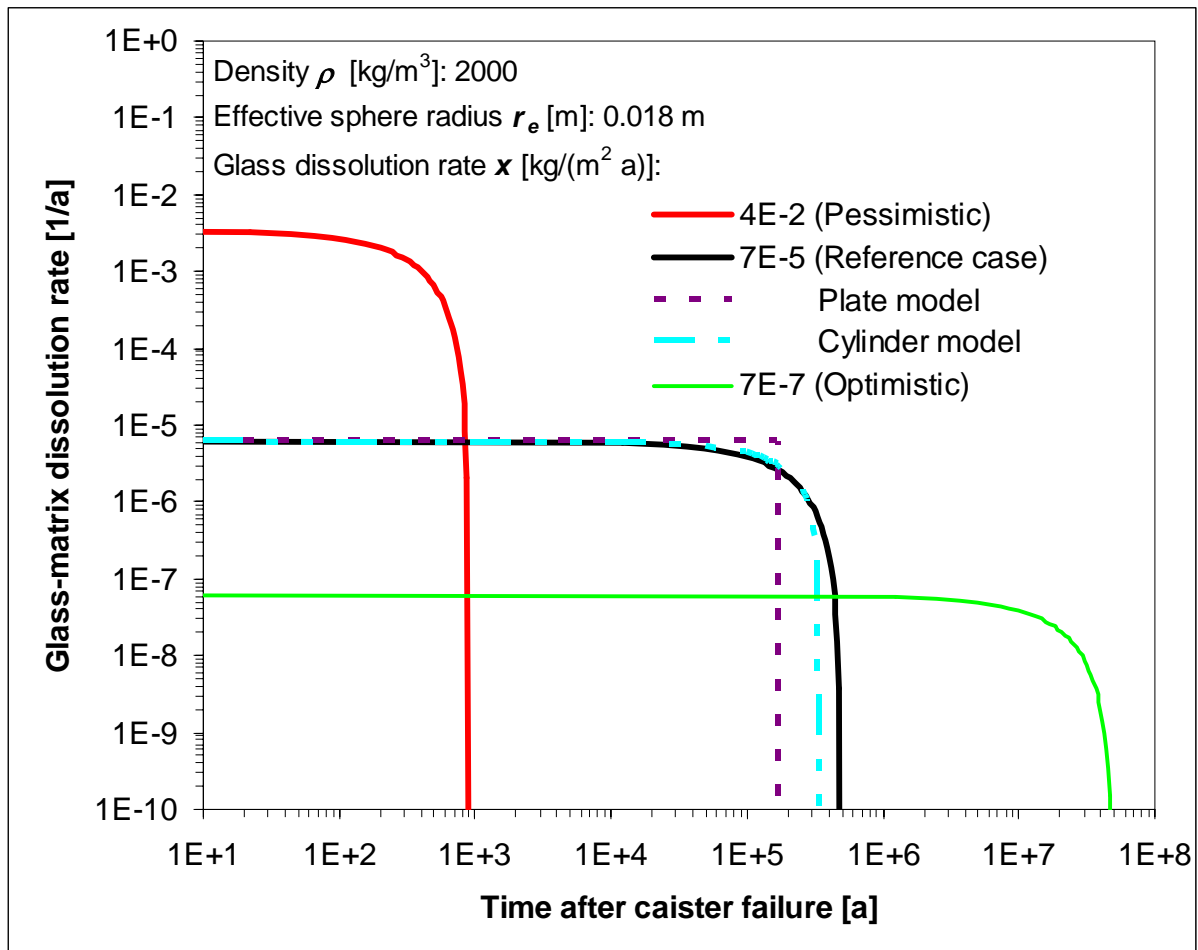


Figure 1: Fraction of the initial glass mass dissolved per year as a function of time

3.5.2.4 Release rate from the bentonite as a function of glass dissolution rate

To evaluate the sensitivity of the glass dissolution rate on the barrier efficiency of the glass matrix the radionuclide release from the bentonite was calculated. Except for the glass dissolution rate, reference conditions were assumed, i.e. reference solubility limits and sorption to the bentonite were included (see Nagra, 2002). The geosphere, however, was not taken into account. Consequently the release rate from the bentonite was directly converted into a dose rate, using biosphere dose conversion factors.

[Figure 2](#) shows the results for the sum of radionuclides and for ¹³⁵Cs only which dominates the dose for about 20 000 years after steel canister breaching. Comparing these results with the ones of a calculation case for which an instant glass dissolution

was assumed (data not shown), one can conclude that the glass matrix is an excellent barrier when it is dissolved with dissolution rate markedly lower than the reference rate of $7 \times 10^{-5} \text{ kg m}^{-2}$. With the reference rate the glass matrix is still a good barrier, in particular for ^{135}Cs for the first 20 000 years. With an initial rate of $4 \times 10^{-2} \text{ kg m}^{-2}$, however, the glass matrix does not have a barrier function within the considered system which includes a bentonite barrier, since the release rate does not differ from the case with instant glass dissolution.

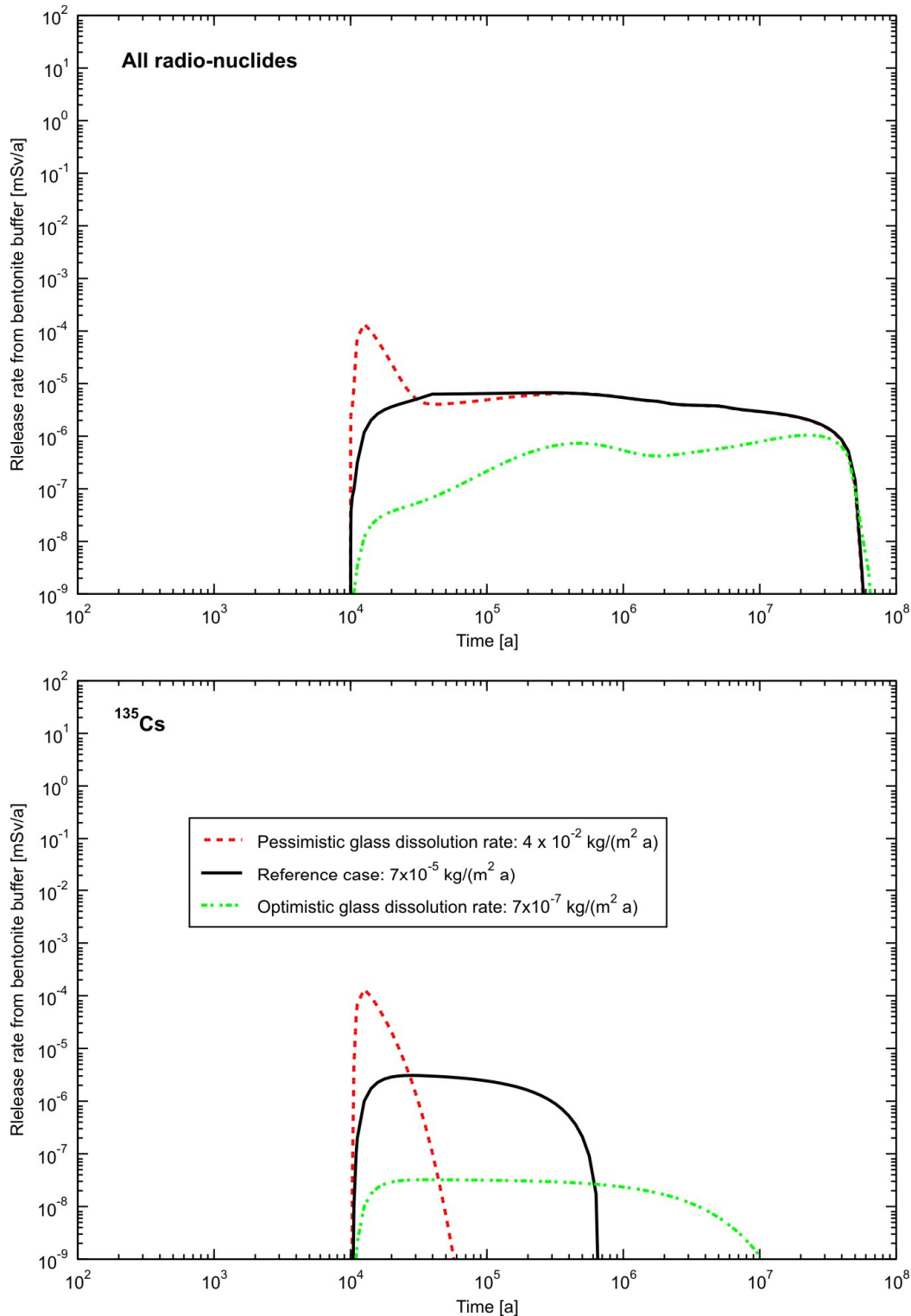


Figure 2: Release rate from bentonite as a function of glass dissolution rate

3.5.2.5 The role of the retention properties of the altered glass

Within the present GLASTAB project the retention properties of the glass alteration products were investigated. Radionuclide sorption and solubility limitation are inherent barrier properties of a glass. The barrier performance within the multi barrier system of the Swiss concept was assessed considering radionuclide sorption and precipitation processes.

The effect of a potential caesium sorption on glass alteration products

During glass dissolution an incongruent release of many elements into the liquid phase is observed. The incongruent behaviour is attributed to retention of these elements by the glass alteration products. The analytical results of the long-term glass leaching experiments carried out at PSI were screened for elements which are strongly retained in comparison to the bentonite barrier. The incongruent behaviour of caesium, which shows extraordinary high retention, was interpreted as sorption to glass alteration products although no independent information on the retention process was available. A K_d value of 4 kg m^{-3} resulted from this interpretation.

In comparison to a non sorption case, such a high sorption value diminishes the release rate from bentonite by more than one order of magnitude during the first 10'000 years when ^{135}Cs is dominating the release rate. For instance, the peak in [Figure 2](#) in the case of the pessimistic glass dissolution rate ($4 \times 10^{-2} \text{ kg m}^{-2}$) is levelled out by the Cs sorption.

The effect of radionuclide solubility limitation

Solubility limits measured in the chemical environment of glass alteration products are found to be similar to the ones derived for the bentonite pore water in the Swiss disposal concept. The latter were therefore used as substitutes to assess the importance of this inherent barrier property of the glass. For the corresponding calculations the full model chain, outlined above, was used.

A comparison between the release rate into the bentonite of a case using solubility limits and a case where solubility limits are switched off, shows a decrease by three orders of magnitude for ^{79}Se but also the release rate for ^{99}Tc is markedly reduced. For the actinide decay chains ($4 \text{ N} + 2$, $4 \text{ N} + 1$, $4 \text{ N} + 3$ and 4 N) a comparison is difficult due to the parallel decay and in-growth of radionuclides. The calculations reveal that mainly the shared solubility of the different uranium isotopes control the release into the bentonite.

The influence of the above mentioned radionuclide solubilities on the release rates into the opalinus clay and the biosphere, respectively, is less pronounced because the strong sorption of these nuclides to the clay minerals superimposes the solubility effect. As an exception, the solubility effect on the ^{79}Se release rate is evident up to the biosphere since no sorption to clay minerals was assigned to this element.

In summary, the solubility limits of ^{79}Se and ^{99}Tc and of U are important chemical barriers for the mentioned fission products and the actinide decay chains.

3.5.2.6 Reference

Nagra (2002): Project Opalinus Clay – Safety report, demonstration of disposal feasibility for spent fuel, vitrified high-level waste and long-lived intermediate-level waste (Entsorgungsnachweis). Nagra Technical Report NTB 02-05. Nagra, Wettingen, Switzerland.

3.5.3 **CONCLUSION**

All the existing operational models are built on the same principle: The quantity of altered glass is calculated by multiplying a matrix alteration rate by a surface area and an effective fracture ratio (the issue of determining this effective fracture ratio was not addressed in the frame of the GLASTAB project). The effect on the environment on the rate is more or less explicitly integrated in the value of the rate, depending on the models: the simpler ones use a single rate value for all the conditions, other ones integrates the effect of temperature, pH, sorption capacity of the environment, etc. But there isn't any completely integrated description of the coupling with environment, particularly from a chemical point of view. This remains a great challenge for future work.

Anyway, this kind of operational models is well designed to be coupled with simplified environmental models, for performance-assessment purpose, as illustrated by the calculations performed by Nagra.

4 General conclusion

Some major points have to be taken into account for performing performance assessment and for getting an overall view of glass performance in disposal conditions:

- The glass alteration kinetics has been studied for a long time and was of particular interest in numerous work packages of the GLASTAB project, either from an experimental or from a modelling point of view. The results of these studies allow justifying the conservative assumptions made when building the different operational models.
- The interactions with environmental materials like clay or corrosion products are of major importance for the glass performance in disposal conditions. The effect of the environment is strongly dependant on the nature of the environmental material (type of clay, of corrosion products). Numerous numerical parameters have to be determined to quantify the effect of these materials. As a consequence, it is necessary to restrain the studies to realistic materials if one wants to reach an exhaustive description of the effects of the environment. The choice of the environment has a direct impact on the overall glass performance.
- The radionuclide retention in the glass alteration products is usually not integrated in the operational models, where only the matrix dissolution is considered. But the studies performed in the frame of the GLASTAB project have confirmed that the radionuclide retention is a phenomenon of major importance, and that integrating it in the performance calculation would lead to greatly improving the overall glass performance in disposal conditions.